Assessing the photo-physiology of cyanobacteria using active fluorescence

Emilie Courtecuisse

Submitted to:

Biological and Environmental Sciences

University of Stirling, Scotland, United Kingdom

April 2023

For the degree of Doctor of Philosophy

Supervisors:

Dr. Stefan G.H. Simis

Dr Gavin H. Tilstone

Dr. Kevin Oxborough

Dr. Evangelos Spyrakos

Dr. Peter D. Hunter

Abstract

Eutrophication and the impacts of climate change are responsible for the increased occurrence of harmful algae blooms. In lakes and reservoirs, cyanobacteria blooms pose particular risk to ecosystems, humans and animals due to the occurrence of toxin-producing species. Several methods exist to monitor cyanobacteria, which vary in cost, time and accuracy. Fluorescence methods developed to monitor cyanobacterial abundance already give rapid, robust and reproducible results. Discrimination between cyanobacteria and algae in fluorescence methods is based on their photosynthetic pigment content, but due to overlapping pigment absorption signatures, the interpretation of fluorescence signals is consequently not straightforward. In this thesis, a range of fluorescence markers were tested on the ability to assess and predict cyanobacteria physiology and growth.

Hyperspectral laboratory experiments with algal and cyanobacteria cultures revealed that excitation wavebands centred on 445 nm and 615 nm, and emission wavebands at 660, 685 and 730 nm allow the best differentiation between cyanobacteria and algae. Broadband actinic light should be preferred to assess the relation between ambient light and photosynthesis. Based on these results, a new multispectral active fluorometer (LabSTAF) was tested to assess the physiology and growth of cyanobacteria in reservoirs exhibiting annual blooms. Fluorescence light curves obtained with a green-orange-red (GOR) and a blue (B) excitation protocol were found to follow cyanobacteria and algae physiology, respectively. The fluorescence emission ratio of photosystem I over II was also significantly correlated with the relative abundance of cyanobacteria. Excitation spectra further distinguish the presence of distinct pigment groups. Finally, the ability of the LabSTAF to determine cyanobacteria growth from photosynthetic parameters was demonstrated on natural samples brought into nutrient replete conditions. ETR (electron transport rate) and P_{max} (maximum specific photosynthetic rate) were found to predict phytoplankton growth by up to 3-4 days, with excitation protocols GOR and B indicating the dominant phytoplankton group.

Acknowledgements

This thesis would have never existed without the support of a lot of people. First of all, I want to thank my internal supervisors at Plymouth Marine Laboratory (PML) Stefan Simis and Gavin Tilstone, my external supervisors at the University of Stirling Peter Hunter and Evangelos Spyrakos, and Kevin Oxborough from Chelsea Technologies, the ICASE partner in this project. I want to thank Stefan in particular as my primary supervisor for his continuous support during this PhD. I want to thank Elias Marchetti, whom I co-supervised for my last research chapter and who did a wonderful job. I want to thank the Plymouth Marine Laboratory, where I was hosted. I had the opportunity not only to do research in new laboratory facilities but also to participate to join field work on the PML research vessel, as a side project. The research in this thesis was funded and made possible by the Natural Environment Research Council.

I want to thank the SCOR Working Group for the opportunity to join them in Vancouver, where I learned a lot and met most of the big names in the research field. I thank the team of the National Meteorological Library and Archive of the UK Met Office for data access. I want to thank South West Water and Bristol Water for nutrient and microscopy data, and the South West Lakes Trust for facilitating access to Roadford Lake. I want to thank Malcolm Woodward (Plymouth Marine Laboratory) for nutrient analysis and Tracey Beacham, Louisa de Dross, Paul Rooks (Plymouth Marine Laboratory) and Philippe Tortell (University of British Columbia) who gave me access to phytoplankton cultures. I want to thank Dr Douglas Campbell and anonymous reviewers who revised the two papers I published thus far.

Most of all, I want to thank my parents who always offered support in every situation. The presence of my dad in the UK for the last week before submission was the reason, I could submit this thesis. Thank you, dad! Thank you, Berne, for believing in myself more than I do. You are one of a kind and I am so glad I shared a part of my PhD and my life with you! Gracias por todo chiquitito! I want to thank my brother, Louis, for never letting me settle in a comfortable position and for opening my horizons! I am so grateful of the time we spend on the phone talking about anything and I am so proud of you! Merci petit Lou! I want to thank all my friends who were always there for me or checking on me at the end of the PhD. Special thanks to Camille, Lauranne, Vincent & Titouan, Paul, Gamze, Tatiana & Rich, Giovanni, El, Elias, Milo, French Tatiana, Will, Ninaï, my friends from home… There are too many to thank ♥

Many thanks to my colleagues at PML, I met so many amazing people there and I had a wonderful time with you guys! I want to thank in particular Patrick, Charlie, Chris 1, Chris 2, Francesco, Franki, Kevin, Rachel, Paul, Zara, Yang, Shauna, Josie, Marc, Louise, Stephanie, Tony, Mike, Nathalie, Hayley, Simone, Ollie, Jazz, Lily Anna, Tom, Lizz, Tom (Applications), Mike, Giovanni, Bror, Joe… Again, there are too many to thank ♥ Special thanks to John! I will give you those cookies one day!

And last but not least, I want to thank the mental health organizations and people who helped me through this PhD. I think of Devon mind (thank you Ed), Head space, Plymouth Livewell, Simply Counselling, Samaritans, Tectona Trust and Sarah. The work you do is absolutely terrific and your help was determining. Without you, I would have never been able to finish this PhD. I am really grateful ! Thanks! ♥

Peer-reviewed publications

Courtecuisse, E., Marchetti, E., Oxborough, K., Hunter, P. D., Spyrakos, E., Tilstone, G. H., & Simis, S. G. (2023). Optimising Multispectral Active Fluorescence to Distinguish the Photosynthetic Variability of Cyanobacteria and Algae. *Sensors*, *23*(1), 461.

Courtecuisse, E., Oxborough, K., Tilstone, G.H., Spyrakos, E., Hunter, P.D., Simis, S.G.H. (2022). Determination of optical markers of cyanobacterial physiology from fluorescence kinetics. *Journal of Plankton Research*, *44*(3), 365-385.

Schuback, N., Tortell, P. D., Berman-Frank, I., Campbell, D. A., Ciotti, A., **Courtecuisse, E.**, ... & Varkey, D. R. (2021). Single-turnover variable chlorophyll fluorescence as a tool for assessing phytoplankton photosynthesis and primary productivity: Opportunities, caveats and recommendations. *Frontiers in Marine Science*, 895.

Hoarau, P. E., **Courtecuisse, E.**, Treilhes, C. R., Lagarde, R., Teichert, N., & Valade, P. B. (2019). Reproductive biology of a small amphidromous shrimp Atyoida serrata on Reunion Island, south-west Indian Ocean. *Limnologica*, 76, 41-47.

Newsham, K.K., Eidesen, P.B., Davey, M.L., Axelsen, J., **Courtecuisse, E**., Flintrop, C., Johansson, A.G., Kiepert, M., Larsen, S.E., Lorberau, K.E., Maurset, M., McQuilkin, J., Misiak, M., Pop, A., Thompson, S., Read, D.J. (2017). Arbuscular mycorrhizas are present on Spitsbergen. *Mycorrhiza*. doi: 10.1007/s00572-017-0785-9

Workshop participation and conference presentations

- SCOR WG 156 (workshop, *Vancouver*, 2019) "Active chlorophyll fluorescence for autonomous measurements of global marine primary productivity ".
- **Oral presentation:** Fluorometry techniques for freshwater cyanobacteria assessment" (BPS conference/PlyMSEF conference, *Plymouth*, 2020)
- **Oral presentation:** "Fluorometry techniques for cyanobacteria assessment in freshwaters areas" (PML Seminar Series, *Plymouth*, 2019)
- **Poster:** "Detection of cyanobacteria *in situ* using fluorescence techniques" (Winter symposium, *Stirling*, 2018)
- **Poster:** "Novel Fluorescence Induction Protocols for Cyanobacteria Detection in Natural Samples" (Ocean Carbon from Space 2022 workshop, *online*)

Contents

List of figures

CHAPTER 1

CHAPTER 2

CHAPTER 3

CHAPTER 4

CHAPTER 5

List of tables

CHAPTER 1

CHAPTER 2

CHAPTER 3

CHAPTER 4

List of abbreviations and symbols

Abbreviations/Symbols	Definition	Unit
HABs and CyanoHABs	Harmful Algae Blooms or Harmful Blooms of cyanobacteria	Unitless
PBS	Phycobilisome	ø
PE	Phycoerythrin	ø
PB	Phycourobilin	ø
PC	Phycocyanin	ø
PEC	Phycoerythrocyanin	ø
APC	Allophycocyanin	ø
LHC	Light Harvesting Complex	ø
PSI (PI) and PSII (PII)	Photosystems I and II	ø
RC1 and RC2	Reaction centres 1 and 2	ø
Chl*a*, Chl*b*, Chl*c*, Chl*d*, Chl*f*	Chlorophyll a, b, c, d and f	ø
d-Chla, d-Chlb	Divinyl chlorophyll a and b	ø
N: P	Ratio of Nitrate over Phosphate	ø
C	Carbon	ø
NPP and GPP	Net Primary Production and Gross Primary	g C m^{-2} $year^{-1}$
NADP and NADPH/$NADPH_2$	Nicotinamide-adenine dinucleotide phosphate and reduced form	ø
PAM	Pulse Amplitude Modulation	ø
FRR	Fast Repetition Rate	ø
STAF	Single Turnover Active Fluorometer	ø
NPQ	Non-Photochemical Quenching	ø
OCP	Orange Carotenoid Protein	ø
DWM	Dual Waveband Measurement	ø
PMT	Photomultiplier Tube	ø
PAR	Photosynthetically available radiation	µmol photons m^{-2} s^{-1}
ā*	Chla-specific spectrally averaged absorption coefficient of phytoplankton weighted by their radiance spectrum	m^2 mg^{-1}
Q_a*	Fluorescence intracellular reabsorption factor	Unitless
ST and MT	Single-Turnover and Multiple-Turnover	ø
R_o	Fraction of the reaction centres in the opened state	Unitless
R_c	Fraction of the reaction centres in the closed state	Unitless

R_{dam}	Fraction of reaction centres damaged	Unitless
λ, λ_{ex}, λ_{em}	Wavelength, Excitation wavelength, Emission wavelength	nm
A_{max}	Maximum of absorbance	Unitless
$a(\lambda)$	Absorption (per wavelength)	m^{-1}
k_f	Rate constant of fluorescence	s^{-1}
k_d	Rate constant of thermal dissipation	s^{-1}
k_p	Rate constant of photochemistry	s^{-1}
k_1	Rate constant of dissipation of energy at damaged reaction centres	s^{-1}
F_o *and* F_o'	Minimum fluorescence obtained in a dark-adapted state and in a light-adapted state	Unitless
F_m or F_m'	Maximum fluorescence obtained after closure of the reaction centres in the dark-adapted state and in the light-adapted state	Unitless
F_v and F_v'	Variable fluorescence ($F_v = F_m - F_o$) in the dark-adapted state and in the light-adapted state	Unitless
F' or F^r	Any point between F_o' and F_m' under light-adapted state	Unitless
F_v/F_m	Maximum quantum yield of fluorescence of charge separation at PSII in the dark-adapted state	Unitless
F_q'	$F_m' - F'$ (fluorescence quenched by photochemistry) in the light-adapted state	Unitless
ϕ_f	Quantum yield of fluorescence in the dark acclimated state	Mol emitted photon (Mol absorbed photon^{-1})
ϕ'_f	Quantum yield of fluorescence not in the dark acclimated state	Mol emitted photon (Mol absorbed photon^{-1})
ϕ_{Fo}	Minimum quantum yield of fluorescence when only the absorption of photosynthetic pigments in PSII is considered	Mol emitted photon (Mol absorbed photon^{-1})
ϕ_{Fm}	Minimum quantum yield of fluorescence when only the absorption of photosynthetic pigments in PSII is considered	Mol emitted photon (Mol absorbed photon^{-1})
ϕ_{PO}^{max}	Maximum quantum yield for energy conservation in RC2	Mol photons used for charge separation (mol absorbed photon)$^{-1}$
FLC or PE	Fluorescence light curve or Photosynthetic vs Energy curve	ø

E_k	Light saturation parameter obtained from the FLC curve	µmol m^{-2} s^{-1}
P_{max}	Maximum photosynthetic rate	µmol m^{-2} s^{-1}
E	Scalar or Photon irradiance	µmol m^{-2} s^{-1}
EST	Irradiance provided to the sample by the LEDs during a ST pulse.	µmol m^{-2} s^{-1}
τ or τ'	Electron transport rates downstream of charge separation in PSII in the dark-adapted state and in the light-regulated state	s
σ_{PII} or σ_{PII}'	Absorption cross-section of PSII in the dark-adapted state and in the light-adapted state	nm^2 $PSII^{-1}$
alpha$_{PII}$	Initial rate at which photons are used to drive PSII photochemistry during a ST pulse	photon $PSII^{-1}$ μs^{-1}
J_{PII} or ETR	Photon flux through σ_{PII} provided by a single PSII complex. Interpreted as electron transport rate if each proton used to drive PSII photochemistry results in the transfer of an electron out of PSII	electrons $PSII^{-1}$ s^{-1}

CHAPTER 1: INTRODUCTION

1. Phytoplanktonic diversity

1.1. Phytoplanktonic productivity in ocean, coastal and inland ecosystems

Phytoplankton communities are as diverse as aquatic ecosystems. Phytoplanktonic diversity and productivity are directly linked to environmental conditions such as water temperature, solar insolation, turbidity, depth and size of the waterbody, nutrient availability and drainage basin properties influencing the periodicity and intensity of nutrient supply (Wetzel 2001).

The productivity of the ocean approximately equals that on land. Thus, oceans constitute an important reservoir of carbon fixation on the planet (Field et al. 1998). In marine environments, the majority of productivity is realized by phytoplankton and highly influenced by the relation between the mixed depth and the critical depth (Kirk 1994) . Productivity in coastal waters (including estuaries, marshes, reefs, mangroves, bays, lagoons) is generally high, according to Mann (1982, 2009). These areas receive nutrients from nearby land, largely from rivers (Mann 1982), and experience substantial nutrient regeneration as convective mixing is more efficient in shallow coastal waters. Moreover, coastal waters see nutrient replenishment from water movement (upwelling), enhancing productivity in these ecosystems (Mann 1982). Even if inland waters bodies (ponds, rivers, reservoirs and lakes) represent less than 1% of the Earth's surface, these include some of the most productive aquatic ecosystems (Likens 1975). Lake productivity is realised by phytoplankton, macrophytes and the periphyton and the contribution of these groups of primary producers is highly variable (Likens 1975). The relative contribution of phytoplanktonic productivity seems to be higher in large and deep lakes and horizontally heterogeneous (Likens 1975; Wetzel 2001). Horizontal variations become significant in very small, very large lakes or in lakes of complex morphometry (Wetzel 2001).

1.2. Phytoplankton group diversity

Phytoplankton are composed of prokaryotic and eukaryotic organisms. Phytoplanktonic prokaryotes are represented by Cyanobacteria (including Prochlorophytes), while the eukaryotic algae constitute a heteroclite and large group of different taxa grouped in several divisions: Euglenophyta, Dinophyta, Chlorophyta, Chlorarachniophyta, Cryptophyta, Haptophyta and Heterokontophyta (Falkowski and Raven 2013). Patterns of microalgal diversity in freshwater bodies are shaped by environmental conditions, and are therefore best understood in terms of functional diversity, i.e. diverse phytoplankton species associated to different microhabitats or ecological niches, notably created by thermal stratification,

turbulence and nutrients gradients (Longhi and Beisner 2010). The functional diversity is assessed by the co-occurrence of *functional types*, determined by *functional traits.* Weithoff *(*2003*)* defines a *functional trait* as a measurable feature or property of an organism which influences functional processes as growth, sedimentation, grazing losses, nutrient acquisition, reproduction, and others. In this case, a *functional type* is represented by different *functional traits* and regroups different types of organisms or species.

Phytoplankton functional groups in freshwater ecosystems are closely linked to nutrient availability, particularly in lakes, with different species assemblages associated with oligotrophic, mesotrophic and eutrophic waters (Wetzel 2001). Additionally, phytoplankton succession is subject to spatial and seasonal differences induced by abiotic factors (light, temperature, buoyancy regulation, inorganic nutrients) and biotic factors (organic nutrients, competition and predation) (Wetzel 2001).

Reynolds (1980) described 14 associations of phytoplankton taxa in lakes and predictable succession of these assemblages, mostly driven by nutrient availability and column stability.

1.3. Ecological diversity of cyanobacteria

Cyanobacteria are found in most types of (illuminated) environment, except in low pH areas, and in different forms, a result of many ecological adaptations. Species of cyanobacteria can be found with the ability to tolerate desiccation, high salinity, high and low irradiation, high UV irradiance, osmotic stress, high and low temperatures, and absence of dissolved nitrogen sources (by fixing N_2), and they are present in some of the most extreme environments including deserts and polar areas (Whitton 1992) .

Cyanobacteria have an important role in carbon and nitrogen cycling in marine environments. In nitrogen-deplete and otherwise oligotrophic areas, N_2-fixing cyanobacteria (*Trichodesmium* and *Richelia* genera) proliferate (Whitton 1992; Whitton and Potts 2000). Picoplanktonic and nanoplanktonic cyanobacteria species are abundant in deep waters, where their pigmentation allows them to use scarce light in the presence of nutrients lacking nearer the surface (Whitton and Potts 2000).

In freshwater environments, the most common cyanobacteria are either picoplanktonic or bloom-forming species (Whitton 1992; Whitton and Potts 2000). Bloom-forming cyanobacteria species tend to be gas-vacuolate and colonial species able to accumulate at or near the water surface (Whitton and Potts 2000). Picocyanobacteria are the major non-bloom forming group

in lakes and these are ubiquitous across lakes of all trophic states (Whitton 1992; Whitton and Potts 2000).

1.4. The photosynthetic apparatus

In eukaryotic phototrophs, photosynthesis takes place in the thylakoid membrane of the chloroplast, a plastid being a sub compartment of the cytoplasm (Staehelin 1986). Prokaryotic photosynthetic organisms (Cyanobacteria and Prochlorophytes) do not possess chloroplasts. Instead, thylakoids are constituted of lamellae adjacent to the periplasmic membrane (Falkowski and Raven 2013, Bryant 1995).

In Prochlorophytes, thylakoids are organised in pairs but in cyanobacteria single forms of thylakoids are found. In phytoplanktonic eukaryotic organisms, the organisation of thylakoids is also varied: in chlorophyta, the photosynthetic apparatus is organised in chloroplasts, enveloped by two membranes in the cytoplasm and thylakoids are found in stacks of three or even more. In some cases, chloroplasts are enveloped by three membranes and thylakoids are found in stacks (Euglenophyta and Dinophyta). In other cases, chloroplasts are enveloped by four membranes and thylakoids organised either in pairs (Cryptophyta) or in stacks of three or more (Heterokontophyta, Haptophyta and Chlorarachniophyta).

1.5. Pigment composition

Taxonomic diversity is closely tied to the pigment composition of the photosynthetic apparatus (Jeffrey, Vesk, and Mantoura 1997). In addition to the main photosynthetic pigment chlorophyll-*a* (Chla), present in all algae and cyanobacteria, accessory photoprotective pigments and light-harvesting pigments are present in each photosynthetic unit (Babin 2008). Photoprotective pigments (or non-photosynthetic pigments) do not transfer the energy they absorb to the photosynthetic apparatus (Bidigare et al. 1997, Babin 2008, Ficek et al. 2000). The light-harvesting pigments or photosynthetic pigments do contribute to photosynthesis and include the chlorophylls (chl *b*, chl *c*, chl *d,* chl *f* and divinyls), carotenoids (carotenes and xanthophylls) and phycobilipigments (or phycobiliproteins) (Johnsen and Sakshaug 2007).

Chlb is found in prochlorophytes, chlorophytes, euglenophytes and chlorarachniophytes (Falkowski and Raven 2013). Chl*c,* co-occurring with Chl*a* and carotenoids, is found in chromophytes (Haptophyta, Cryptophyta and Heterokontophyta) and dinoflagellates (Zapata, Garrido, and Jeffrey 2006, Falkowski and Raven 2013). Divinyl chlorophylls (d-Chla and d-Chl b) are modified forms of respectively Chla and b and are found in prochlorophytes (Falkowski and Raven 2013, Wright and Jeffrey 2006). Chld is a rare form of chlorophyll which has been found by Manning and Strain (1943) only in the cyanobacterium *Acaryochloris marina* (Larkum and Kühl 2005). Chld is not only a light-harvesting pigment but also (almost) replaces Chla in the photochemical reactions (Hu et al. 1998, Chen and Blankenship 2011). Chlf *is* the last chlorophyll discovered, found in stromatolites, and isolated from a cyanobacterium (Chen and Blankenship 2011, Chen et al. 2010) as an accessory pigment (approximately 10-15% total chlorophylls).

Carotenoids (carotenes and xanthophylls) include light-harvesting pigments and photoprotective pigments. Although the main role of xanthophylls is photoprotection (Demmig-Adams 1990), some transmit energy to Chl*a*, like fucoxanthin, peridin and violaxanthin (Falkowski and Raven 2013). Xanthophylls are involved in the *non-photochemical quenching* process described later (Huot and Babin 2010). Some carotenoids, such as echinenone, 4-ketomyxol 2'-fucoside and myxol 2'fucoside, are uniquely found in certain species of cyanobacteria and are not found in others phytoplanktonic organisms (Gault and Marler 2009).

Phycobiliproteins, which are found in Cyanobacteria (Prochlorophytes excepted), Cryptophyta and Rhodophyta (red algae), are principally light-harvesting pigments. Moreover, phycobilins and especially phycocyanin pigment can also play a role as nitrogen reserve (Allen 1984, Kromkamp 1987).

Phycobiliproteins consist of four main pigment groups: phycoerythrin, phycocyanin, allophycocyanin and phycoerythrocyanin. In the case of phycoerythrin and phycocyanin, several forms are described in literature: C-Phycoerythrin/R-Phycoerythrin and C-Phycocyanin/R-Phycocyanin. C-Phycocyanin and C-Phycoerythrin refer to the form originally found in Cyanobacteria and R-Phycocyanin/R-Phycoerythrin to the form of phycobiliproteins found in red algae. It has since been established that phycobilipigments are comprised of pairs of four possible subunits or phycobilins: phycocyanobilin, phycoerythrobilin, phycoviolobilin, also known as cryptoviolin, and phycourobilin (O'Carra, Murphy, and Killilea 1980, Falkowski and Raven 2013), and therefore multiple forms of each pigment are possible and found across

taxa. In the photosynthetic apparatus, pigments are bound by proteins (apoproteins) and form pigment-protein complexes (Johnsen and Sakshaug 2007).

The specific molecular structure of pigments results in distinct absorption and (sometimes) fluorescence properties. Absorption spectra of individual pigments are presented in Figures 1 A. Non-photosynthetic and photosynthetic carotenoids have maximum absorption *in vivo* in the 400-600 nm range of the light spectrum. Chla in vivo absorption maxima are found for wavelengths of approximately 440 and 675 nm, corresponding to the absorption maxima by PSII Chla. Chl*c*, Chlb, d-Chlb and d-Chla, in sequence, have absorption maxima around 450-490 nm. Phycobiliproteins, on the other hand, absorb more efficiently in the 450-700 nm spectral range, with peaks of phycoerythrin (≈490 and ≈570 nm), phycocyanin (≈620 nm) and allophycocyanin (≈650 nm) with increasing wavelength. This complementary arrangement of absorption peaks is illustrative of the energy transfer between these pigments, discussed further below (Gantt 1975). Generally speaking, phycobilipigments have absorption maxima in the wavelength range 500-650 nm and are a typical indication of the presence of cyanobacteria, as observed in Figure 1B in *Anabaena cylindrica* at wavebands ranging from 550 to 650 nm. In comparison, in figure 1B, *Chlorella sp.* does not show high absorption in wavebands 550-650 nm.

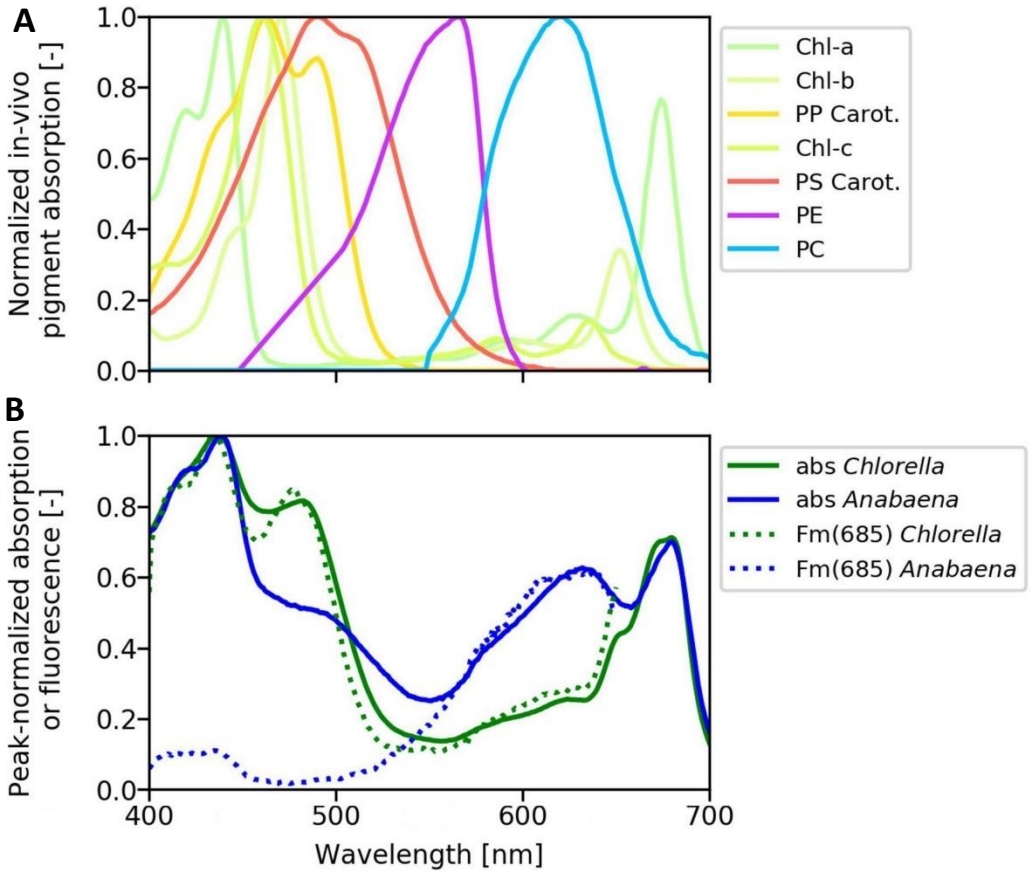

Figure 1. Absorption spectra of *in-vivo* pigments and absorption spectra as well as $F_m(685)$ excitation spectra of one algal species (*Chlorella sp.*) and one cyanobacteria species (*Anabaena cylindrica)*. A: *In-vivo* pigment-specific absorption spectra normalized to their maximum value. Abbreviations: Chl, chlorophyll (a/b/c); PS Carot., photosynthetic carotenoids; PP Carot., photoprotective carotenoids (Bidigare et al. 1990); PE, phycoerythrin; and PC, phycocyanin (including allophycocyanin; Simis and Kauko (2012)). B: Pigment absorption (solid lines) and $F_m(685)$ fluorescence excitation spectra (dashed lines) of *Chlorella sp.* (green) and *Anabaena cylindrica* (blue). This figure was adapted from Schuback et al. (2021), under Creative Common License.

Interactions between the absorption spectra of individual pigments alter the optical behaviour of the cell as a whole. Shading, fluorescence and re-absorption contribute to a relatively complex absorption envelope. The cellular pigment concentration is directly linked to environmental conditions and photoacclimation. For example, absorption differences between two phytoplankton species (*Emiliana huxleyi* and *Synechococcus sp.*) under different light conditions (low light to high light) shows that light conditions influence pigment composition and, conversely, the magnitude and shape of absorption spectra (Organelli et al. 2017).

Nutrient concentrations can also influence absorption properties. Under light-limited growth, increased pigment production may be observed. Increased cellular nutrient concentration leads to the pigment *package effect*, decreasing the bulk light harvesting efficiency of

photosynthetic pigments (Kirk 1994) and consequently decreasing mass-specific absorption coefficients and dampening of absorption spectra.

Spectral groups of phytoplanktonic organisms have been defined by several authors according to their pigment contents and corresponding optical properties. For example Hunter et al. (2008) discriminate four "colour groups" : blue-green, green, brown and red algae differentiated by their optical properties, which directly translates into their potential separation using optical detection methods.

2. Photosynthetic electron transport, structure of light harvesting systems and energy transfer

2.1. Photosynthetic electron transport

The photosynthetic apparatus is composed of several photosynthetic units. The concept of a *photosynthetic unit*, composed of chlorophyll molecules, has been proposed by Emerson and Arnold (1932) and developed later by Arnold and Kohn (1934) and Gaffron and Wohl (1936). The latter described a photosynthetic unit as "the mechanism which must undergo the photochemical reaction to produce one molecule of oxygen or reduce one molecule of carbon dioxide". Emerson and Arnold (1932) tried to determine the "size" of each unit at approximately 2500 molecules per molecule of CO_2 or O_2. This "Emerson-Arnold number" has been derived from their experiments and is still widely used for the determination of the "size" of the photosynthetic unit in algae.

One photosynthetic unit is composed of two photosystems, PSI and PSII. A photosystem constitutes a reaction centre and a pigment antenna. The main role of PSII is to oxidize water, in order to drive the complete electron transport chain, while the main aim of PSI is to reduce NADP to NADPH, needed for the Calvin Cycle (Mimuro 2004), which is the photosynthetic carbon reduction cycle transforming inorganic carbon (CO_2) into carbohydrate. The reaction centres related to each photosystem are referred to as RC1 and RC2, respectively, and are where charge separation takes place. Pigment antennae collect photons and transmit derived energy (individual units called *excitons*) to the reaction centre. The pigment composition of the antennae is different between the two photosystems and also specific to phytoplankton taxonomic groups (Falkowski and Raven 2013). This difference will be discussed later, with specific focus on the cyanobacteria antenna pigment composition.

The main role of the photosynthetic electron transport chain is to transform energy derived from absorption of light (photons) into chemical energy. Photochemistry conforms to two

main laws: the *Grotthuss-Draper law* and the *Stark-Einstein law*. The first law stipulates that only absorbed light can promote chemical reactions and the second law stipulates that one quantum of light absorbed (photon) can influence only one molecule (Falkowski and Raven 2013). The transport of electrons follows from the oxidation of water along the light-harvesting pigment complex (LHC), and through PSI and PSII (Figure 2A). The photosynthetic electron transport chain and molecular structure on thylakoids is specific in cyanobacteria (Figure 2B).

A photochemical reaction is thus directly linked to two charge separations, described below on the photosynthetic electron transport chain, occurring in the two photosystems. Moreover, the photochemical reaction necessitates two photoreactions in series for the assimilation of the inorganic carbon. Oxidation of two water molecules requires four electrons (Eq.1. below), so with two reactions centres working in series, a minimum of eight photons s are necessary to produce a molecule of dioxygen (O_2), (Krall and Edwards 1992):

$$2H_2O + light \rightarrow O_2 + 4H^+ + 4e^- \qquad (1)$$

Electrons produced by the oxidation of water (Eq. 1) are transmitted to four atoms of manganese (Mn) and further to the amino acid tyrosine (Yz). The oxidation of the primary electron donor in PSII (P680) forms the reduced P680* and provides a high charge separation of 1.7 V induced by the light energy (Figure 2A). This light energy, as described above, originates from the pigment antennae of PSII. Then, the phaeophytin anion reduces the primary acceptor in PSII, the quinone Qa, and the latter transmits two electrons to the second acceptor of PSII, the quinone Qb. Between PSII and the cytochrome b_6/f complex, a plastoquinone pool occurs.

The cytochrome transfers, in turn, electrons to the protein plastocyanin (PLC) which transfers them to P700. Another photon caught and brought to PSI reaches P700 and enables another charge separation of 1.6 V. An electron is then transmitted through different electron carriers: A_0, a chlorophyll monomer, A_1, phylloquinone, F_X, an iron sulfur cluster, F_A and/or F_b, iron-containing proteins and F_d, a molecule of ferredoxin. Finally, the electron is transmitted to the NADP oxidoreductase, which reduces NADP to $NADPH_2$. Once produced, $NADPH_2$ is used for the fixation of inorganic carbon in dark reactions or to sustain metabolic activity of the cell (e.g., Mehler reaction, photorespiration, nitrogen reductions)

Ultimately, eight electrons are required for the fixation of one carbon. Two molecules of $NADPH_2$ are required for each carbon fixation, two electrons are required for the reduction of

each molecule of NADP (Huot and Babin 2010) and as mentioned above, reactions centres of each photosystem work in series.

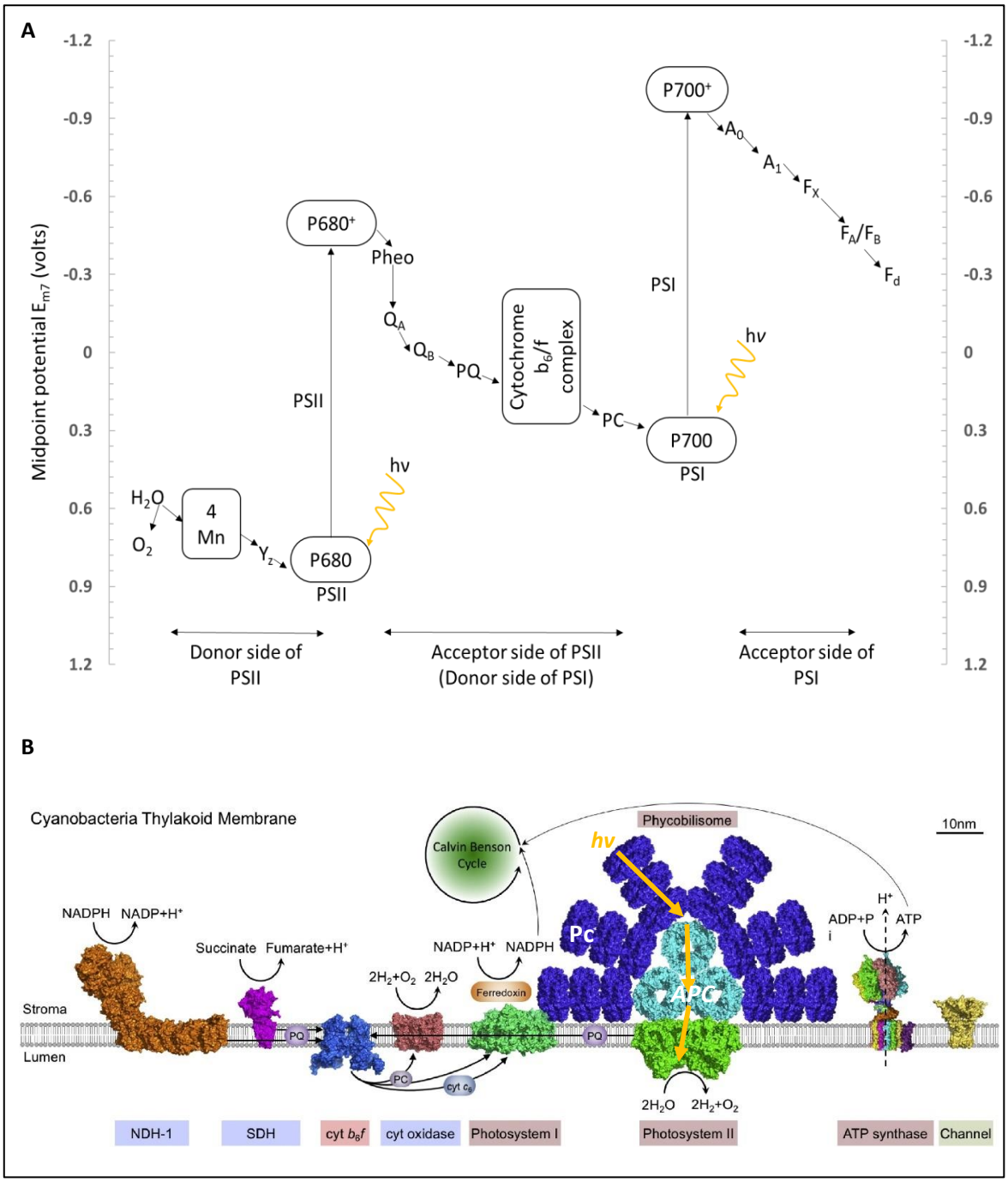

Figure 2. A: Photosynthetic electron transport chain represented in a "Z-diagram". Abbreviations Mn: Manganese atoms, Y_z: amino acid tyrosine, P680: primary electron donor in PSII, P680*: reduced form of P680, Phaeo: phaeophytin anion, Q_A: quinone secondary electron acceptor of PSII, Q_B: plastoquinone molecule bound to PSII, PQ: Plastoquinone pool, PC: Plastocyanin, P700: reaction center of PSI, P700*: reduced form of P700, F_X: ferredoxin, , A_0: chlorophyll monomer, A_1: phylloquinone, F_X: iron sulfur cluster, F_A/F_B: iron-containing proteins, F_d: Ferredoxin, PSI: Photosystem I, PSII: Photosystem II, ,. *hv* represents the photon. P680, P680* and P700 are named in relation to their absorption maximum, respectively obtained for the wavelength 680 nm and for the wavelength 700 nm. B: Photosynthetic and respiratory electron transport component in the cyanobacterial thylakoid membrane (based on

knowledge of *Synechocystis* 6803 thylakoids) and structure of the *hemidiscoidal* phycobilisome (PBS). The PBS is in "state 1" (see Section 2.2). Photosynthetic electron transfer complexes include phycobilisome, Pc, APC, PSII and PSI, cyt b_6f and ATPase and respiratory electron transport chain complexes are NDH-1, SDH and cyt oxidase. Cyt b_6f, PQ and PC are shared by both electron transport pathways. There are also potassium channel proteins in the thylakoid membrane indicated by the tag "channel". Black arrows indicate the electron transduction reactions. The pathway of the excitation energy (*exciton*), collected by the light-harvesting antenna, is represented by yellow arrows. *hv* represents the photon. Abbreviations: ADP: adenosine diphosphate, APC: allophycocyanin, ATP: adenosine triphosphate, cyt b_6f : cytochrome b_6f, cyt c_6: cytochrome c_6, cyt oxidase: cytochrome oxidase, NADP(H): nicotinamide-adenine dinucleotide phosphate (reduced form), NDH-1: type 1 NADPH dehydrogenase, Pc: phycocyanin, PC: plastocyanin, PQ: plastoquinone, SDH: succinate dehydrogenase. The protein structures are achieved from PDB database: allophycocyanin, PDB ID: 1KN1; NDH-1, based on the Complex I structure from *Thermus thermophilus*, PDB ID: 4HEA; cyt b_6f, PDB ID: 4H13; cyt oxidase, PDB ID: 1OCO; potassium channel protein, based on the *Magnetospirillum magnetotacticum* KirBac3.1 potassium channel crystal structure, PDB ID: 1XL4; phycocyanin, PDB ID: 3O18; PSI, PDB ID: 1JB0; PSII, PDB ID: 3WU2; and SDH, based on the *E. coli* SDH crystal structures, PDB ID: 1NEK. Figure A has been recreated and adapted from Falkowski and Raven (2013) and figure B was adapted from Liu (2016), under Creative Common License. Phycobilipigments specifications in *Synechocystis* 6803 are based on Elmorjani, Thomas, and Sebban (1986) study.

2.2. The cyanobacterial phycobilisome

In cyanobacteria and rhodophytes, the LHC is called the *phycobilisome* (Allen 1984). A LHC is a protein-pigment complex directly linked to the reaction centre (RC). The phycobilisome (PBS) is a hydrophilic macromolecule composed of phycobilipigments and situated on the stromal side of the thylakoid membrane (Bryant et al. 1979; Falkowski and Raven 2013). In comparison, in microalgae and plants, light harvesting complexes are internal and not attached to the thylakoid membrane (Whitton and Potts 2000). The phycobilisome is also composed of linker proteins, mostly non-pigmented, which have a functional and structural organisation role (Falkowski and Raven 2013, Sidler 1994). For example, these proteins serve to attach rods to the core or also to attach the core to the surface of the thylakoid membrane (Bryant 1995).

The phycobilisome is composed of a core directly linked to the reaction centre and bounded by rods, producing generally a "hemidiscoidal" structure. Nevertheless, other, less common, morphological types of PBS have been described: these are "hemiellipsoidal", "bundle-shaped" and "block-shaped" structures (Bryant 1995). The core possesses a triangular structure comprised of three stacks and mainly constituted of allophycocyanin (Bryant et al. 1979), associated with core linker polypeptides (Gault and Marler 2009). Usually, the core is surrounded by six rods in cyanobacteria. Each rod is composed of disks of 6 nm in thickness and 11 nm in diameter and the number of disk on rods depends on the organism and also on environmental conditions (light and nutrient availability). The length of the rod varies between 12 and 36 nm (Bryant 1995). While the core of the phycobilisome mostly contains

allophycocyanin (APC) trimers (A_{max} at 650 nm), rods can be composed of hexamers of phycocyanin (PC) (A_{max} at 620 nm), phycoerythrin (PE) (A_{max} at 565 nm) and phycoerythrocyanin (PEC) (A_{max} at 570 nm) (Whitton and Potts 2000). It is possible for the rods to contain only PC, both PC and PE or, more rarely, PC and PEC, but PC is always present. Rod composition in phycobiliproteins varies between species and with environmental conditions. Certain species of cyanobacteria use complementary chromatic adaptation (CCA); they can change their PBS composition in phycobiliproteins under different light conditions (e.g. red vs green light), offering a mechanism to optimize the efficiency of light absorption and thus their growth or competition for light (Campbell 1996, Whitton and Potts 2000, Gault and Marler 2009). One PBS is linked to two PSII reaction centres (Falkowski and Raven 2013). Nevertheless, the PBS can, under certain environmental conditions (low or suboptimal temperature, saturating light conditions), be attached to PSI, moving on thylakoid membranes and transmitting energy directly to PSI (Gault and Marler 2009). This process, describing PBS movements between each RC, is called a *state transition*. When the PBS is linked to PSII, the PBS is in "state 1" and when the PBS is attached to PSI, the PBS is in "state 2" (Mackey et al. 2013). State transitions are reversible, e.g. by dark-acclimating cells as these will, over time, return to state 1. Figure 2B represents a *hemidiscoidal* PBS in "state 1" whose rods are composed of PC.

2.3. Light harvesting process

Energy collected by the light-harvesting antenna is transmitted by pigments to Chla in each photosystem. Moreover, two forms of energy transfer exist in a photosynthetic unit: homogenous and heterogeneous energy transfer, indicating transfer between identical or different pigments, respectively (Rabinowitch and Govindgee 1969). Homogenous energy transfer is realised, for example, between two molecules of Chla in the same photosynthetic unit. Transfer along the antenna of each photosynthetic unit, between light-harvesting pigments, is an example of heterogeneous transfer, also called *resonance energy transfer* and sometimes "Förster transfer" (Förster 1960, 1948). This is possible if the emission (fluorescence) band of the donor pigment overlaps with the absorption band of the acceptor pigment, and while the distance between donor and acceptor pigments is small, and both donor and acceptor oscillators have approximately the same frequencies (Förster 1960). During each transfer, a fraction of energy is lost in the form of heat and the amount of energy ultimately arriving at Chla in the RC is therefore less than that collected by the original light-harvesting pigment (Figure 3).

2.4. Energy transfer in cyanobacteria

The energy transfer along the light-harvesting antenna in cyanobacteria depends on pigments present in the PBS and this transfer is most markedly different between 'red' and 'blue' cyanobacteria. Parésys et al. (2005) define red cyanobacteria as cyanobacteria containing (a variable amount) of PE in addition to at least one PC per rod, while blue cyanobacteria do not contain PE (Figure 3). Moreover, according to Falkowski and Raven (2013), freshwater red cyanobacterial species contain phycoerythrobilin at the distal ends of the rods whereas marine species contain phycourobilin. Exceptions also occur, with some marine species having a PE complex formed of both phycoerythrobilin and phycourobilin subunits (Stadnichuk, Romanova, and Selyakh 1985, Swanson et al. 1991).

In cyanobacteria and red algae, energy transfer in the phycobilisome is particularly rapid and efficient (>99%, Porter et al. (1978)) and most of the energy is transferred to PSII. In cyanobacteria, most Chla (> 80%) is contained by PSI, rather than by PSII (Mimuro and Fujita 1977).

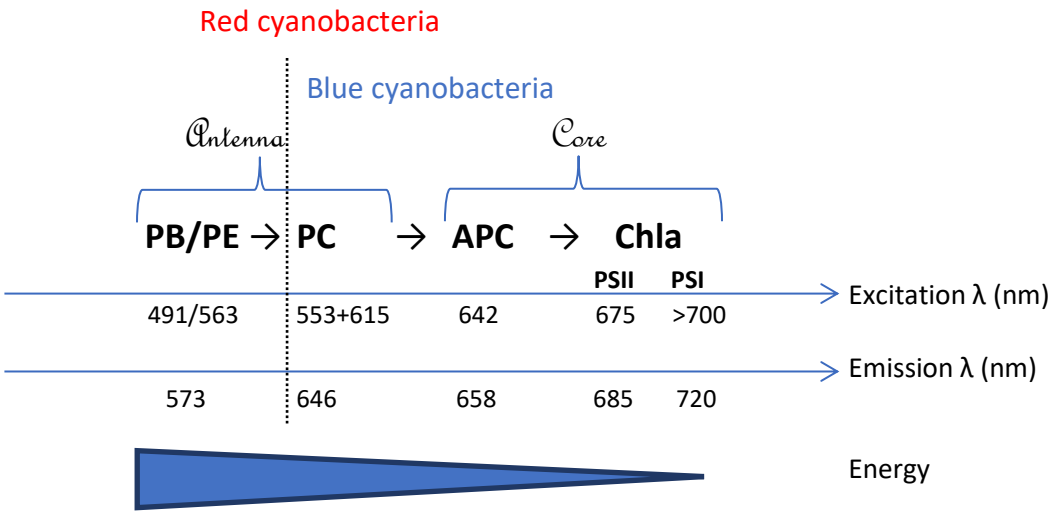

Figure 3. Schema of the energy transfer in cyanobacteria (red and blue types) in a photosystem (PSI or PSII). Peak excitation and emission wavelengths for each pigment group are also represented (PB = Phycourobilin, PE = Phycoerythrin, PC= Phycocyanin, APC = Allophycocyanin, Chla = Chlorophyll a), λ = wavelength. The energy being transferred along the light harvesting antenna is also represented by the blue gradient. Based on a model of the marine cyanobacterium Synechococcus WH8103 (Falkowski and Raven 2013).

2.5. Principles of fluorescence

Once absorbed, the energy of a photon has several possible futures: energy can be dissipated as heat, used for charge separation (photochemistry) or fluoresce (Huot and Babin 2010). In the visible part of the spectrum, a photon has sufficient energy once absorbed, to transition from one electronic state to another (Kirk 1994). The transition from the first state to the ground state can produce a photon of lower energy (longer wavelength λ) (Babin 2008). This photon emission following absorption is called *fluorescence*.

The quantum yield of fluorescence (ϕ_f) is the fraction of absorbed photons re-emitted as fluorescence among the other pathways for absorbed energy, expressed as (Falkowski and Raven 2013):

$$\phi_f = \frac{k_f}{\left(k_f + k_d + k_p\right)} \qquad (2)$$

where k_f, k_d and k_p are the rate constants of respectively fluorescence, thermal dissipation, and photochemistry (charge separation).

A more elaborate way to express the probability of fluorescence is to take into consideration the state of the reaction centre (opened/closed) as well as the dissipation of energy associated with the light acclimated state ("energy dependant quenching"), both related to *in vivo* conditions. This can be expressed as (Huot and Babin 2010):

$$\phi'_f = R_o \frac{k_f}{\left(k_f + k_d + k_p + k_{qe}\right)} + R_c \frac{k_f}{\left(k_f + k_d + k_{qe}\right)} \qquad (3)$$

where R_o and R_c represent, respectively, the fraction of the reaction centres in the opened and the closed state ($R_o + R_c = 1$) and k_{qe} is the rate constant of the dissipation of energy associated with the light acclimated state. In Eq. 3 the quantum yield of fluorescence is noted ϕ'_f instead of ϕ_f because the yield is not limited to the dark acclimated state while k_{qe} can be 0.

In vivo, cells (and reaction centres) can be damaged by an excess of light. Including this process in a third term results in Huot and Babin (2010):

$$\phi'_f = R_o \frac{k_f}{\left(k_f + k_d + k_p + k_{qe}\right)} + R_c \frac{k_f}{\left(k_f + k_d + k_{qe}\right)} + R_{dam} \frac{k_f}{\left(k_f + k_d + k_{qe} + k_1\right)} \qquad (4)$$

where R_{dam} is the fraction of damaged reaction centres (so that $R_o + R_c + R_{dam} = 1$) and k_1 is an additional rate constant corresponding to the dissipation of energy at damaged reaction centres.

3. Methods to quantify photosynthesis

Photosynthesis can be quantified using gross photosynthesis or its equivalent gross primary production (GPP), net photosynthesis and net primary production (NPP). GPP is defined as a rate of electron flow, dependant of light, from water to electron acceptors which leads to photosynthetic carbon fixation during that time interval (Wetzel 2001, Falkowski and Raven 2013). GPP doesn't include respiratory losses, which are defined by all metabolic processes which lead to the oxidation of CO_2 and the production of O_2 (Falkowski and Raven 2013). Net photosynthesis is calculated as the difference between GPP and the respiratory losses in the light (Kirk 1994). NPP is further defined as the difference between net photosynthesis and the respiration of photoautotrophs in the dark (by night) (Falkowski and Raven 2013).

3.1. The ^{14}C method (radiocarbon method)

The radiocarbon method has long been the benchmark method to quantify photosynthesis in natural phytoplanktonic communities (Falkowski and Raven 2013). This method was developed by Einar Steemann Nielsen and is based on the use of the isotope ^{14}C as a tracer in the photosynthetic reaction (Nielsen 1952). The uptake of carbon in the photosynthetic reaction is given as:

$$H_2O + CO_2 + energy\ (light) \rightarrow CH_2O + O_2 \qquad (5)$$

The rate of assimilation of radioactive inorganic carbon ($^{14}CO_2$) into organic carbon is proportional to the rate of assimilation of non-radioactive inorganic carbon ($^{12}CO_2$) (Falkowski and Raven 2013). Radioactivity (β^- radiation) is measured with a liquid scintillation counter (Falkowski and Raven 2013).

There are limits in using this method. One such limit is the "bottle effect", largely due to the need to use small volumes of measurement. Measurements in sealed bottles also imply a non-consideration of irradiance changes that normally occur in natural environment. *In situ* bottle incubations are a solution to achieving natural changes of light conditions (Bower et al. 1987), but are logistically challenging.

3.2. The ^{18}O method

This method is based on the utilisation of the stable isotope ^{18}O as a tracer. $H_2{}^{18}O$ (water labelled with ^{18}O) is added to the sample, on which we want to measure photosynthetic rate. The O_2 labelled with the stable isotope produced during photosynthesis is measured (Bender and Laub 1987). This method measures GPP as the major oxygen isotope is ^{16}O and only a negligible amount will be consumed by respiration (Bender and Laub 1987). The isotope abundance is measured with a mass spectrometer, which due to its cost makes the method neither common nor convenient to measure GPP (Falkowski and Raven 2013). Another disadvantage in using this method, is the fact that the labelled oxygen produced can be recycled in the cell, reducing the rate of observed oxygen evolution (Bender and Laub 1987).

3.3. Fluorescence methods to determine phytoplankton physiology

3.3.1. Measurement principles

The basic configuration of a fluorometer consists of the illumination of a sample in one direction and detection of the fluorescence emission in the perpendicular plane. An example of a benchtop spectrofluorometer, used to control the wavelength of excitation light and quantify the spectral emission using a pair of monochromators, is shown in Figure 4. To account for variation in the light source, a reference detector is used to normalize the fluorescence signal. This configuration is typically used to collect excitation spectra and emission spectra, or an excitation-emission matrix by looping over both properties.

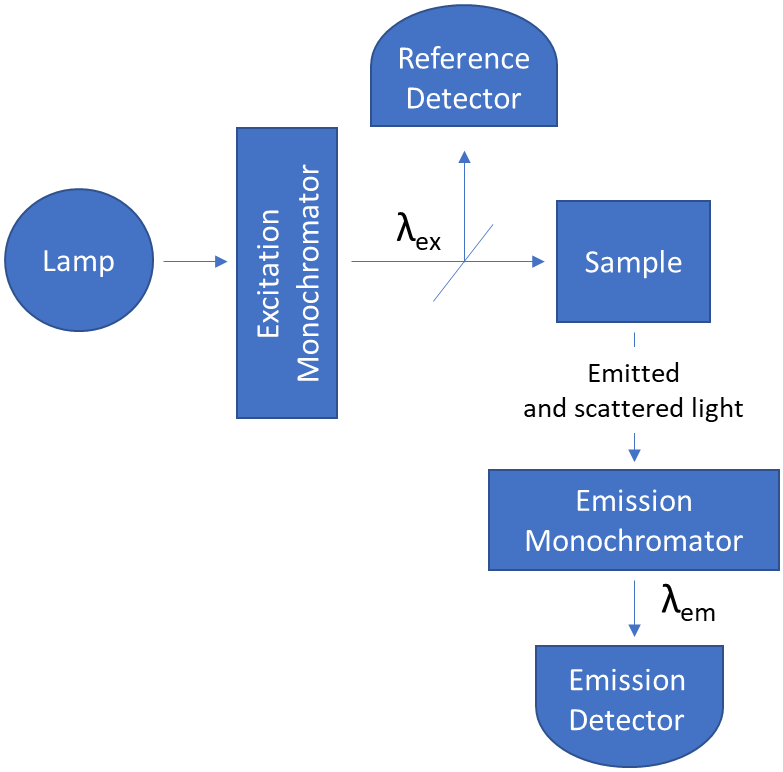

Figure 4. Optical set-up of a benchtop spectrofluorometer. This figure is recreated from Huot and Babin (2010). λ_{ex} and λ_{em} represent respectively the excitation waveband and the emission waveband.

The use of fluorescence to quantify photosynthesis focusses on determining one or more of the rate constants of energy transfer, upstream from the fixation of carbon or evolution of oxygen. Two techniques have been widely applied: passive and active fluorescence methods (Kolber and Falkowski 1992). Passive fluorescence methods use solar-stimulated fluorescence to quantify the rate of photosynthesis (Chamberlin et al. 1990), and are not discussed here. Active fluorescence methods use an artificial light source to generate a fluorescence signal. The focus here is on instruments designed to resolve the rate constants of energy transfer by manipulating, in one way or other, the light dosage to saturating irradiance, while polling the fluorescence response in time. There also exist a wide range of 'fluoroprobes,' simpler in design, which record the time-integrated fluorescence response from a non-saturating light pulse, often used as a first estimate of group-specific biomass following a calibration of the fluorescence yield to pigment extracts. These instruments cannot be used to determine productivity. Instruments in the fluoroprobe category are based on the principle that fluorescence is proportional to Chla concentration while photosynthetically available radiation (PAR) is constant, and if the product of the quantum yield of *in vivo* fluorescence (φf), the Chla-specific spectrally averaged absorption coefficient of phytoplankton weighted by their radiance spectrum ($\tilde{a}^*$), and the fluorescence intracellular reabsorption factor ($Qa*$), may be considered constant (Babin, 2008). However, $\varphi f^{-} a*Qa*$ is not constant but varies under

different environmental conditions and biological conditions, such that frequent calibration of the signal is needed.

Among active fluorescence instruments designed to estimate productivity, two types exist: those that deliver saturating light intensity within the time needed to complete a single turnover (ST) of the RCs, and those that achieve this over a period which is likely to include multiple turnovers (MT). In both cases, the fluorescence transient from a state where a fraction of reaction centres are opened, to where all reaction centres are closed, forms the basis of fitting models of energy transfer to determine phytoplankton physiology. Saturation of RC with ST rather than MT implies more costly electronics which explains why MT instruments are generally less expensive than ST instruments . Both categories of instruments have portable options, and some have been designed to resolve the activity of distinct pigment groups by using several excitation wavebands in sequence. All instruments are also able to record the Photosynthesis vs Energy (PE) curve which is the measurement of photosynthetic rate as a function of irradiance (Kirk, 1994). The most full-featured instruments contain multiple excitation light sources (and/or filters), emission wavebands, and the potential to measure excitation spectra though careful calibration of the light source(s) and optics.

3.3.2. Determining the rate constants

The principle of ST and MT fluorometers for productivity estimates is to measure the quantum yield of fluorescence (ϕ_f) and variable fluorescence (F_v) derived from the minimum fluorescence F_o, obtained in a dark-adapted state, and the maximum fluorescence obtained after closure of all reaction centres, F_m (Babin 2008). F_v is the difference between these two states, also termed variable fluorescence. The parameter F_v/F_m corresponds to the maximum quantum yield of fluorescence of charge separation at PSII.

In the same way that the quantum yield of fluorescence (ϕ_f) can be modelled, the efficiency of photochemistry can also be determined and linked to F_m, F_o and F_v. First, the maximum (ϕ_{Fm}) and the minimum (ϕ_{Fo}) quantum yield of fluorescence, in the case of the dark acclimated state (k_{qe}=0) and undamaged reaction centres (R_{dam} = 0), can be determined according to Eq. 3 and presented below:

$$\phi_{Fo} = \frac{k_f}{\left(k_f + k_d + k_p\right)} \qquad (6)$$

$$\phi_{Fm} = \frac{k_f}{(k_f + k_d)} \qquad (7)$$

In the case of $\phi_{Fo,}$ in Eq. 3, R_o equals 1 and R_c equals 0, while in the case of $\phi_{Fm,}$ R_o equals 0 and R_c equals 1.

F_v/F_m and the maximum quantum yield for energy conservation in RC2 (ϕ_{PO}^{max}) can now be derived from Eqs. 6-7:

$$\frac{F_v}{F_m} = \frac{\phi_{Fm} - \phi_{Fo}}{\phi_{Fm}} = \frac{k_p}{(k_f + k_d + k_p)} = \phi_{PO}^{max} \qquad (8)$$

The maximum quantum yield for energy conservation in RC2 (ϕ_{PO}^{max}) indicates the efficiency of photochemistry and photosynthetic processes at PSII and ultimately the phytoplankton physiology.

Closure of all RCs from a dark-acclimated state allows both F_m and F_o to be fitted. Gradual closure during exposure to saturating irradiance allows F_m and F_o to be fitted more accurately by extrapolation of the induction curve, whilst additional photosynthetic variables can be fitted such as the absorption cross section of PSII (σ_{PSII}) and secondary parameters including the photochemical flux per PSII or electron transport rate, respectively noted JPII or ETR or post-saturation relaxation rate, an indication of NPQ (Non-Photochemical Quenching) (Schuback *et al.,* 2021). An example of induction curve is shown in Figure 5, showing the parameters F_o, F_m, F_v and σ_{PSII} in the dark-adapted state. Full closure of RCs can also be achieved by chemical treatment. A widely used method is the addition of DCMU (3-(3, 4-dichlorophenyl)-1, 1-dimethylurea), an herbicide which acts as photo-inhibitor in *ex situ* measurements. The first uses of DCMU, in order to derive variable fluorescence, started in the 1970s and 1980s, linking the action of DCMU with the photosynthetic capacity and fluorescence characteristics of various species (Vincent 1980). DCMU prevents the re-oxidation of Q_a, and maintain all reaction centres closed (in this case, in Eq. 3, R_o= 0, R_c= 1 and k_{qe}= 0) (Huot and Babin 2010). Fluorescence is then measured before (F_o, using a low light dose) and after (F_m) the addition of the electron flow inhibitor. The action is non-reversible and relatively stable, such that traditional benchtop fluorometers (Figure 4) may be used to collect spectrally detailed excitation-emission properties of variable fluorescence.

JPII or ETR, as described earlier, corresponds to the photochemical flux per PSII or the rate of charge separation in individual photochemically active PSII. JPII is measured in aquatic measurements as a proxy of C-fixation (Hughes et al. 2018). Different models currently exist to estimate JPII but are submitted to different sources of errors. Schuback et al. (2021) determined a new way to estimate JPII, taking in account dark and light-regulated state, the calculation of the baseline fluorescence and the amplitude of ST chlorophyll fluorescence and is shown in Eq. 9 (Schuback et al. 2021).

$$J_{PII} = E \times \sigma'_{PSII} \times \left[1/\left(1 + (\sigma'_{PSII} \times E \times \tau')\right)\right] \quad (9)$$

Where E is the scalar irradiance (in photon m^{-2} s^{-1}) , σ'_{PSII} is the absorption cross-section of PSII in the light-regulated state (in nm^2 $PSII^{-1}$)) , and τ' is the electron transport rates downstream of charge separation in PSII in the light-regulated state (in seconds). In Eq. 9, 1/τ' represents the rate of re-opening RCII (Schuback et al. 2021). J_{PII} units are electrons $PSII^{-1}$ s^{-1}.

3.3.3. Photosynthesis-Energy curves

PE curves are measured in fluorometers using induction protocols and induction curves (Figure 5). An ideal PE curve is characterized by an initial linear response of the photosynthetic rate (*P*) to increasing irradiance E produced by an actinic light source, followed by a reduction in *P* up to a plateau with increasing E. P can decrease at higher intensities as a result of photoinhibition. The PE curve can be fitted to derive the maximum photosynthetic rate (P_m) which is the maximum P obtained, and E_k which is the intersection point between the initial extrapolated linear response section of PE curve and the horizontal line at P_m (Kirk, 1994). An example of PE curve is shown in Figure 6.

3.3.4. Instrumentation

Induction fluorometers designed to deliver saturating light energy use ST methods or MT methods, as previously described. MT method include the multiple turnover pulse amplitude modulation (PAM) method. The pulse amplitude modulation (PAM), introduced by Schreiber, Schliwa, and Bilger (1986) uses multiple non-actinic flashes to determine F_o followed by a long actinic multiple-turnover suturing flash of 600 ms, supported by short non-actinic flashes, from which F_m and consequently F_v are derived.

ST methods include pump-and-probe and fast repetition rate (FRRf) techniques. The pump-and-probe method was first described by Mauzerall (1976). This technique is based on the alternation between “Probe flash “and “Pump flash”. A single “Probe flash”, a non-actinic-

turnover flash, is applied to determine F_o, then follows a "Pump flash", a saturating actinic flash, and finally a last "Probe flash" is applied. The fluorescence measured after the second "Flash probe" permits to determine F_m and also the variable fluorescence (F_v). The FRRf method was first described by Kolber, Prášil, and Falkowski (1998). The FRRf method is based on a series of short (~1 µs) non-actinic single-turnover flashes, at a frequency of about 0.35 MHz (Babin 2008). The initial rise of fluorescence during this process is proportional to σ_{PSII}. The FRRf is also able to measure MT, and Kolber, Prášil, and Falkowski (1998) compared the determination of primary chlorophyll fluorescence parameters using MT and ST. Suggett et al. (2001) describe the FRRf method as a method more rapid, robust and more accurate for measurements *in situ* compared to the pump and probe method. Moreover, this method is more sensitive than the PAM method in open ocean or in low chlorophyll *a* concentration areas (Suggett et al. 2003). The main differences between FRRf and PAM methods is, however, that FRRF saturates RC2 within a single turnover period (<150 µs), which allows the functional absorption cross section of PSII to be accurately determined. The 600-ms saturation period of the PAM corresponds to multiple turnovers of the RC2, and generally leads to higher estimates of F_m. The FRRf method determines the proportion of closed RCIIs by including a relaxation protocol which consist of 40 to 80 flashlets at intervals varying exponentially from 50 µs to 50ms (Kolber, Prášil, and Falkowski, 1998). A new method based on ST, developed by Chelsea Technologies Group, the STAF method (Single Turnover Active Fluorescence) uses a dual ST pulse which is a "set" pair on ST pulse as a relaxation method (Oxborough 2021). An increasing time interval between the two pulses, ranging between 200 to 6400 µs, is applied to assess the proportion of closed RCIIs. The first instrument which apply this method is called LabSTAF and includes, in other, a high signal sensitivity for oligotrophic conditions and seven excitation wavebands to target a range of photosynthetic pigments and ultimately a range of phytoplankton types. An example of an induction curve is shown in Figure 5. This induction curve is issued from the first step of the PE curve shown in Figure 6 and corresponds to the very first acquisition in the dark (E=0 µmol m^{-2} s^{-1}).

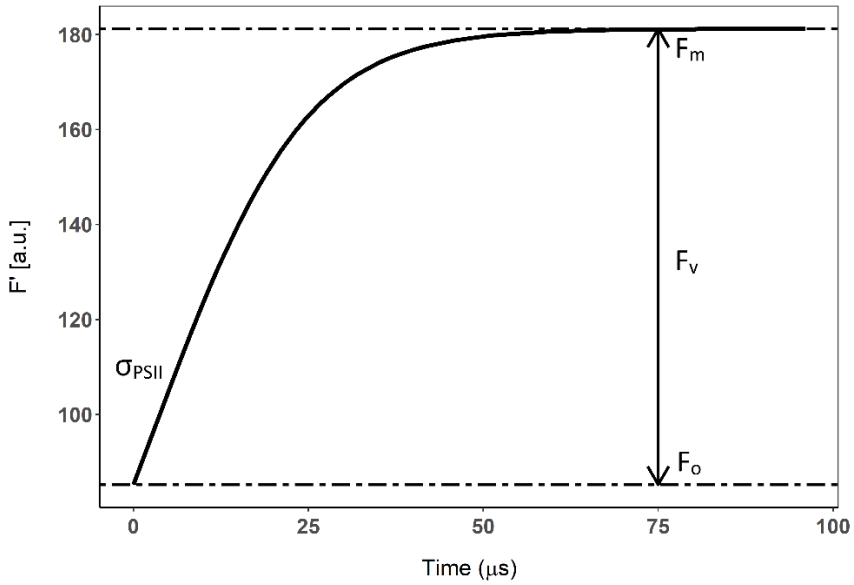

Figure 5. Induction curve generated by the LabSTAF instrument in the dark adapted state. F_o, F_m and F_v corresponds respectively to the minimum , maximum and variable fluorescence. σ_{PSII} is the absorption cross-section for PSII in the dark-regulated state, which can be derived from the initial rise of fluorescence in the induction curve. This induction curve is issued from the first step of the PE curve shown in Figure 5 and corresponds to the very first acquisition in the dark (E=0 µmol m^{-2} s^{-1}). In the light-adapted state, F_o, F_m and F_v and σ_{PSII} will be noted respectively as F', F_m' and F_q' and σ'_{PSII}.

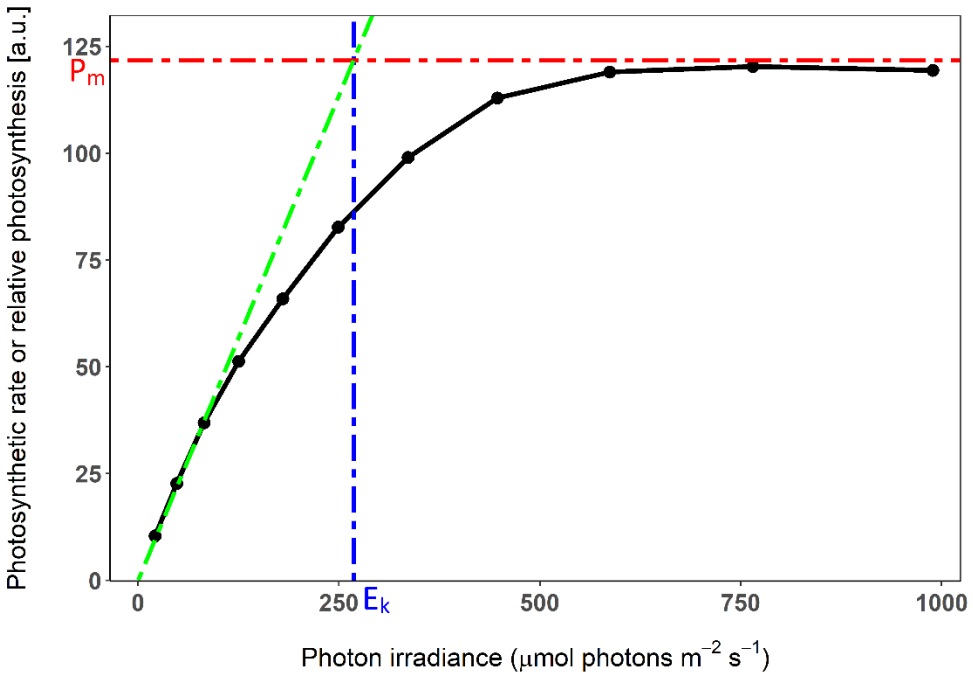

Figure 6. PE curve or Photosynthetic light curve generated by the LabSTAF instrument. The green line corresponds to the initial extrapolated linear response section of the curve, the red horizontal line determines the maximum photosynthetic rate (P_m). The intersection of the green and red line determines E_k (in blue). On the LabSTAF, the relative photosynthesis is reported on a unitless scale but the units are actually µmol photons m^{-2} s^{-1}.

4. Observing physiological change in nature

4.1. Nutrient availability

There are multiple factors controlling phytoplankton growth in nature. Phytoplankton require organic nutrients, trace metals and vitamins to efficiently use light for growth. Further factors controlling growth are water temperature and pH. Nitrogen and phosphorus are essential nutrients for growth (Redfield 1958), and in turn, phytoplankton influence environmental nitrogen to phosphorus (N: P) ratios. Every species has specific optimal growth conditions with algae generally favouring N: P molar ratios > 16 and cyanobacteria < 16. However, Geider and La Roche (2002) suggest that the Redfield N:P ratio is more likely to be between 15 and 30. Some species of cyanobacteria have the possibility to fix elemental nitrogen, further widening their range for growth below the 16:1 Redfield N:P ratio. The presence of cyanobacteria in natural samples is therefore more often controlled by phosphorus availability than nitrogen (Whitton and Potts 2000).

4.2. Light availability

Light availability controls the potential for growth when other requirements are met. Each species has an optimum light environment; however several cellular acclimation mechanisms can be regulated to overcome energetically suboptimal light conditions.

High irradiance conditions are common at the water surface and, over time, induce photoinhibition. According to Long, Humphries, and Falkowski (1994), photoinhibition is the "light dependent and slowly reversible retardation of photosynthesis, independent of any developmental change" which decrease the photosynthetic rate and maximum quantum yield for CO_2 uptake. If cells are submitted to an excess of light for a long period, photo-oxidation of the cell and in the case of cyanobacteria, detachment of PBS from the thylakoid membrane will result in lasting damage.

Cyanobacteria have adapted a number of mechanisms to overcome rapid alterations of quality and quantity of light (Whitton and Potts 2000). These mechanisms broadly classify into those requiring protein synthesis and those which do not..

Non-Photochemical Quenching (NPQ), dissipates excess energy as heat to limit the damage caused by intense illumination (Giacometti and Morosinotto 2013). Examples of regulation without protein synthesis and being part of NPQ mechanisms, include the aforementioned "state transitions", distributing excitation energy between the two photosystems in timescales

from seconds to minutes (Mullineaux, Tobin, and Jones 1997). When PSII becomes saturated, state transitions will favour PSI. In many cyanobacteria, this process is induced by exposure of orange carotenoid protein (OCP) to blue-green light (Tian et al. 2011). The activation from the inactive form of the OCP (OCP^o) to the active form (OCP^r) induces the "quenching state" and leads to a decrease of the energy arriving to reaction centres and a decrease of the PBS fluorescence. Reciprocally, the "non-quenching state" is induced by another protein: the Fluorescence Recovery Protein (FRP) which permits the recovery of the full antenna capacity under low irradiance (Gwizdala, Wilson, and Kirilovsky 2011). In plants and algae, NPQ is activated by all visible light, while the quenching state is only induced under blue-green light in cyanobacteria (Giacometti and Morosinotto 2013). The recovery of the inactive form of the OCP (OCP^o) is temperature dependant, recovering faster with increasing temperature. Maximum fluorescence quenching is dependent on the OCP-to-PBS ratio (number of OCP per PBS); a higher ratio decreases the time necessary to reach the maximum fluorescence quenching (Sluchanko et al. 2017, Gwizdala, Wilson, and Kirilovsky 2011). The maximum fluorescence quenching is attained after several minutes and differences are obtained among different environmental conditions (pH, phosphate concentrations) and light-adaptation of cells (Kirilovsky and Kerfeld 2012, Gwizdala, Wilson, and Kirilovsky 2011). The reverse process is also slower, in the order of tens of minutes.

Other mechanisms, based on production and degradation of proteins, are diverse. Some cyanobacteria species are able to alter the number and the size of phycobilisomes and photosynthetic units per cell in response to light availability (Raps et al. 1983, Kana and Glibert 1987, Grossman 1990, Whitton and Potts 2000). Under growth-inhibiting high irradiance, the number and the size of PBS can be decreased by dilution (as cells divide, gene expression for PBS units and pigments is downregulated) whereas under low light and nutrient replete conditions PBS and pigment production increase. Certain species can regulate the production of PC (group II) or both PC and PE per PBS (group III), a mechanism called complementary chromatic adaptation (CCA, (Whitton and Potts 2000). This mechanism may be triggered by the light availability in specific wavebands (De Marsac and Houmard 1988, Grossman 1990). Generally, under green light, PBS synthetized contain PE and PC whereas under red light, PBS contains only PC (Whitton and Potts 2000). CCA is based on the regulation of PE and PC gene expression; under green light (GL), PE gene expression is induced and PC gene expression is mostly repressed while under red light (RL), the induction of PC gene expression and repression of the PE gene expression are observed (Campbell 1996). Changes of photosystems (PSI and PSII) number as well as the PSI: PSII ratio, exist also in certain species of cyanobacteria

under different light and nutrient conditions. Cyanobacteria grown under weak white light, are likely to exhibit a higher PSI: PSII ratio grown under strong white light (Kawamura, Mimuro, and Fujita 1979, Whitton and Potts 2000). These processes act slower than the NPQ process and depend on acclimation time, growth conditions and the intensity and quality of light.

Finally, phytoplanktonic species are able to repair PSII damage through a high turnover of the D1 protein, but this process is unstable under high light conditions (Inagaki 2022). However, some species of cyanobacteria, living in extreme conditions, are known to be remarkably resistant to photoinhibition and have the ability to repair PSII damage, even under high intensity light (Rascher et al. 2003, Harel, Ohad, and Kaplan 2004).

5. The case for improved near-real time monitoring of cyanobacterial water quality

5.1. Water quality assessment frameworks

Water quality can be assessed through several biological, physical, and chemical variables. These can be translated into water quality indices, or indicators, to be deployed on a national or global level (Katyal 2011). An index or indicator represents a single value of water quality based on the status of one or multiple measured variables, facilitating interpretation in terms of ecosystem health (Abbasi and Abbasi 2012). They express water quality as classes or numerical indices of pollution or other pressures.

In Europe, the *Water Framework Directive* 2000/60/EC (WFD), adopted by the European Union (EU) on the 23rd of October 2000, aims to improve the water quality across member states. More precisely, goals of the directive are to avoid deterioration and assign targets marking "Good Environmental Status" for ground and surface waters. The WFD covers a wide range of water quality aspects and takes into consideration the designation of water bodies including as bathing or drinking water resource. Each member state is obliged to implement a River Basin Management plan. Objectives of the WFD are submitted to strict monitoring deadlines to encourage water quality improvement with a deadline for Good Environmental Status set for 2027 ('Water - Environment - European Commission' 2018). National regulatory bodies (e.g. the Environment Agency, Scottish Environment Protection Agency, Northern Ireland Environment Agency, Natural Resources Wales) subsequently determine the ecological and chemical status of waterbodies by measuring biological and physical elements.

Substance concentrations are measured regularly, although the frequency of observations varies widely between countries and water bodies (Birk et al. 2012, Poikane et al. 2019).

Results are compared to targets to define the ecological status and chemical status of water bodies, and sometimes seasonally aggregated. The water quality assessment is broadly grouped into physio-chemical variables and biological variables. Physio-chemical elements include pH, turbidity, temperature, water colour, conductivity, alkalinity, total solids (suspended and dissolved), heavy metals and toxic elements, nutrients (phosphate, ammonium, nitrite and nitrate), dissolved oxygen, dissolved carbon dioxide, chemical oxygen demand, total hardness and chlorides (Trudgill et al. 1997, Simeonov et al. 2003, Hurley, Sadiq, and Mazumder 2012, Patil, Sawant, and Deshmukh 2012, Rahmanian et al. 2015). Several biological elements are also included, such as total organic carbon and biological oxygen demand (Simeonov et al. 2003). The water quality bioassessment is primarily implemented by periodically assessing periphyton, plankton, fish and macrobenthos assemblages (Metcalfe 1989, Barbour 1999). Macrobenthos communities are used to assess river water quality and may be expressed in specific indices such as the Marine Biotic Index, the Biotic Index or the Benthic Response Index (Borja, Franco, and Pérez 2000, Diaz, Solan, and Valente 2004, Pinto et al. 2009).

5.2. Harmful algae blooms (HABs)

Industrial, agricultural and urban activities contribute to nutrient enrichment of water bodies, a process referred to as eutrophication (H. W. Paerl and Huisman 2008). Hydrological modifications and climate change further contribute to more frequent blooms of cyanobacteria, which are understood to be favoured by nutrient enrichment, warm water, enhanced stratification, and increased atmospheric CO_2 (H. W. Paerl and Huisman 2008; Hans W. Paerl and Huisman 2009). In freshwater areas, cyanobacteria blooms are particularly driven by elevated nutrient concentrations (Paerl *et al.,* 2011; Paerl and Paul, 2012; Wurtsbaugh *et al.,* 2019). These blooms can affect water taste, odour, and appearance. Among bloom-forming cyanobacteria some species are considered more likely than others to form harmful algae blooms (CyanoHABs), related to the production of a diverse range of toxins (Whitton and Potts 2000). CyanoHABs can affect human and animal health as well as human activities (water supply, irrigation, fishing and recreational), aquatic ecosystems and food webs (Whitton and Potts 2000; H. W. Paerl and Huisman 2008; Hans W. Paerl and Huisman 2009). Blooms of cyanobacteria can take multiple forms and accumulate into biofilms, mats, or surface scum, and they are found in fresh and brackish waters, lakes, lagoons and even some marine areas (Codd et al. 2005). According to Cronberg, Carpenter, and Carmichael (2003), more than 55 species, belonging to 30 genera, have been recorded to produce toxins, with the

majority found in freshwater environments. Ongoing discovery of toxins in previously unsuspected species are alarming and detecting toxins at scale, in order to prevent risks to human and animal life, remains challenging.

Risk management of CyanoHABs is realised notably through indices related to the drinking water quality, tolerable daily intakes and Guideline values (Codd, Morrison, and Metcalf 2005). These indicate, for each specific cyanobacteria toxin, the maximum healthy intake level for a life-time of drinking water (Whitton and Potts 2000). Providing a cyanotoxicosis diagnosis still remains difficult. Indeed, toxicity can vary between strains of the same species but also between clones of the same isolate (Whitton and Potts 2000). Moreover, a bloom dominated by species known to be toxic, does not guarantee that this bloom is actually hazardous. Different environmental factors such as light, pH, temperature, nutrient availability and trace metals have an influence on the toxicity of some species or on the proportion or diversity of toxins produced by toxigenic strains (Paerl and Otten 2013, Jacoby et al. 2000, Whitton and Potts 2000). Moreover, the accumulation of biomass to toxic levels is often dependent by vertical mixing, and thus weather dependent.

5.3. Water quality assessment and cyanobacteria blooms

HABs can be assessed through a range of methods: *in situ* fluorescence measurements, *in situ* sampling associated with analyses in laboratory (taxonomic species identification, molecular analyses, High-performance liquid chromatography (HPLC) of toxins), biological and physical modelling, and a range of Earth observation methods (including satellite remote sensing). Those methods vary in cost, time, and accuracy. A non-exhaustive list of these methods is presented in Table 1. The duration of getting samples, analysing them, and obtaining diagnostic results will influence the frequency of the measurements and ultimately the timeline of the assessment of potential cyanobacteria bloom. CyanoHAB assessment will be based on a trade-off between cost, time, and accuracy of the methods, but the ideal set of methods should be available at relatively low cost, easy to use and provide an accurate assessment to prevent risks to water users.

Taxonomic methods, molecular and toxicity analysis, are relatively time-consuming (up to days of analysing) and therefore costly, but have the advantage of being highly accurate. Remote sensing has the advantage of visualizing the full extent of blooms (Shen et al. 2012), but satellites equipped with the appropriate wavebands cannot resolve the majority of (relatively

small) water bodies. *In situ* optical methods used to assess cyanobacterial biomass include flow cytometry, spectrophotometry, and active fluorescence measurements.

Spectroscopic techniques, including UV absorption and fluorescence properties, have been developed as alternative techniques for environmental monitoring (Hur, Hwang, and Shin 2008). Flow cytometry, combining fluorescence properties and light scattering of cells, has been used to discriminate between phytoplankton taxa (Trask, Van den Engh, and Elgershuizen 1982). Flow cytometry can estimate cell numbers rapidly and include pico-cyanobacteria. However, this technique is not well suited for samples containing filamentous cyanobacteria (Table 1). Spectrophotometry can discriminate between pigment groups, but not at the taxonomic level below required to assess risk (Table 1). Spectrophotometry is also used to determine the concentration of Chla in samples as a measure of biomass.

Fluorescence methods have been considered in research context for water quality assessment, pollution, and algal monitoring in marine and inland waters, for a variety of reasons. Most prominently, fluorescence methods are rapid which allow a high frequency of measurement, giving immediate results, and they are non-intrusive, do not produce waste and can be used *in situ* (Table 1). Active fluorescence include fluorometers which indicate the physiology and the potential to grow of phytoplankton as well as NPQ processes. However, fluorometers can only discriminate between phytoplankton belonging to different pigment groups and they cannot indicate the potential toxicity of cyanobacteria (Table 1). The advantage of using fluorescence to target cyanobacteria is based on the fact that phycobilipigments are the main-light harvesting pigments in cyanobacteria and are only found in cyanobacteria, rhodophytes and glaucophytes. Rhodophytes and glaucophytes do not proliferate in environments subjected to cyanobacteria blooms (Dodds 2002, Dittami et al. 2017, Price et al. 2017), which indicates that fluorescence signal characteristic of PBS and phycobilipigments is diagnostic of cyanobacteria. Moreover, fluorescence is particularly suitable for monitoring cyanobacteria blooms, as a preventive method. Fluorometers which are able to estimate both the physiology and biomass of cyanobacteria can predict cyanobacteria growth according to nutrients concentration and light level. Early prediction of cyanobacteria blooms is useful to give warnings to water quality managers and prevent risk on potential users. Early warnings are also possible with satellite earth observation methods but these methods are not suitable for small water bodies and cannot determine accurately cyanobacteria physiology.

Table 1. Comparative table of methods currently used to monitor cyanobacteria HABs. Advantages, limitations and timing of each method are considered. This table is based on Hallegraeff et al. (2004).

Methods	Advantages	Limitations	Timing of results
Fluorescence	- *In situ* deployment - High reproducibility - Non-destructive - Non-intrusive - High sample turnover - Rapid results - Cyanobacteria biomass and physiology assessment - Early warnings	- Cost - No information on toxins - Training required - Specific instrumentation needed to observe cyanobacteria - Specific to pigment groups rather than taxonomic groups	- Minutes to hours
Spectrophotometry	- High reproducibility - High sample turnover - Rapid results - Cyanobacteria biomass estimation from Chla and phycobilipigment absorption	- No physiology information - Pigment content is influenced by light/nutrient history - No information on toxins - Specific to pigment groups rather than taxonomic groups	- Minutes
Flow cytometry	- Differentiates cyanobacteria - Cell counts	- High cost - Training required - No information on toxins - Sample preparation - Not suitable for filamentous cyanobacteria - No physiology information	- Minutes

Identification by light microscopy	- Highly precise - Species identification - Cell counts	- No information on toxins - Training required - Time consuming - No physiology information	- Hours
Molecular analysis	- Highly precise - Biomass estimation - Toxicity analysis - Species identification	- Needs consumable (expensive) - Training required - Time needed for analysing	- From hours to days depending on the method
***In vitro* assays for phycotoxins**	- Specific to toxins - Highly precise - Highly sensitive - Rapid and affordable test kit (can be used *in situ*)	- Method expensive to develop	- Minutes to hours
Chromatographic methods	- Highly precise - Identification and quantification of toxins	- Training required - Consumables cost	- Minutes to hours
Satellite Earth observation	- Detect cyanobacteria blooms across spatial scales - Validated by *in situ* data - High automation potential - High repeat frequency - Early warning	- No information on toxins - No information on species - Computing infrastructure required	- Latency 1-2 days
Biological and physical modelling	- Prediction of cyanobacteria biomass in a specific waterbody - Biogeochemical insights (nutrients, light, competition, grazing…) - Validated by *in situ* data	- Model development cost - *In situ* for model calibration - No information on toxicity	- Hourly estimates possible

5.4. The state-of-the-art of fluorometric assessment of cyanobacteria

5.4.1. Sensor availability

Several fluorescence sensors are commonly available to target cyanobacteria in mixed populations *in situ* and a non-exhaustive list of these sensors are presented in Table 2). Instruments targeting cyanobacteria can measure variable fluorescence (PAM or FRR) or measure non-kinetic fluorescence to estimate biomass *in vivo*. They are found in different formats (benchtop, handheld, or submersible), can be deployed to analyse discrete or continuous measurements, on-site or in the laboratory. All fluorometers in Table 2 target the PC pigment in cyanobacteria while several instruments additionally target PE. Several fluorometers measuring variable fluorescence present a range of actinic light colour or have several emission bands. The choice of actinic light is important to consider when targeting cyanobacteria. Indeed, different type of phytoplankton are excited by different excitation wavebands due to their different composition in photosynthetic pigments (as seen in section 1.5 and Figure 1). Cyanobacteria are excited by the red part of the spectrum while algae are excited by the blue part of the spectrum. Actinic light spectra will consequently influence the fluorescence signal in algae and cyanobacteria. Moreover, actinic light color is susceptible to induce NPQ mechanism, found only in cyanobacteria. NPQ induced by the OCP protein occurs only in cyanobacteria (Wilson et al. 2008) and is photo-activated by white or blue-green light (Wilson et al. 2008, Tian et al. 2011, Giacometti and Morosinotto 2013).

Table 2. Optical specifications, deployment, and specific advantages of fluorometers targeting cyanobacteria. PAM: Pulse Amplitude Modulation, ST: Single Turnover, PC: Phycocyanin (pigment), PE: Phycoerythrin (pigment). The list of non-kinetic instruments is not intended to be exhaustive.

Type of fluorometry	Type of saturation technique	Fluorometer configuration	Fluorometer name (supplier)	Advantage (application and target of cyanobacteria)
Variable	PAM	Benchtop fluorometer	**PhycoLabAnalyser** (bbe-Moldaenke)	Target PC Emission windows: 2 ranges 640-700 nm Actinic light colour: 660 nm
			MULTI-COLOR-PAM (WALZ)	Target PC and PE Multi-wavelength actinic LED array Saturating single or multiple turnover flashes
			DUAL-PAM-100 (Walz)	Record fluorescence at longer wavelengths than 700 nm Multiple choice of actinic light colour Saturating single or multiple turnover flashes
			Phyto-PAM II (WALZ)	Target PE and PC Multiple choice of actinic light colour Saturating single or multiple turnover flashes
		Hand-held	**AquaPen AP 110-C** & **AquaPen AP 110-P** (Photon Systems Instruments)	Target PC Instantaneous chlorophyll fluorescence can also be measured
	ST or flash sequences	Benchtop fluorometer	**LabSTAF** (Chelsea Technologies Group)	Target PC and PE Can run continuous measurements Dual emission waveband (685 and 730 nm)
			Mini-FIRe (mini-FIFe Fluorometers)	Target PC and PE High sensitivity and signal-to-noise ratio
			LIFT-FRR fluorometer (Soliense)	Target PC and PE 6- position filter for emission bands

				Available as submersible instrument
		Submersible, profiling system	**Fast Ocean** (Chelsea Technologies Group)	Target PC and PE
Non-kinetic	Not applicable	Handheld fluorometer (not *in situ*)	**CyanoFluor** (Turner Designs)	Target PC
		Handheld fluorometer (*in situ*)	**FluoroSense** (Turner Designs)	Target PC
			AlgaeTorch (bbe-Moldaenke)	Target PC Submersible to 10 m
		Submersible	**NanoFlu** (TriOs)	Target PC
			MatrixFlu VIS (TriOs)	Target PC Quasi-synchronous detection of excitation-emission matrices
			UniLux, **TriLux**, (Chelsea Technologies Group)	Target PC and PE
			ECO FL (Sea Bird scientific)	Target PC and PE Can be used for long term field measurements
			PhytoFind (Turner Designs)	Target PC and PE
		Submersible (flow-through measurement)	**FluoroProbe III** (bbe-Moldaenke)	Target PC and PE A lab-based version exists
			WETStar (Sea-Bird Scientific)	Target PC and PE

5.4.2. Current challenges in the fluorometric determination of cyanobacterial physiology

Fluorometers designed to target and discriminate cyanobacterial photo-physiology and, ultimately, determine the potential for population growth, are subject to the specific challenges of diagnostically interpreting *in vivo* fluorescence, and the technical challenges of building a performant fluorometer.

The diagnostic challenge follows from the overlap in absorption spectra of photosynthetic pigments that are characteristic of the main phytoplankton groups (Figure 1). As a result, isolating the response from cyanobacteria in a natural community is subject to some uncertainty, likely requiring multiple optical markers to determine the cyanobacterial signal contribution. A combination of excitation wavebands, including those targeting Chla and phycobilipigments, are already used (Table 2). These will induce a strong signal in cyanobacteria, but also a (weaker) signal from algae (Simis et al. 2012). A challenge, therefore, is to determine the difference between a strong, positively diagnostic signal from a small population of cyanobacteria, and a weaker signal from a population dominated by other phytoplankton groups.

Other challenges could comprise the fluorescence signal induced by non-phytoplanktonic chromophores or organisms. These non-photosynthetic substances or organisms include, in other, CDOM (Chromophoric Dissolved Organic matter), humic and fulvic substances, uncoupled pigments, as well as photoheterotrophic bacteria which contains bacteriochlorophyll *a*. However, only the photoheterotrophic bacteria is able to produce variable fluorescence and the maximum fluorescence emission of bacteriochlorophyll *a* is found at a longer wavelength (≈ 880 nm) than Chla maximum fluorescence emission wavelengths (≈ 685 nm) (Kolber et al. 2001). Moreover, maximum fluorescence emission of CDOM and humic/fulvic substances are generally found at much shorter wavebands than phytoplanktonic organisms and obtained under shorter excitation wavebands (Kowalczuk et al. 2003, Xiaoli et al. 2012, Fukuzaki et al. 2014).

Saturating PSII, which is translated by reaching the maximum F_m, has been a significant challenge in the design of active fluorometers which is most likely to be overcome by using (banks of) high intensity LEDs.

New opportunities to exploit differences between cyanobacteria and algal fluorescence may present themselves, in fluorometer design. Recording fluorescence at PSI emission, as well as

the ratio of PSI emission over PSII emission, have potential to identify cyanobacteria in mixed-communities. Most fluorometers record fluorescence at 685 nm, corresponding to PSII Chla emission (Table 2). However, in cyanobacteria, Chla is mostly contained in PSI (Mimuro and Fujita 1977), and PSII fluorescence is mainly induced by light harvesting phycobilipigments. It has been assumed that PSI fluorescence is non-variable and that the contribution of the PSI in Chla fluorescence, in room temperature, at wavelengths lower than 700 nm is relatively low (Franck, Juneau, and Popovic 2002). However, Schreiber and Klughammer (2021) induced PSI variable fluorescence using high signal/noise ratio and high light intensity in a cyanobacterial species.

Finally, to provide a practical tool for assessment of cyanobacteria physiology and potential to grow, globally and for the majority of users, the cost of the fluorometer will have to be considered. The cost of a fluorometer is linked to its electronical and optical features. In order to keep cost low, the number of excitation and emission wavebands requiring specialist optics may need to be limited. The colour of actinic light has to be carefully chosen because a limited number of actinic light colour should be added to keep the cost low. The intensity range of the actinic light has to be carefully chosen not only because it is determining for creating PE curves and calculating photosynthetic rate, but also because the intensity potential of the actinic light will influence ultimately the cost of the instrument. A choice should also be made between single and multiple turnover excitation and subsequent data processing, with the former more expensive but delivering additional information on phytoplankton physiology.

6. Research aims

The first aim of this thesis is to identify the **specific optical characteristics or optical markers which can be exploited for the detection of cyanobacteria in mixed freshwater phytoplanktonic communities.** The optical markers include emission-excitation pair bands, actinic light colour and maximum intensity, and the length of the fluorescence kinetics protocol which should be implemented in a fluorometer measuring variable fluorescence. Moreover, the optical properties of the NPQ mechanism, linked to the OCP protein and induced by blue-green light in cyanobacteria, are explored as part of this first explorative research aim, to determine if this mechanism could be used as a diagnostic optical marker for cyanobacteria.

The second aim of this research is **to identify if the single turnover fluorometer LabSTAF, designed to differentiate the fluorescence response from several types of phytoplankton,**

can be used to target the cyanobacterial component of natural phytoplankton populations. As follow-on aim, the research will determine whether any shortcomings of the labSTAF can be ameliorated with optical features that were previously identified in the laboratory.

The final aspect of the research is to **determine if cyanobacterial growth characteristics can be quantified from natural samples**, using the optimised measurement configuration and the sensor that was previously tested. A secondary aim of this research direction is to establish whether physiological information derived from continuous fluorescence observations can serve to provide early warnings of cyanobacterial growth, and to establish the likely maximum lead time for such predictions.

7. Research approach and hypotheses

This thesis is organised in several research chapters which address the research aims (Section 6) in turn. Chapter 2 explores the potential of several optical markers to discriminate cyanobacteria, expanding on previous work in this direction using spectrally highly resolved excitation-emission matrices on laboratory-grown cultures. In addition, fluorescence kinetics of these cultures are measured using the same spectrofluorometer with an added actinic light source, following some optimisation experiments to determine a light intensity that reveals fast and gradual changes in fluorescence emission. Fluoresce emission spectra are recorded against two excitation wavebands, selected to target the main light-harvesting pigments in cyanobacteria and algae, for a period of one hour. Finally, to explore if the NPQ is ubiquitous to most cyanobacteria species and has a common fluorescence kinetic response which can be exploited to target cyanobacteria, the effect of using a blue-green actinic light source compared to white actinic light is studied. For these experiments, we expect fluorescence quenching and fluctuations to occur over a period of one hour, which is considered a realistic maximum duration for eventual sample screening in field conditions. The selected excitation wavebands are expected to induce distinct fluorescence responses between cyanobacteria and algae and stronger fluorescence emission or changes should be found at distinct emission wavebands between cyanobacteria and algae. The sensitivity and timing of NPQ induced by OCP is expected to be common to all cyanobacteria cultures (where OCP is present).

Chapter 3 presents the first validation of the single turnover fluorometer LabSTAF in assessing the physiology of cyanobacteria in a reservoir where cyanobacterial blooms are observed annually. Samples from the reservoir are analysed in the laboratory from early spring to late summer to capture the typical seasonal abundance of cyanobacteria. A range of optical

features of the LabSTAF are tested for their ability to capture cyanobacteria physiology. These optical features include PSII excitation spectra obtained with a protocol targeting cyanobacteria and a protocol targeting algae, fluorescence light curves obtained using a combination of excitation wavebands as well as the emission of 730 nm over 685 nm using two excitation protocols designed to have sensitivity towards either algae or cyanobacteria. Excitation protocols designed to target exclusively algae and cyanobacteria based on their main light-harvesting pigments are expected to capture fluorescence responses from both groups exclusively. PSII excitation spectra are expected to show the distinct pigments composition between cyanobacteria and algae, as it has been shown before. Finally, the ratio of emission at 730 nm over 685 nm is expected to higher for cyanobacteria and algae for the two excitation protocols but distinct responses are however expected.

In chapter 4, the LabSTAF fluorometer is set up to continuously measure fluorescence in a vessel where cyanobacteria growth is promoted through nutrient addition. Fluorescence light curves are recorded with protocols previously found to target cyanobacteria and algae, respectively, and run simultaneously using two systems sampling the experimental vessel in parallel. This chapter explores the potential of the photosynthetic parameters derived from the light curves to predict the growth of cyanobacteria versus algae, following nutrient addition. Cyanobacteria blooms are expected to be induced by nutrient addition (adjusted N:P ratio) so that phytoplankton community shifts may be observed. Photosynthetic parameters derived from light curves are expected to predict the growth of cyanobacteria versus algae, using the two excitation protocols and following the nutrients addition.

CHAPTER 2: DETERMINATION OF OPTICAL MARKER OF CYANOBACTERIAL PHYSIOLOGY FROM FLUORESCENCE KINETICS

This chapter is based on : Courtecuisse, E., Oxborough, K., Tilstone, G.H., Spyrakos, E., Hunter, P.D., Simis, S.G.H. (2022). Determination of optical markers of cyanobacterial physiology from fluorescence kinetics. Journal of Plankton Research, 44(3), 365-385.

Author Contributions to the paper: Conceptualisation, E.C., S.G.H.S., G.H.T., E.S., P.D.H. and K.O.; methodology, E.C. and S.G.H.S.; formal analysis, E.C.; investigation, E.C.; resources, K.O.; data curation, E.C.; writing—original draft preparation, E.C.; writing—review and editing, S.G.H.S., G.H.T., E.S., P.D.H., and K.O.; visualisation, E.C.; supervision, S.G.H.S., G.H.T., E.S., P.D.H. and K.O.; project administration, S.G.H.S.; funding acquisition, S.G.H.S. and K.O.

1. Abstract

Compared to other methods to monitor and detect cyanobacteria in phytoplankton populations, fluorometry gives rapid, robust and reproducible results and can be used *in situ*. Fluorometers capable of providing biomass estimates and physiological information are not commonly optimized to target cyanobacteria. This study provides a detailed overview of the fluorescence kinetics of algal and cyanobacterial cultures to determine optimal optical configurations to target fluorescence mechanisms that are either common to all phytoplankton or diagnostic to cyanobacteria. We confirm that fluorescence excitation channels targeting both phycocyanin and chlorophyll *a* associated to the Photosystem II are required to induce the fluorescence responses of cyanobacteria. In addition, emission channels centered at 660, 685 and 730 nm allow better differentiation of the fluorescence response between algal and cyanobacterial cultures. Blue-green actinic light does not yield a robust fluorescence response in the cyanobacterial cultures and broadband actinic light should be preferred to assess the relation between ambient light and photosynthesis. Significant variability was observed in the fluorescence response from cyanobacteria to the intensity and duration of actinic light exposure, which needs to be taken into consideration in field measurements.

KEYWORDS: fluorescence kinetics; optical markers; cyanobacteria; algae; fluorometry

2. Introduction

Phytoplankton blooms increase in magnitude, duration and frequency in response to nutrient enrichment and climate change (rising temperature and hydrological changes) in marine and freshwaters ecosystems (Paerl and Huisman, 2008, 2009; O'Neil et al. 2012). In freshwater systems, cyanobacterial blooms are specifically associated with elevated nutrient concentrations (Paerl et al. 2011; Paerl and Paul, 2012; Wurtsbaugh et al. 2019). Excessive cyanobacterial blooms can change the water taste, odor and appearance and can be directly harmful to aquatic life and human health if the dominant species produce toxins (Codd, Morrison, and Metcalf 2005, Codd et al. 2005, Whitton and Potts 2000). Such blooms affect ecosystem function (through oxygen depletion, increased turbidity, decreased plant growth and fish kills), animal and human health as well as industrial, agricultural and urban activities. Early detection of cyanobacterial species and subsequent monitoring of their potential to develop into blooms is essential to manage affected ecosystems. Several conventional and emerging

methods have already been recognized and reported to achieve this. These include microscopic identification and quantification, toxicity analysis (Carmichael and An, 1999; Baker et al, 2002; Oehrle et al, 2010), genetic and genomic methods, such as qPCR (quantitative Polymerase Chain reaction) and microarrays (Pearson and Neilan, 2008; Srivastava et al, 2013), and methods based in optics such as *in vivo* fluorometry (Beutler et al, 2002), flow cytometry (Becker et al, 2002) and imaging flow cytometry (Campbell et al, 2013). The accuracy, specificity, operational cost and transferability of these methods varies, with microscopic analysis being the most specific and also most laborious and with optical methods generally not discriminating beyond group taxonomic level but allowing higher throughput of samples.

Phytoplankton fluorescence methods target the light-harvesting system and include a broad set of approaches to provide rapid and relatively robust results that are reproducible and non-destructive and can be used *in situ* (Zamyadi et al. 2016). Within the phytoplankton, the eukaryotic algae and prokaryotic cyanobacteria display specific light-harvesting and fluorescence behaviors. First, light-harvesting pigments and structures are distinct between algae and cyanobacteria. Cyanobacteria (Prochlorophytes excepted) produce phycobilipigments [allophycocyanin (APC), phycocyanin (PC) and phycoerythrin (PE)], which also exist in Cryptophyta, Glaucophyta and Rhodophyta (Falkowski and Raven, 2013) but are not commonly found in abundance alongside cyanobacteria. In Cyanobacteria, Glaucophyta and Rhodophyta, these phycobilipigments are located in light-harvesting protein-pigment complexes (LHC) called phycobilisomes (PBS), attached to the thylakoid membrane (Beutler et al, 2002). In other phytoplankton groups, the LHC are embedded in the thylakoid membrane and do not include phycobilipigments. In Cryptophyta, phycobilipigments may be found which are not directly attached to the LHC. Phycobilipigments organized in a PBS induce a discernible fluorescence response to excitation in wavebands targeting phycobilipigment absorption peaks, which are typically in the "green gap" between the absorption of light by chlorophylls and carotenoids. Excitation wavelengths targeting phycobilipigments are proven optimal markers to discriminate cyanobacteria from other phytoplankton (Beutler et al, 2002; Gregor and Marsálek, 2005; Gregor et al, 2007; Seppälä et al, 2007). While glaucophytes and rhodophytes do possess PBS and their pigment fluorescence could be confused with cyanobacteria, rhodophytes are rarely found in freshwater areas and none of these groups are likely to be abundant in environments susceptible to cyanobacterial blooms (Dodds, 2002; Dittami et al, 2017; Price et al, 2017). A strong phycobilipigment fluorescence signal in freshwater bodies is therefore likely associated with cyanobacteria and is a suitable proxy for early warning.

Differences in the LHC structure and corresponding functioning of the light-harvesting and quenching apparatus further define fluorescence responses between the main phytoplankton groups. The energy from a single photon absorbed by a photosynthetic pigment can be lost through one of three pathways: it can be re-emitted as fluorescence, lost through heat dissipation or used to drive photochemistry. Photochemical quenching is caused by an increase of photochemistry, while non-photochemical quenching (NPQ) regroups a range of mechanisms dissipating energy as heat, some of which are not shared between algae and cyanobacteria. NPQ mechanisms found in both algal and cyanobacterial species include "state transitions," which allow relatively rapid adjustment of the energy delivered from LHCs to Photosystem II (PSII). The photoreceptors triggering these transitions provide group-specific optical markers. NPQ induced through the orange carotenoid protein (OCP), a water-soluble protein linked with the PBS, occurs only in cyanobacteria (Wilson et al, 2008) and is photo-activated by blue-green (BG) light or bright white light, changing OCP between its inactive orange form and its active red form. Kerfeld et al. (2017) reported 113 genomes of cyanobacteria which contained the protein OCP-1, which is present in almost every phylogenetic subclade. If this response is nearly ubiquitous in cyanobacteria, instruments could be designed to trigger a group-specific response to detect the presence of cyanobacteria in a mixed phytoplankton assemblage. Detailed spectrofluorometric studies to determine whether this mechanism can be observed as a targeted fluorescence response have not yet been reported.

The "ideal" fluorometric solution would assess both the biomass and physiology (potential for growth) of cyanobacteria in a water body in mixed phytoplanktonic communities. Such a solution does not yet exist in concept in scientific literature nor on the market. Estimating phytoplankton biomass using *in vivo* fluorescence is based on the assumption that fluorescence is proportional to chlorophyll *a* (Chla) concentration while photosynthetically available radiation (PAR) is constant, and as long as the product of the quantum yield of *in vivo* fluorescence (ϕ_f), the Chla-specific spectrally averaged absorption coefficient of phytoplankton weighted by the irradiance spectrum ($\bar{a}^*$), and the fluorescence intracellular reabsorption factor (Q_{a^*}), may be considered constant (Babin, 2008, Huot and Babin, 2010). Fluorometers giving a diagnostic assessment of (relative) biomass of cyanobacteria are at relatively low cost, can have an easy deployment method and generally give results in short time scale (minutes). However, the product $\phi_f \, \bar{a}^* \, Q_{a^*}$ is subject to environmental, biological and physiological variability (Babin 2008) . While $\bar{a}^*$ and Q_{a^*} cannot be estimated directly from *in vivo* fluorescence, active fluorescence methods are able to measure the quantum yield of

fluorescence.

Active fluorescence, previously established using flash-stimulated techniques, measure the photochemical efficiency of the sample while saturating it with light (Huot and Babin, 2010). This is done via the determination of the minimum quantum yield of fluorescence F_o (in dark-adapted state, all reaction centers opened) maximum quantum yield of fluorescence F_m (all reaction centers closed) and the variable fluorescence F_v, which is the difference between F_o and F_m (Schuback et al, 2021). Two instrument types are widely used for the active, saturating fluorescence approach: those which saturate PSII over multiple turnovers (reaction centers open and close repeatedly), such as pulse amplitude modulation fluorometers, and those that are able to achieve the same within a single turnover of the photosystem using order-of-magnitude higher excitation intensity, such as fast repetition rate fluorometers and other well-characterized fluorometers which capture the rise of fluorescence in the microsecond scale (Suggett et al, 2006). Single-turnover fluorometers provide the added advantage of running samples at a higher frequency, interpreting the rate of fluorescence induction as a measure of the functional absorption cross section of photochemistry as well as the kinetics of fluorescence relaxation, which can reveal the state of NPQ of the sample (Schuback et al, 2021). Active fluorometers include predominantly benchtop instruments, but until recently, few were designed with sensitivity to cyanobacteria in mind, and the single-turnover category of instruments required relatively more costly electronics.

Bringing down the cost of fluorometric solutions while optimizing their specificity to cyanobacteria physiology remains a challenge. Several factors should be considered to optimize fluorometer design, starting from a suitable combination of excitation and emission wavebands to achieve specificity, actinic light spectral properties and the range of excitation and actinic light intensity to reliably induce and saturate photosynthetic responses as well as other engineering challenges such as temperature and flow control. To date, these design steps have been guided foremost by technically feasibility and not by what would provide the optimal separation of signals from algae and cyanobacteria.

Current fluorometers which do target the bio-optical properties of cyanobacteria have excitation wavebands targeting PE and/or APC and record Chla PSII emission. Wavebands targeting PC, which exists in all cyanobacteria, tend to be centered at shorter wavelengths (e.g., 590 nm) than the peak absorption of the pigment (615 nm) to avoid cross-talk with emission detection windows and to limit cross-excitation of Chla. While the selection of excitation bands to target cyanobacteria-specific pigments is relatively straightforward, the interpretation of the PSII response is not. It is known that, in cyanobacteria, >80% of Chla

tends to be associated with Photosystem I (PSI) rather than PSII because Chla is not a major light-harvesting pigment serving PSII in this phytoplankton group (Mimuro and Fujita, 1977). Caffarri et al. (2014) also suggest that, compared to algae, the number of Chla molecules in the PSII core is lower in cyanobacteria. These findings suggest that estimation of cyanobacteria biomass based on PSII fluorescence is likely negatively biased. Reciprocally, we can hypothesize that the relationship between the concentration of Chla in a sample and the fluorescence observed from PSII versus PSI may hold information on the fraction of cyanobacteria out of the total phytoplankton biomass. The question remains to what extent these nuances are observable in nature and which fluorescence markers (notably fluorescence emission windows) could be exploited to quantify these properties among the various, changing fluorescence responses of diverse phytoplankton samples. It has generally been assumed that PSI fluorescence is non-variable (F_v equal to 0) but Schreiber and Klughammer (2021) showed variable PSI fluorescence in a green algal species, a cyanobacterial species and in a light-green ivy leaf using a high-resolution time and high signal/noise ratio as well as high light intensity. Considering that a small percentage of Chla is linked to PSI compared to PSII in algae while the opposite is observed in cyanobacteria (Johnsen and Sakshaug, 1996, 2007), the discovery of PSI variable fluorescence opens the possibilities of using PSI fluorescence as an optical marker to discriminate cyanobacteria in a mixed phytoplankton assemblage.

In this study, we aim to identify an optimal set of optical markers to discriminate both biomass and physiological parameters of cyanobacteria using fluorescence responses. Both excitation and emission band optimization are considered. A secondary aim of this work is to inform the development of low cost *in situ* fluorometric techniques that can diagnostically target the physiology of cyanobacteria in natural samples using active fluorescence techniques and actinic light dosing. The low-cost perspective implies that markers which can be observed by dosing actinic light, even over relatively long timescales, are preferred to those which require highly sensitive or additional detectors since these components largely determine cost.

Fluorescence kinetics measurements obtained under a range of optical configurations (blue and orange excitations, emission windows over the 650–750 nm range, BG and broadband actinic light options) are recorded in this work during experiments lasting up to 1 hour in nutrient-replete laboratory strains of three cyanobacterial and three algal species. The dataset is characterized by high spectral resolution to inform band selection and is used to inform our analysis. In summary, we hypothesize that the temporal nature of the fluorescence response is more heterogeneous between than within the main phytoplankton groups (algae/cyanobacteria), which is similar to what is known spectral fluorescence responses.

Further, we expect that the use of blue actinic light, while resulting in low electron transport for PSII, can induce NPQ in cyanobacteria over time such that observable fluorescence kinetics (e.g., OCP) can be assessed using a single actinic light color. However, the rate of these kinetics may well differ between algae and cyanobacteria, providing further optical markers to distinguish their response. Third, we expect that any predictable temporal aspects of fluorescence emission from PBS pigments, changing in relation to PSII and potentially also PSI fluorescence emission during exposure to actinic light, follow the mechanics known as state transitions in cyanobacteria, which are related to the movement of PBS toward and away from PSII. Variability and consistency in the emission response rates between phytoplankton groups to actinic light treatment would inform the selection of specific emission markers and light treatments for operational use. Finally, it is expected that actinic light exposure exhibits a larger response in the change of emission at 730 nm (associated with PSI) in cyanobacteria than in algae.

3. Method

3.1 Phytoplankton cultures

Phytoplankton cultures used in this study included three PC-rich cyanobacteria, one chlorophyte, one eustigmatophyte and one diatom species. *Synechocystis* sp. UTEX 2470 (UTEX Culture Collection of Algae at the University of Texas at Austin, Austin, USA) is a unicellular freshwater cyanobacterium isolated from Berkeley (USA). The N_2-fixing pluricellular cyanobacterium *Anabaena cylindrica* CCAP 1403/2A (culture collection of algae and protozoa, SAMS limited, OBAN, Argyll, Scotland) was originally isolated from a pond in Surrey (UK). This strain grows photoheterotrophically following glycolate uptake (Renström-Kellner and Bergman 1990). *Spirulina platensis* TBSH1-5 is a freshwater filamentous cyanobacterium isolated from a culture starter (Terra Biosphere, Paignton, UK).

The unicellular chlorophyte *Chlorella* sp. was isolated at Plymouth Marine Laboratory (UK) from a lake water sample taken in the Hanoi municipality in Vietnam. *Nannochloropsis oceanica* CCAP 849/10 is a marine eustigmatophyte isolated from an operational hatchery in western Norway. The unicellular diatom *Phaeodactylum tricornutum* UTEX 646 (UTEX Culture Collection of Algae at the University of Texas at Austin) was originally isolated from a rock pool in Segelskär (Finland).

Batch cultures were grown at relatively low light intensity (25 μmol m^{-2} s^{-1}) at a 16/8 hour light/dark photoperiod using white, blue and red LED banks. Cultures were kept in a

temperature controlled room at 22°C. All cultures were in their exponential growth phase when fluorescence kinetics measurements were achieved. *Synechocystis* sp. UTEX 2470 was grown in BG11 medium, *A. cylindrica* CCAP 1403/2A and *Chlorella* sp. in JM medium, *P. tricornutum* UTEX 646 and *N. oceanica* was grown in the f/2Q "quad" medium (higher nitrate and phosphate concentrations than f/2 medium) and *S. platensis* was grown in modified Zarrouk's medium (Delrue et al. 2017).

3.2. Absorption measurements and dilution targets

Spectrophotometric measurements were carried out using a PerkinElmer (Waltham, MA, USA) model Lambda1050 spectrophotometer equipped with a 150- mm integrating sphere. Samples were placed in a 10-mm quartz cuvette at the center of the sphere to minimize the influence of light scattering on the absorbance measurement. Culture medium was used as blank reference, subtracted from the absorbance of each sample.

To achieve comparable cell densities between the experiments, we adapted the dilution targets established by Simis et al. (2012) who set absorbance targets of $D(675) = 0.022$ and $D(437) = 0.043$ in a 1-cm cuvette for nutrient-replete algae and cyanobacteria cultures, respectively. Absorbance targets provide roughly equivalent photosynthetic light absorption while minimizing the risk of multiple scattering by the cell suspension, as stated by Mitchell et al. (2002) and Werdell et al. (2018). Here, to allow for increased signal-to-noise ratio and faster repeated fluorescence measurements, these targets were doubled to $D(675) = 0.044$ (algae) and $D(437) = 0.086$ (cyanobacteria).

Absorption (a, units m^{-1}) was derived from absorbance as follows:

$$a(\lambda) = \ln(10) \times \frac{D(\lambda)}{0.01}$$

where ln(10) converts from 10-based to a natural logarithm and 0.01 corresponds to the path length of the cuvette in meters. Absorption spectra were finally zeroed at 750 nm, following blank subtraction, to remove any remaining scattering or subtraction effects caused by minor variations between blank and sample, or cell positioning in the sphere, due to the low absorption signal of the diluted samples.

3.3. Fluorescence measurements and experiment set-up

All samples were low light adapted (<17 μmol m^{-2} s^{-1}) for at least 20 minutes prior to fluorescence measurements. Fluorescence was recorded in a 10-mm quartz cuvette in a Varian Cary Eclipse (Agilent, Santa Clara, CA, USA) spectrofluorometer. This instrument comprises a red-sensitive photomultiplier tube (PMT) detector to enhance sensitivity up to 900 nm. Samples were stirred and kept at 22°C throughout the measurements using a Peltier temperature control and a mini-stirrer unit. The spectrofluorometer uses a xenon flash lamp to provide repeated high-intensity excitation flashes, the xenon flash lamp gives a peak power in excess of 75 kW and switches on and off 80 times every second which corresponds to a flash lasting less than 12.5 ms. The short duration of flashes coupled with the relatively long interval between flashes prevent the saturation of PSII (Simis et al. 2012). A dark signal between excitation flashes is recorded by the instrument and is used to offset the observed fluorescence. An actinic light source was placed directly above the cuvette and through a cover to keep out any other source of light. This actinic light source does not interfere with the excitation-emission measurement because the "ambient light" signal in the period between excitation flashes is already subtracted from the fluorescence signal. Fluorescence responses are expressed here as a function of excitation and emission waveband, $F_x(\lambda_{ex}, \lambda_{em})$, with λ being the center wavelength in nm and F_x being one of F_o, or F^r or to indicate the dark-adapted and transitory fluorescence response, respectively. During fluorescence kinetics measurements, emission spectra were recorded every 15 seconds for 1 hour at $F^r(445, \lambda)$ and $F^r(615, \lambda)$ to target Chla and PC, respectively. Emission was recorded in 10-nm wide bands at 2-nm intervals between 500 and 750 nm for $F^r(445, \lambda)$ and between 635 and 750 nm for $F^r(615, \lambda)$. To accommodate weaker fluorescence from cyanobacteria under blue excitation, the PMT detector voltage was set to 600 V for cyanobacteria and to 400 V for algal cultures with 445- nm excitation. With 615-nm excitation, the PMT voltage was set to 400 V for cyanobacteria and to 600 V for algal species. Corrections to adjust for the detector gain are described in the next section.

Actinic light was used to induce quenching, while fluorescence kinetics measurements were performed at intensities ranging from low (27–41 μmol m^{-2} s^{-1}), intermediate (152–168 μmol m^{-2} s^{-1}) and bright (578–597 μmol m^{-2} s^{-1}) to intense (1931–1960 μmol m^{-2} s^{-1}). Following initial measurements conducted over the course of 1 hour to determine the range over which temporal fluorescence responses could be discerned, further experiments were carried out under bright intensity light exposure. Light intensity was adjusted before each experiment

using a Biospherical instruments Inc (San Diego, USA) PAR sensor, cross-calibrated with a calibrated spherical Micro Quantum PAR sensor, US- SQS/L (Walz). Actinic light was generated using a white LED bulb (neutral white, 540 lm, Diall) with optional BG filter (Jade 323, LEE filters) to create "white actinic" and "BG actinic" light treatments. OCP has been activated in previous studies by intense BG illumination centered at 500 nm (Tian *et al.,* 2011) and in the 400–550 nm range (Wilson *et al.,* 2008) and accordingly, in this study, the BG filter was chosen because of its high transmittance at 500 nm. White actinic produced a broad spectrum between 425 and 700 nm with peak intensity around 600 nm (Figure 1). The BG filter combined with the white actinic light bulb induced high light intensity in the 500–545 nm range (Figure 1). Actinic light was switched on 15 seconds after starting each experiment, i.e*.,* after recording the first set of emission spectra on the low light-adapted sample.

3.4. Signal normalization

Spectral calibration of the spectrofluorometer was performed according to Kopf and Heinze (1984). In summary, excitation correction factors were obtained using a quantum counter [Oxazine 1, molar absorption coefficient (641 nm) = 117 000 $M^{-}1\ cm^{-}1$] in a triangular cuvette. Five excitation spectra were recorded from 200 to 700 nm (emission at 730 nm) and were averaged to obtain the excitation correction spectrum. For the emission correction, a diffusor was placed in the path from incident beam to detector, and an attenuator was placed in front of the detector. Five scans of synchronous excitation- emission measurements in the range of 200–800 nm were recorded and averaged. The excitation correction spectrum was divided by the synchronous excitation-emission spectrum to obtain the emission correction spectrum. Both correction spectra were applied to all fluorescence data shown in this study.

An instrument-specific gain correction factor was obtained to normalize fluorescence data, where different PMT voltages were selected to optimize the instrument signal-to-noise levels. Fluorescence was recorded from a polymer block reference standard of Rhodamine (Starna Scientific Ltd) at excitation 445 nm and recorded the peak emission of the same standard (≈ 574 nm) to obtain a correction curve as a function of PMT voltage. The correction factor (≈ 45.44) was applied to fluorescence obtained at a detector voltage of 400 V to align the response with fluorescence obtained at 600 V.

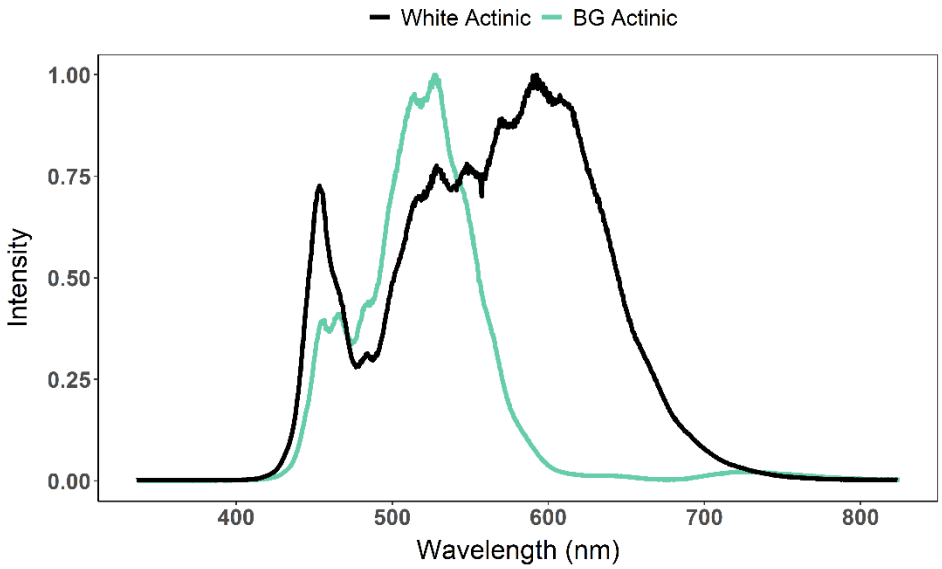

Figure 1. Light spectrum of the white actinic light bulb (white actinic) and light spectrum of the white actinic light bulb combined with the BG filter (BG actinic).

3.5. Data fitting

Generalized additive models (GAM, package "mgcv" v1.8-31 for *R* v3.6.1) were used to fit localized spline regression models to the fluorescence kinetics data.

This data smoothing procedure was used to identify subtle trends in fluorescence emission to capture the dominant curvature for data visualization and to handle noise in the data, particularly in spectral regions with weak fluorescence. The performance of the GAM fit was evaluated using the adjusted *r*-squared and the proportion of the null deviance explained by the model. Relative fluorescence was calculated from fitting results (to the first value) to compare fluorescence kinetics between species. Derivatives of the GAM fitting between each time step (15 seconds) were calculated to plot the slope of fluorescence change over time.

4. Results

4.1. Optical variability between phytoplankton cultures

The most prominent absorption features were the distinct Chla peak absorption in the blue region at around 440 nm in all species tested and the PC absorption peak in the 610–630 nm region for the cyanobacterial species (Figure 2). The absorption peak primarily associated with PC was found at shorter wavelengths in *S. platensis* (618 nm) and *Synechocystis* sp. (622 nm) compared to *A. cylindrica* (634 nm), suggesting variable intracellular ratios of PC, APC and Chla,

which have partially overlapping absorption signatures (Figure 2B). Absorption around the peak associated with PC exceeded that of the red Chla peak at 675 nm by ~15% in *Synechocystis* sp. In the other cultures, these pigment absorption peaks were of the same order of magnitude.

In the 450–500-nm region, absorption can be primarily attributed to non-photosynthetic carotenoid pigments in cyanobacteria and the eustigmatophyte, to the presence of carotenoids and photosynthetic chlorophyll-*b* in the chlorophyte species and to carotenoids and photosynthetic chlorophyll-*c* in the diatom (Figure 2). A significant absorption tail in the 500–560-nm region in the diatom *P. tricornutum* can be attributed to fucoxanthin (Figure 2A). Blue-to-red absorption ratios were of similar magnitude in all cultures, confirming that culture conditions favored expression of photosynthetic over photo-protective pigments, the latter being expressed primarily in the blue part of the spectrum (Kirk, 1994).

4.2. Low-light adapted fluorescence features of cyanobacteria and algae

Orange ($F_o(615, \lambda)$) versus blue ($F_o(445, \lambda)$) light excitation resulted in the typical divergent fluorescence response of algae and cyanobacteria (Figure 3). In algae, fluorescence emission was consistently higher under $F_o(445, \lambda)$, while cyanobacteria exhibited several orders of magnitude higher $F_o(615, 685)$ than $F_o(445, 685)$ (Figure 3). Regardless of which excitation band was used, algal cultures presented a narrow fluorescence emission band around 685 nm associated with PSII Chla and relatively low $F_o(\lambda, 700–750)$ (Figure 3A and 3C). The near infra-red emission ranged between 16 and 23% of the PSII peak and should be mostly attributed to Chla associated with PSI Chla (see, e.g. Itoh and Sugiura (2004)).

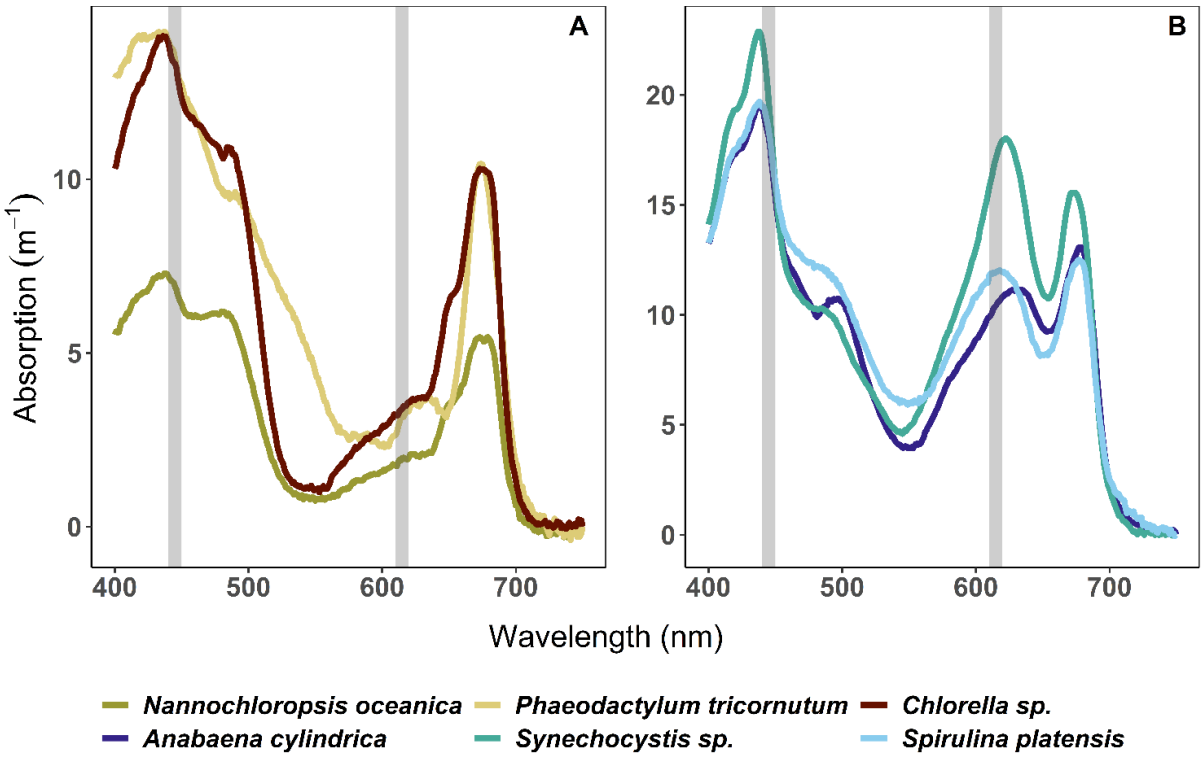

Figure 2. Absorption spectra of algae (A) and cyanobacteria (B) species. Gray rectangles represent two excitation wavelengths used in this paper: blue (445 nm) and orange (615 nm).

By contrast, F_o(445, 685) in cyanobacteria was part of a systematically broader emission feature (Figure 3B), which was associated with overlapping phycobilisomal fluorescence toward shorter wavelengths and a relatively higher PSI Chla contribution, ranging from 31 to 92% of the PSII peak, measured as the emission ratio of 734 over 684 nm. The *S. platensis* exhibited the highest (92%) relative fluorescence amplitude of PSI Chla compared to PSII Chla. A Raman scattering feature around 525 nm (Lawaetz and Stedmon 2009, Murphy 2011) is discernible in the cyanobacterial emission curves (Figure 3B), owing to a relatively low fluorescence response under blue excitation.

The F_o(615, λ) in cyanobacteria was high in the region 640–695 nm and showed two local peaks, centered at F_o(615, 660) and F_o(615, 685) (Figure 3A), corresponding to PC and APC and PSII Chla F_o, respectively. PSII Chla fluorescence peak contributed, between the cyanobacterial cultures, to 65-70% of the PC and APC peak, measured as the emission ratio [F_o(615, 684) over F_o(615, 660)]. Fluorescence attributed to PSI Chla was evident at wavelengths >700 nm and decreased gradually beyond 730 nm (Figure 3A). The contribution of PSI Chla fluorescence ranged between 18 and 25% (in algae) and between 32 and 37% (in cyanobacteria) of the PSII Chla peak, (Figure 3A) measured as the emission ratio [F_o(615, 734) over F_o(615, 684)].

4.3. Actinic light exposure experiments

4.3.1. General kinetics features

Bright (≈ 588 μmol m^{-2} s^{-1}) white actinic light treatment induced gradual quenching within the time frame of our experiment in *Chlorella* sp. and *A. cylindrica* (Figure 4) and was therefore considered as suitable to assess the temporal aspects of fluorescence responses over the 1-hour duration of the experiments. By comparison, intense (≈ 1946 μmol m^{-2} s^{-1}) white actinic light treatment induced rapid quenching at the beginning of the experiment and lower intensities induced no quenching or a rapid quenching followed by a long increase in fluorescence (Figure 4).

Fluorescence emission during continuous light exposure experiments remained consistently higher under $F^{r}(615, \lambda)$ compared to $F^{r}(445, \lambda)$ in cyanobacteria and for $F^{r}(445, \lambda)$ in algae (Figs 5 and 6). The specific wavebands where maximum fluorescence emission was observed differed between cyanobacterial cultures, whereas all algae showed consistent peak fluorescence emission around 685 nm (Figs 5 and 6).

Under white actinic exposure, maximum fluorescence emission was of similar magnitude between the three cyanobacterial cultures, whereas *N. oceanica* had 2-fold higher fluorescence emission compared to the other two algal cultures.

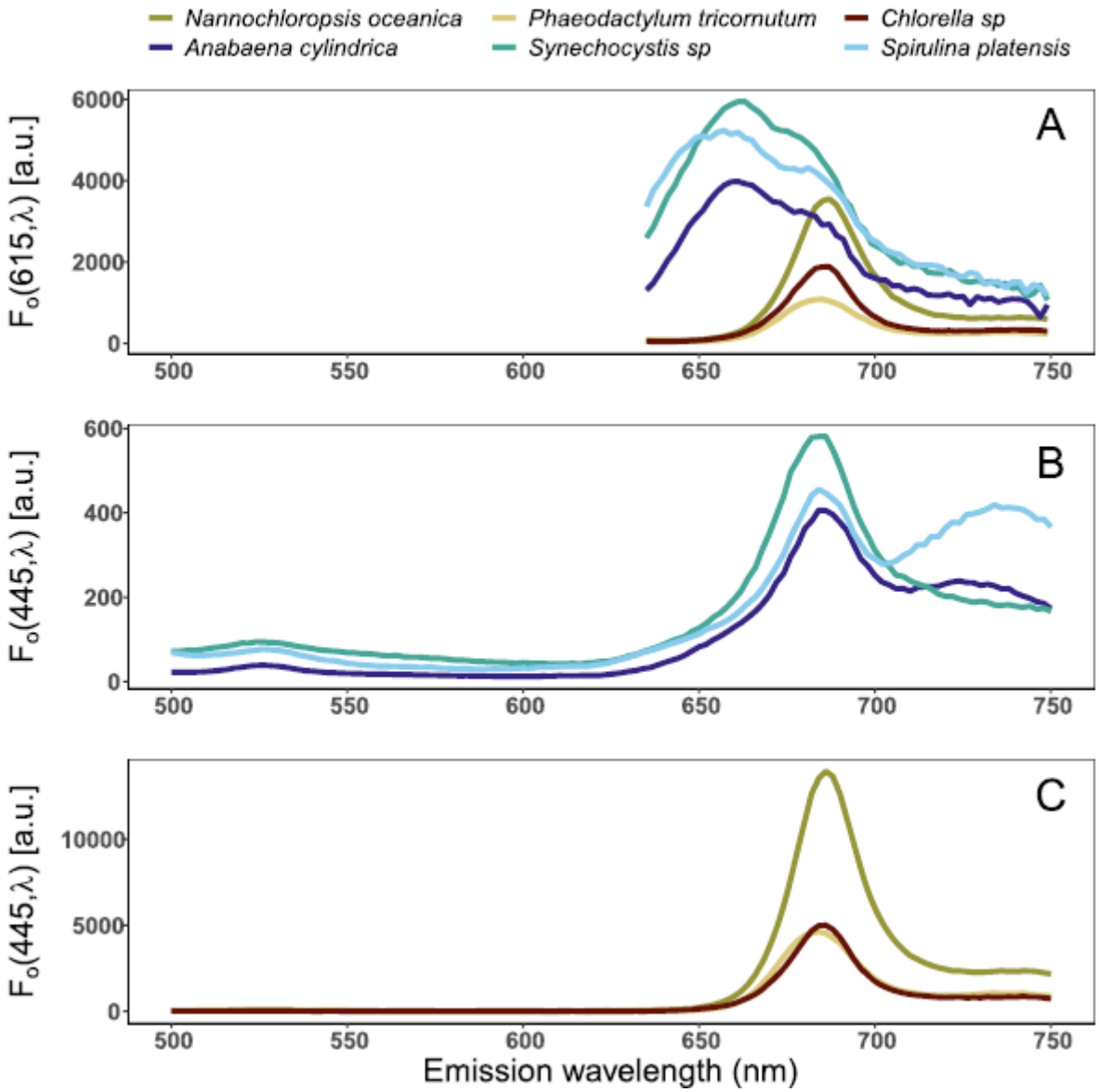

Figure 3. Emission spectra (F_o) of all cultures under orange excitation (615 nm) (A), cyanobacterial (B) and algal (C) cultures under blue excitation (445 nm).

4.3.2. Kinetics of algae

Algal species systematically exhibited maximum fluorescence at $F^r(\lambda, 685)$ which was quenched over time under both BG and white actinic exposure (Figure 5). Quenching appeared to be spectrally uniform except in the region of the emission of PSII Chla ($F^r(\lambda, 680–690)$) where quenching occurred earlier. This response was most clearly observed in *N. oceanica* and *P. tricornutum* under white actinic exposure and in *Chlorella* sp. under blue actinic exposure on the relative fluorescence data (Figure 7). The relative fluorescence for cyanobacterial cultures is shown in Figure 8. For each emission waveband, the slope of fluorescence change is derived from data shown in Figs 5 and 6 (i.e. the derivatives of the GAM fitting between each time

step) and is presented in Figs 9 and 10. These results indicate, at each emission waveband, the extent to which a photosynthetic or photoprotective mechanism was triggered, which could be considered as optical markers to differentiate cyanobacteria and algae responses to different light treatments. Fluorescence change over time (Figure 9) was steepest (fastest) at $F^r(\lambda, 685)$ and steeper (faster) at $F^r(445, \lambda)$ than $F^r(615, \lambda)$. The observed changes established more quickly under white actinic light in *N. oceanica* and *P. tricornutum* but under BG Actinic exposure in *Chlorella* sp. (Figure 9). In Figure 9, small regular variations (every 10-15 mins), are observed. These variations are likely attributed to the GAM smoothing process, which can enhance subtle variations in the signal (GAM overfitting), although relatively slow adjustment of sample temperature or unexplained fluorescence variations during quenching cannot be ruled out.

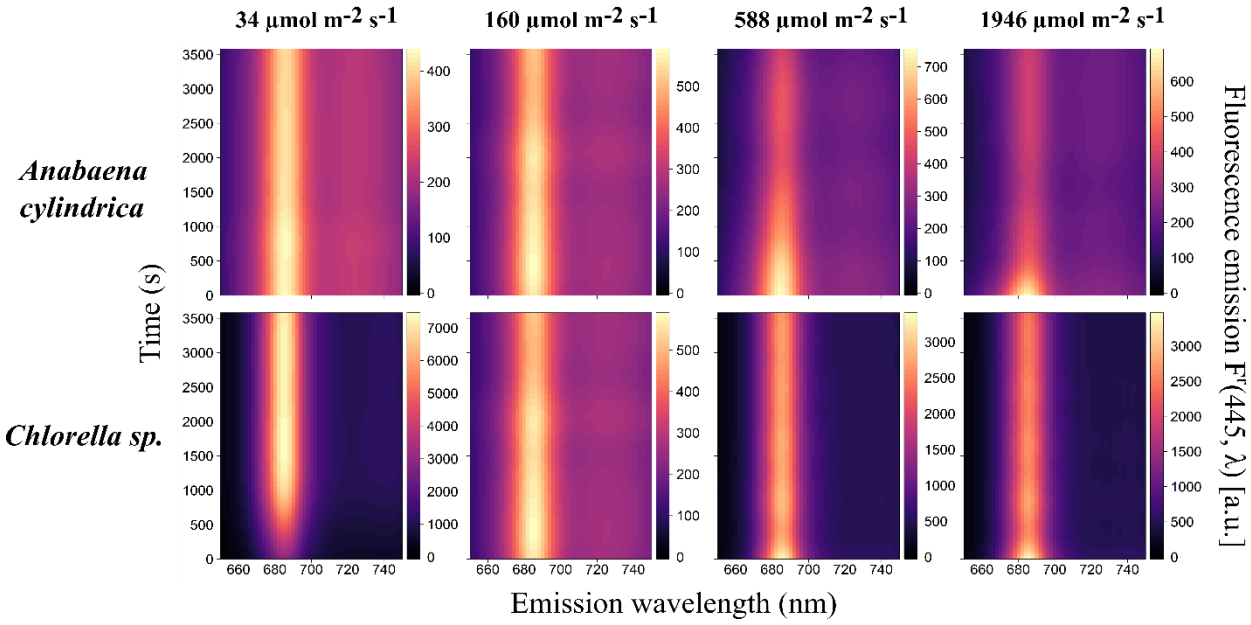

Figure 4. Kinetics measurements of *A. cylindrica* and *Chlorella* sp. under blue excitation (445 nm) and subjected to different intensities of white actinic light treatment. Data shown are fluorescence emission, $F^r(445, \lambda)$. Intensity values presented are the median of each of the following light treatment's intensity range: low (27–41 μmol m^{-2} s^{-1}), intermediate (152–168 μmol m^{-2} s^{-1}), bright (578–597 μmol m^{-2} s^{-1}) and intense (1931–1960 μmol m^{-2} s^{-1}).

Within-group similarities in the responses to continued actinic light exposure may present at different times during the experiment as an increase or decrease in observed fluorescence. This information is contained in the slope of change-over-time spectra but is not straight forward to visualize in this context. Whether the response was net positive or negative can be shown in "cumulative spectral change" plots (Figure 11) showing the net change per wave- band over the duration of the light exposure. The steepest slopes observed between subsequent wavebands are summarized in Table I and highlight wavebands where the fluorescence emission spectrum

is most likely to change during actinic light exposure. In algal species, these key wavebands were, expectedly, found in the $F^{r}(\lambda, 683–688)$ range irrespective of the light treatment. Key emission wavebands in the cyanobacterial cultures are described further below.
Spectral emission responses can be net zero over time when multiple photoadaptive processes occur within one emission waveband but with opposite responses.

Therefore, the timing of these changes was extracted by carrying out a similar procedure as described above but along the temporal (instead of emission) axis of the fluorescence change-over-time spectra. Results of this procedure should indicate when the strongest emission changes occurred (here, considered regardless of the emission waveband) in each light treatment. The "cumulative (or net) temporal change" is shown in Figure 12, and Table II summarizes the most prominent events of changing fluorescence emission. Cumulative temporal change (Figure 12A and B) highlighted the differences between BG Actinic and white actinic light treatments and the two excitation wavebands. In algae, only downward trends in fluorescence emission were observed, except for short-term oscillations, notably in *Chlorella* sp. and *P. tricornutum.* These small variations are likely attributed to the GAM smoothing process, the slow adjustment of sample temperature or unexplained fluorescence variations, as seen in Figure 9.
Evidence of fluorescence quenching was observed within 15 seconds after light exposure in *P. tricornutum* and *Chlorella* sp., whereas the same extent of fluorescence decrease established over 870–1020 seconds in *N. oceanica* (Figs 5, 7 and 9, Table II). Exposure to BG actinic led to slower quenching compared to white actinic in this culture (Table II). Using $F^{r}(615, \lambda)$, quenching was slower than under $F^{r}(445, \lambda)$ (Table II). This trend was not observed in the other algal species.

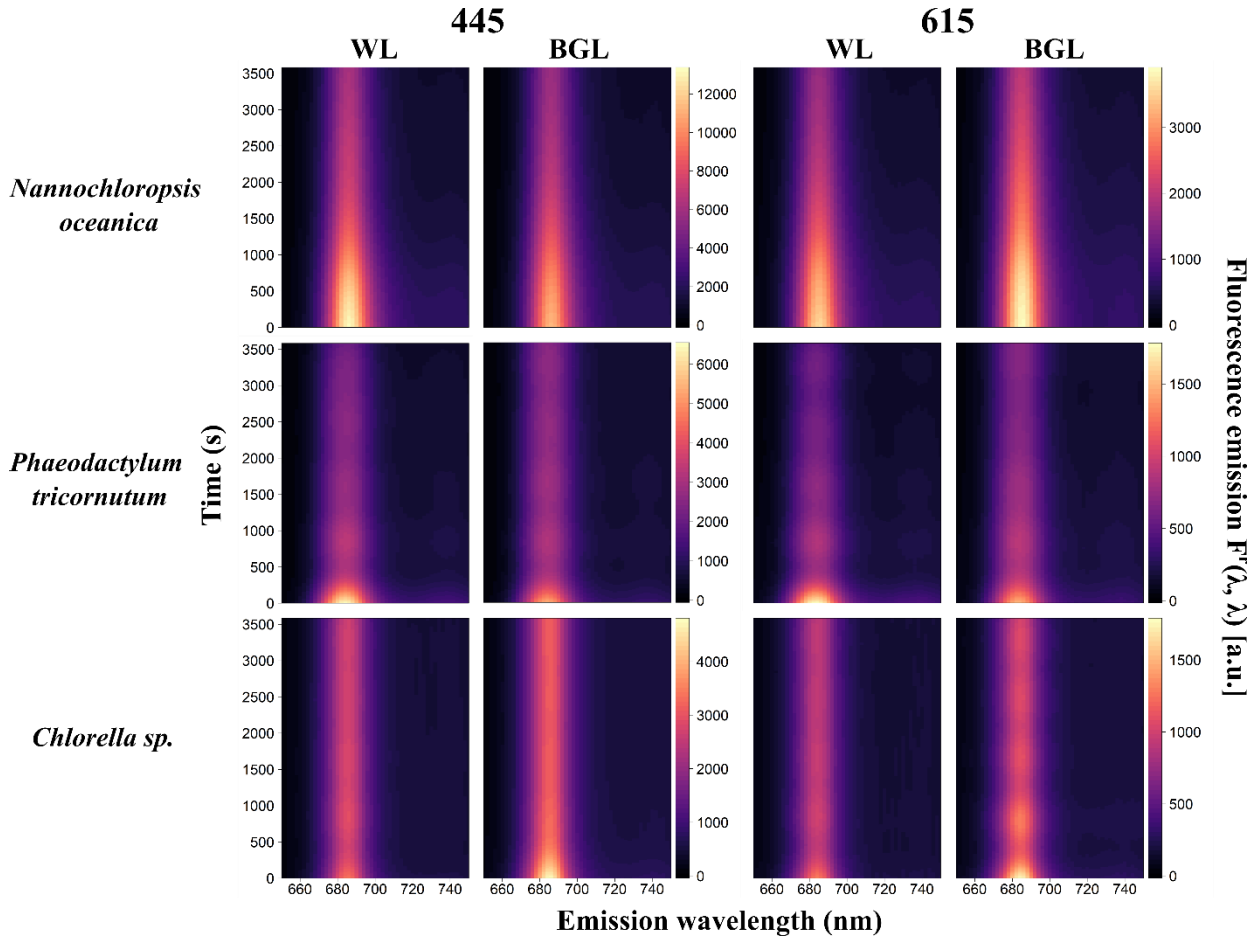

Figure 5. Kinetics measurements of algal species under blue (445 nm) and orange excitations (615 nm) and subjected to white actinic (WL) and BG actinic (BGL) light treatments. Data shown are fluorescence emission, $F^r(\lambda, \lambda)$.

Table 1. Wavebands (nm) which displayed the strongest change in fluorescence emission, determined from the cumulative spectral change (Figure 11): the steepest slopes observed between subsequent wavebands were identified as well as the waveband where it was identified; results are shown for species exposed to white actinic and BG actinic and under blue (445 nm) and orange (615 nm) excitations.

Species	White actinic		BG actinic	
	445	615	445	615
S. platensis	738	661	734	675
A. cylindrica	684	679	684	683
Synechocystis sp.	682	677	684	679
N. oceanica	688	685	686	687
P. tricornutum	684	685	684	683
Chlorella sp.	686	685	686	685

4.3.3. Kinetics of cyanobacteria

Relatively more diverse responses were found between the three cyanobacterial cultures. With orange excitation, the highest fluorescence emission was found around $F^r(615, 660)$ and $F^r(615, 685)$ (Figure 6). With blue excitation, fluorescence emission was generally lower, peaking around $F^r(445, 685)$ and in the near infrared ($F^r(445, >710)$) in *S. platensis* (Figure 6). The $F^r(\lambda, 650–750)$ under white actinic exposure yielded higher fluorescence than BG actinic exposure. This was consistent between both excitation wavebands and all cyanobacterial cultures (Figure 6).

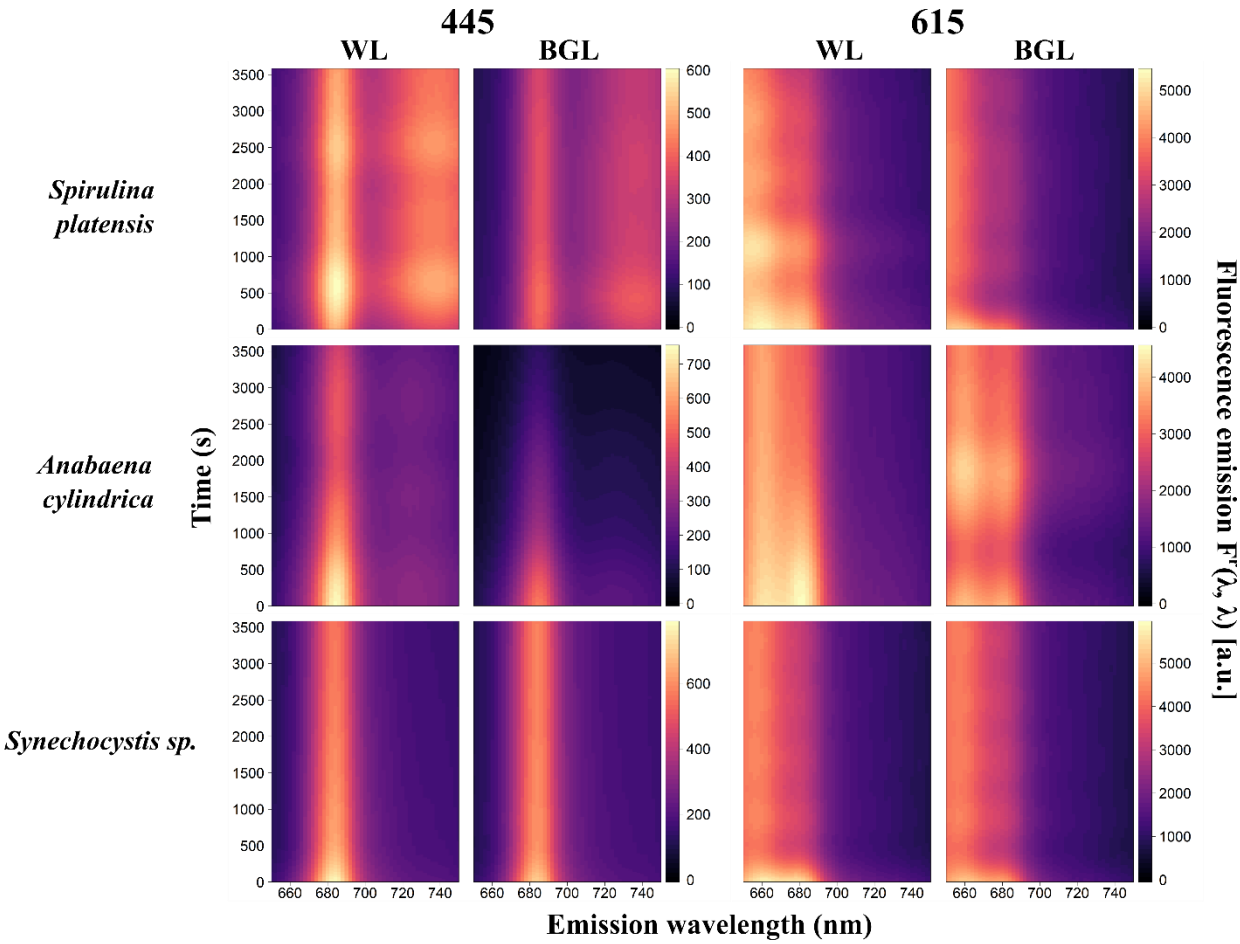

Figure 6. Kinetics measurements of cyanobacterial species under blue (445 nm) and orange excitations (615 nm) and subjected to white actinic (WL) and BG actinic (BGL) light treatments. Data shown are fluorescence emission, $F^r(\lambda, \lambda)$.

Table 2. Timing (s) of the strongest fluorescence emission change determined from the cumulative temporal change (Figure 12): the steepest slopes observed between subsequent time steps were identified as well as the timing when it was identified; results are shown for species submitted to white actinic and BG actinic and under blue (445 nm) and orange excitations (615 nm).

Species	White actinic		BG actinic	
	445	615	445	615
S. platensis	30	1410	15	15
A. cylindrica	630	630	600	195
Synechocystis sp.	15	15	15	15
N. oceanica	870	1005	930	1020
P. tricornutum	15	15	15	15
Chlorella sp.	15	15	15	15

Quenching was predominant in $F^{r}(\lambda, 650–685)$ in *S. platensis* and *A. cylindrica* (Figure 8). In *Synechocystis* sp., quenching prevailed at $F^{r}(445, 650–660)$ range and at $F^{r}(615, 685)$ (Figure 8). White actinic also caused quenching at $F^{r}(615, 730–750)$ (Figure 8).

In contrast to all other cultures, *S. platensis* and *A. cylindrica* exhibited both positive and negative fluorescence emission trends over the period of actinic light exposure. Under BG actinic, $F^{r}(615, \lambda)$ of *A. cylindrica* showed quenching during the first 600 seconds of exposure, followed by an increase up to 1750 s into the experiment (Figs 6, 8 and 10). White actinic exposure of *S. platensis* similarly resulted first in a period of quenching of $F^{r}(615, \lambda)$, followed by a fluorescence increase until 1100 s after the beginning of the experiment, followed by another decrease (Figs 6, 8 and 10). The $F^{r}(445, \lambda)$ increased from the first measurement to peak only after 600 seconds. Following a period of quenching, another peak occurred around 2600 seconds (Figs 6, 8 and 10). Under BG actinic exposure, $F^{r}(445, \lambda)$ in *S. platensis* increased from the start of light exposure to reach a maximum after around 500 seconds (Figure 8). These negative and positive emission trends were also observed on the cumulative temporal changes in *S. platensis* and *A. cylindrica* (Figure 12C–D).

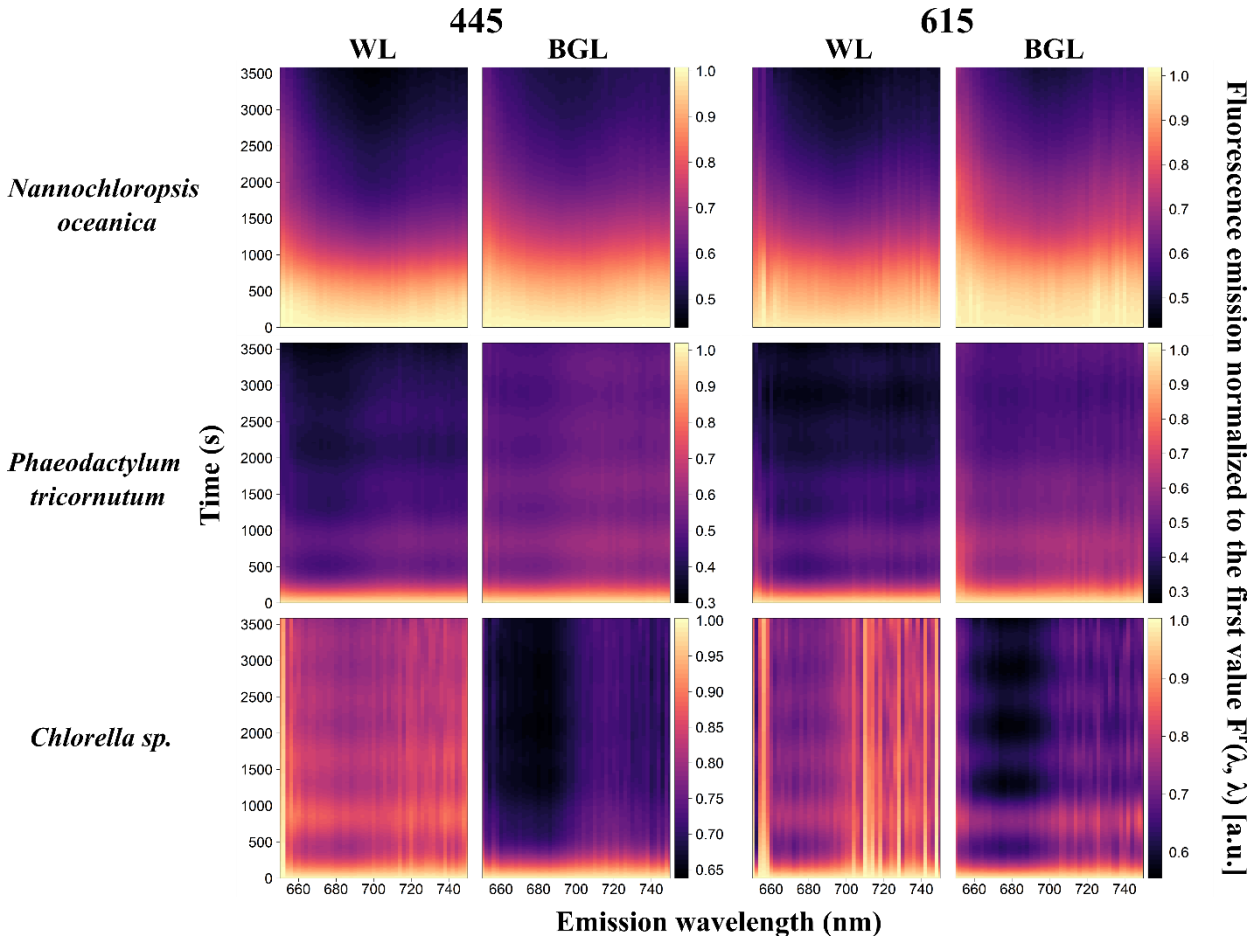

Figure 7. Kinetics measurements of algal species under blue (445 nm) and orange excitations (615 nm) and subjected to white actinic (WL) and BG actinic (BGL) light treatments. Data shown are fluorescence emission normalized to the first value, $F^r(\lambda, \lambda)$.

The observed fluorescence increases in *A. cylindrica* and *S. platensis* were observed in the 650–750-nm region, except for the region around $F^r(615, 685)$ and $F^r(445, 660–685)$ (Figure 8). Short-lived variability in fluorescence was also observed in cyanobacterial cultures (Figure 10). These short-lived variations were also observed in algal cultures under BG and white actinic light (Figure 7 and Figure 9) and appears as background fluorescence variations in comparison to larger variations. Short-lived variability in fluorescence is therefore likely attributed to artifacts from data post-processing or slow adjustment of sample temperature.

Fluorescence changes observed during actinic light exposure were more clearly expressed as $F^r(615, \lambda)$ compared to $F^r(445, \lambda)$ for cyanobacteria (Figure 10), with the strongest fluorescence changes observed over the 661–738-nm wavelength range (Table I). These changes were observed at longer wavelengths under blue excitation compared to orange excitation (Table I). Under BG actinic, changes were found at longer wavelengths compared to white actinic exposure and differences were clearly observed under orange excitation (Table I). The *S.*

platensis was an exception because changes observed under blue excitation were observed at longer wavelengths under white actinic (Table I). The changes in fluorescence were larger in *S. platensis* and *A. cylindrica* under BG actinic compared to white actinic, while the opposite behavior was observed in *Synechocystis* sp., as illustrated in the cumulative spectral changes in Figure 11C and D.

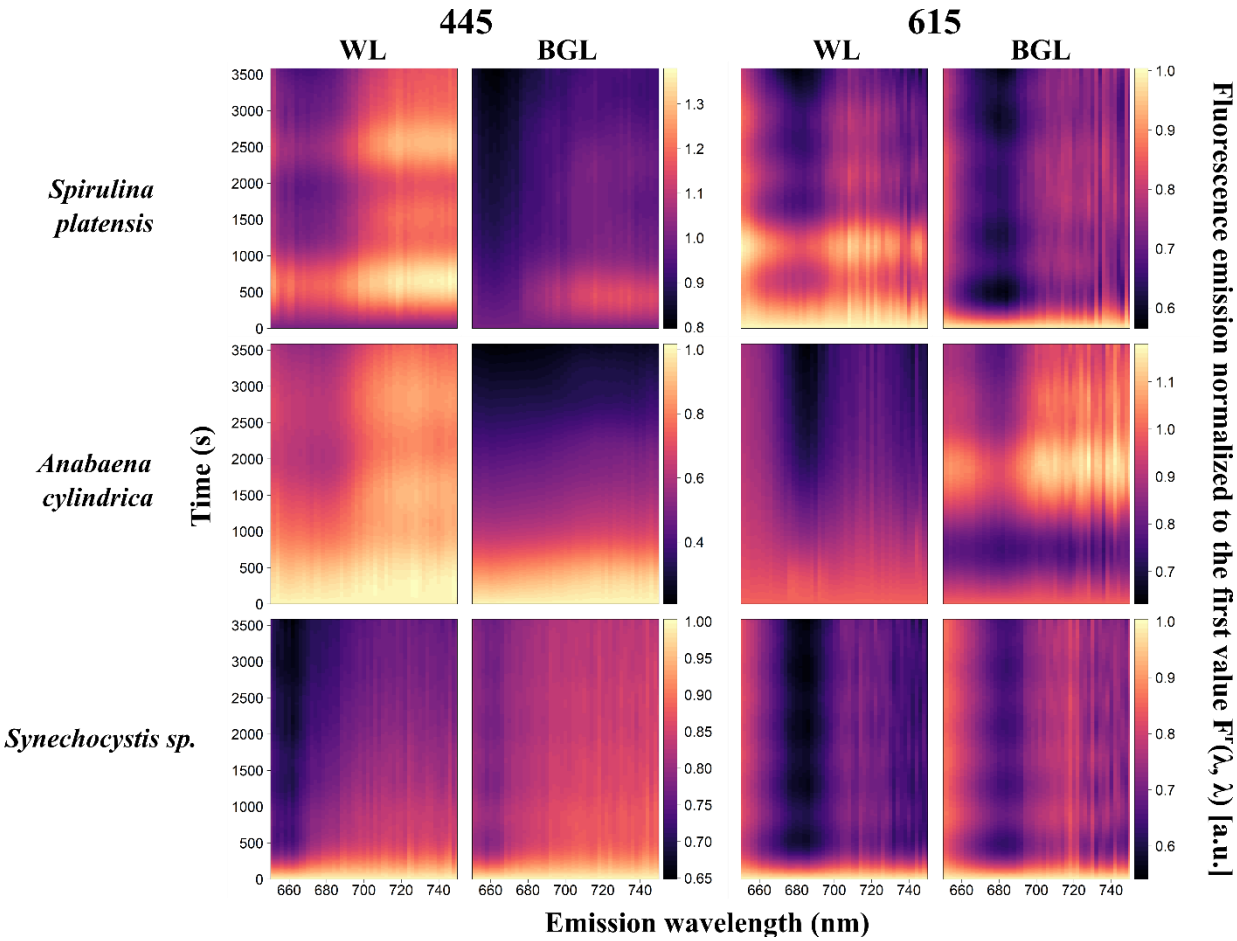

Figure 8. Kinetics measurements of cyanobacterial species under blue (445 nm) and orange excitations (615 nm) and subjected to white actinic (WL) and BG actinic (BGL) light treatments. Data shown are fluorescence emission normalized to the first value, $F^r(\lambda, \lambda)$.

In cyanobacteria, the strongest fluorescence changes occurred at different times and under different excitation wavebands and color of actinic light (Figure 10, Table II). In *Synechocystis* sp., the largest fluorescence changes occurred 15 seconds into the experiment under all excitation and actinic light treatments. In the other species, the most significant fluorescence changes, under BG Actinic exposure and orange excitation, occurred earlier. For example, the most significant $F^r(615, \lambda)$ changes in *S. platensis* were observed at 1410 s into the experiment under white actinic compared to just 15 seconds under BG Actinic (Figure 10, Table II).

For *A. cylindrica*, the largest fluorescence changes $F^r(615, \lambda)$ occurred 195 seconds after the beginning of the experiment under BG actinic compared to 630 seconds under white actinic (Table II, Figure 10). These species presented earlier quenching under BG actinic compared to white actinic (Figure 6).

4.3.4. Fluorescence emission ratios

The ratio of $F^r(445, 734)$ over $F^r(445, 684)$ was higher in cyanobacterial cultures than in algal cultures (Figure 13). In all algae, the ratio was around 0.2, whereas in cyanobacteria, it varied between 0.27 and 0.93 (Figure 13). This ratio increased over time in all cyanobacterial cultures under both white actinic and BG actinic exposure, particularly in *S. platensis* and *A. cylindrica*. The ratio of $F^r(445, 660)$ over $F^r(445, 684)$ was higher at around 0.3 in cyanobacteria compared to around 0.1 in algae (Figure 13). Under BG actinic exposure, in cyanobacterial cultures, this ratio was lower than under white actinic exposure. In algal cultures, it increased over time of exposure as a result of ongoing quenching around 684 nm.

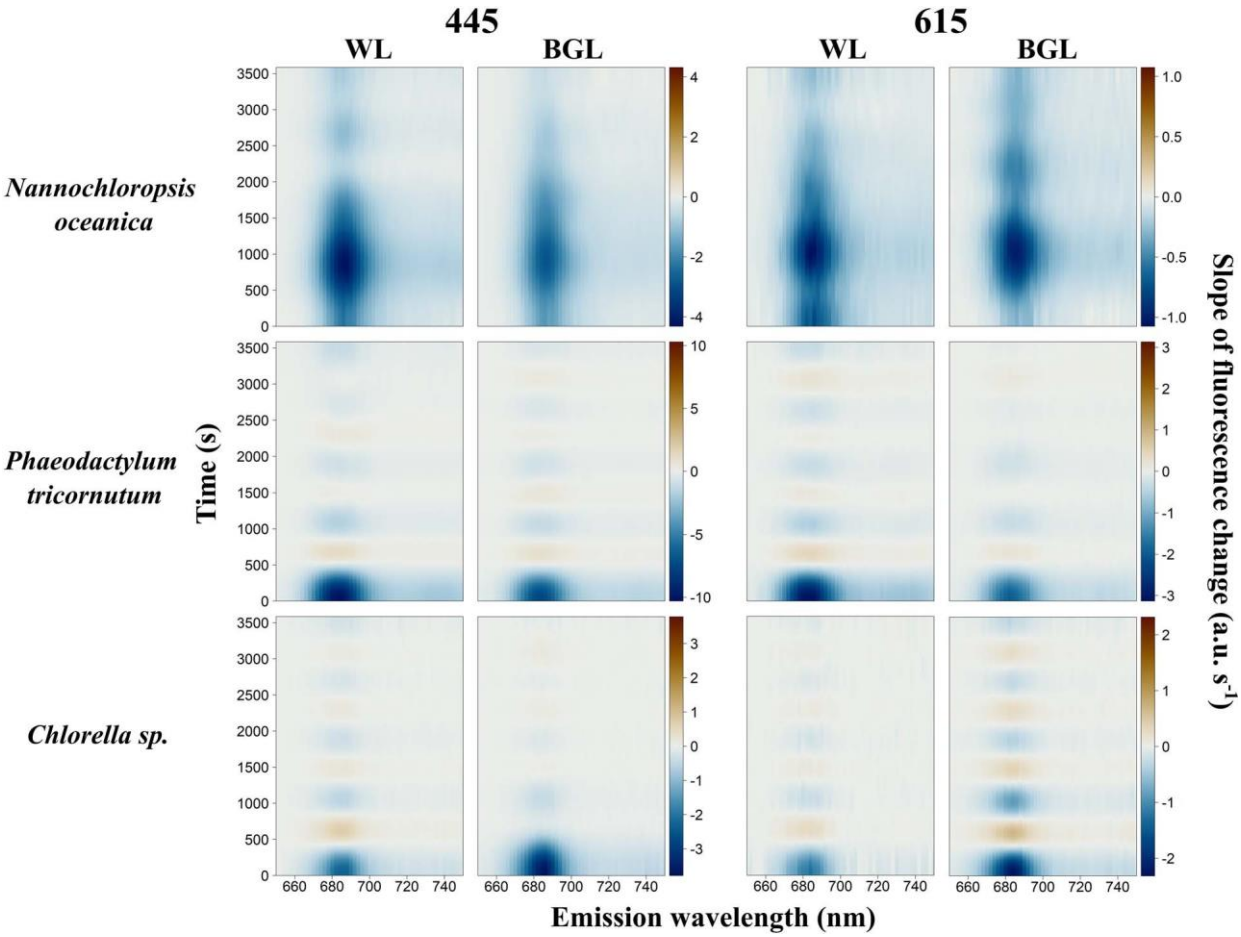

Figure 9. Kinetics measurements of algal species under blue (445 nm) and orange excitations (615 nm) and subjected to white actinic (WL) and BG actinic (BGL) light treatments. Data shown are the slope of fluorescence change (a.u.s^{-1}).

5. Discussion

5.1. Kinetic fluorescence responses in algae and cyanobacteria

A high degree of variability in fluorescence responses during continued light exposure was found between cyanobacterial cultures, both in terms of where along the emission spectrum and when any significant transitions occurred. By contrast, algal cultures showed a high level of consistency in their fluorescence responses over time. Cyanobacterial cultures presented events of increased fluorescence along the kinetics experiments under both actinic light colors and both excitation wavelengths as well as quenching which was observed in all experiments. These results were observed in both *A. cylindrica* and *S. platensis* but were not uniform between the two species. The events occurred neither at the same time nor under the same light conditions (excitation wavelengths and actinic light color). The events of increased fluorescence in our results after quenching episodes, observed in *S. platensis* and *A. cylindrica*, suggest a recovery of NPQ mechanisms and the possibility of succession or cooccurrence of

different NPQ mechanisms. To help distinguish different NPQ mechanisms, a recovery period after inducing low light exposure could be tested, but this is more suitable for an experiment employing single-turnover fluorescence instruments. Moreover, to obtain more information about photochemistry efficiency, time-resolved fluorescence measurements could be conducted.

Variability of the expression of quenching mechanisms under continued light exposure, as observed in the cyanobacterial cultures, is particularly important to consider as it highlights the difficulty to determine a generic light treatment protocol to elicit a diagnostic, targeted response in cyanobacterial fluorescence markers. On the other hand, homogeneity of algal responses is reassuring as their response can be largely predicted.

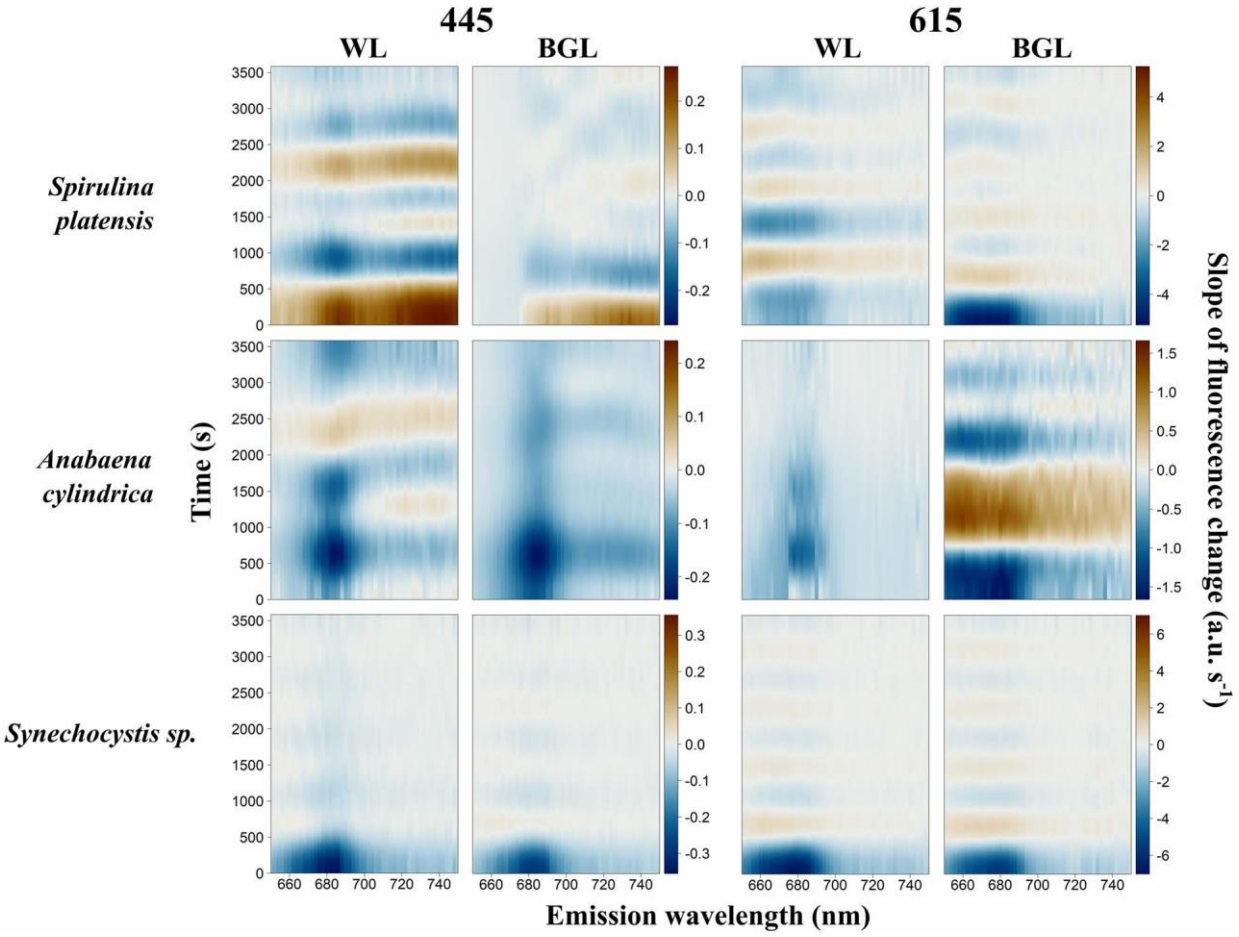

Figure 10. Kinetics measurements of cyanobacterial species under blue (445 nm) and orange excitations (615 nm) and subjected to white actinic (WL) and BG actinic (BGL) light treatments. Data shown are the slope of fluorescence change (a.u.s^{-1}).

5.2. BG actinic light and OCP-induced quenching

The choice of actinic light spectrum requires further consideration. BG actinic induced lower maximum fluorescence values than white actinic in all cyanobacterial cultures. The lower maximum emission under BG actinic is attributed to the fact that BG actinic mainly excites Chla linked to PSII, the number of Chla molecules in the PSII core complex is low (Caffarri et al. 2014) and ancillary chlorophylls linked to PSII are missing or in low quantities in most nutrient-replete cyanobacteria (Mimuro, 2004). The cyanobacterial PSII excitation spectrum is weak in the blue part of the spectrum compared to longer wavebands (Yentsch and Yentsch 1979, Schubert, Schiewer, and Tschirner 1989, Simis et al. 2012). BG actinic nevertheless appeared to induce more rapid fluorescence quenching at the beginning of the actinic light exposure experiments in two out of three cyanobacteria (*A. cylindrica* and *S. platensis*, Figs 6 and 8) under both orange and blue excitations. The BG actinic treatment was selected to highlight this feature and to explore whether it would induce NPQ quenching related to OCP protein as a photoreceptor in cyanobacteria. It has been shown that the genera *Anabaena*, *Synechocystis* and *Spirulina* all contain strains possessing genes encoding for OCP (Kerfeld et al. 2017). Higher quenching observed at the beginning of the experiment in *A. cylindrica* and *S. platensis* under BG actinic compared to white actinic support the assumption of NPQ induced by OCP in these strains. Moreover, abrupt changes in the cumulative emission change shortly after the start of the BG actinic experiment (compared to white actinic) and particularly under orange excitation support the theory of OCP-induced NPQ. The quenching process was not observed in *Synechocystis* sp., and fluorescence responses were not uniform between the two cultures that did show this behavior. In algae, none of these processes were observed and there was no marked difference between BG actinic and white actinic exposure. In conclusion, using only BG actinic (as has been practiced with some active fluorometers) risks overlooking the response of cyanobacteria due to a low signal amplitude but can show an abrupt quenching reaction in part of the cyanobacteria community which has potential diagnostic use. Overall, a broad actinic light spectrum is more likely to illicit a common response in all taxa and should be part of standard measurement protocols. The ability to modulate the spectral quality of the actinic light source should be considered to further study taxonomic differences in instrument designs intended for experimental use. For example, using multiple LEDs in a bank, the blue part of the spectrum could be activated first, followed by broad white LEDs.

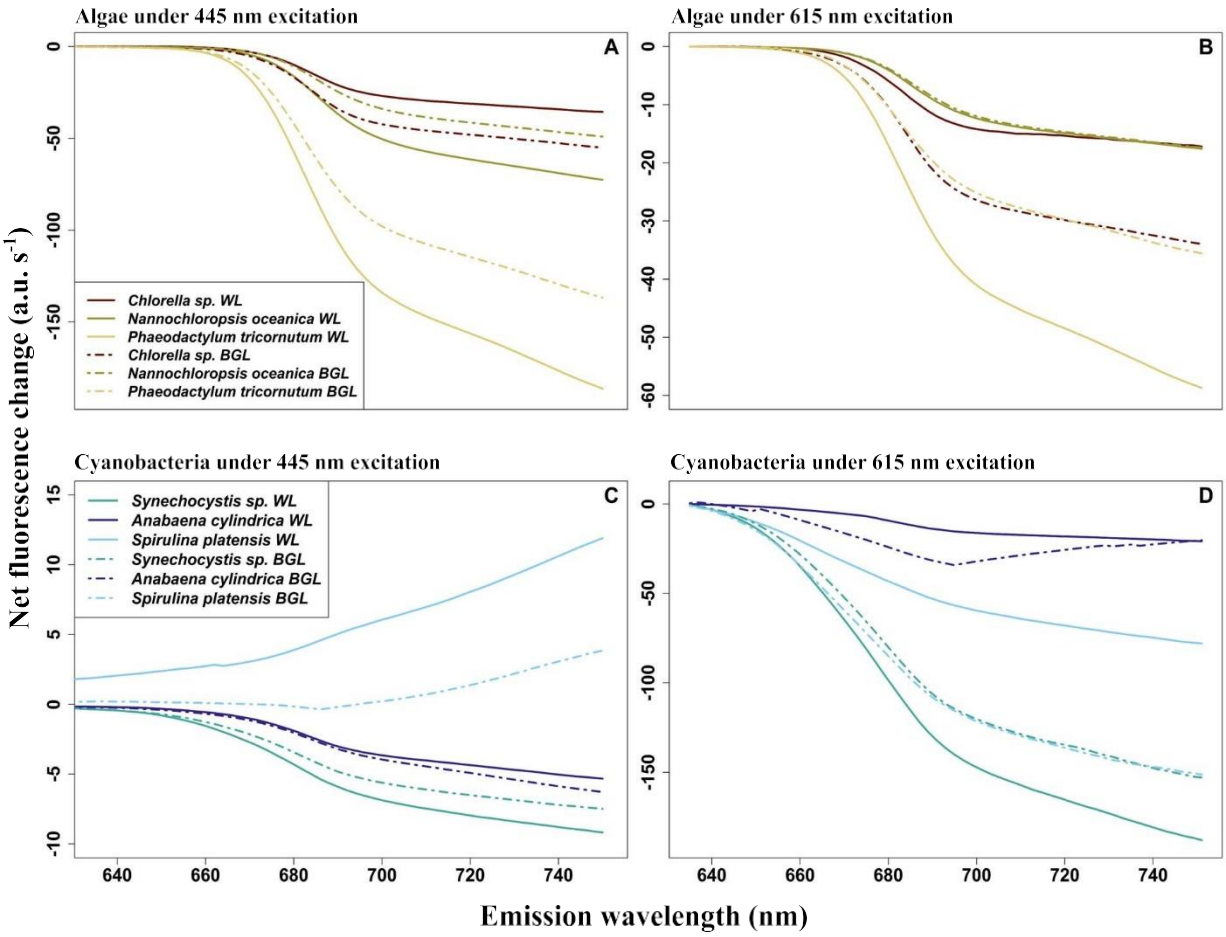

Figure 11. Cumulative spectral change under white actinic and BG actinic (BGL) light. The data are derived from Figure 9 and Figure 10. (A) Algae under blue excitation (445 nm), (B) algae under orange excitation (615 nm), (C) cyanobacteria under blue excitation (445 nm) and (D) cyanobacteria under orange excitation (615 nm). Note different vertical axis scalings.

5.3. PBS, PSII and PSI fluorescence emission wavelengths as emission markers

The role of the PBS pigments in cyanobacteria underlies the traditional naming of this taxonomic group as "BG algae." Low-light acclimated and nutrient-replete cultures show a clear distinction between the photosynthetic energy harvested using PBS in the 500–650-nm range in cyanobacteria and the well-described "green gap" in photosynthetic pigmentation in algae. The most prominent fluorescence emission markers, to distinguish cyanobacteria from algae, are therefore in $F_o(615, \lambda)$ and attributed to PBS fluorescence. Several experimental results further detail the role of PBS emission around 660 nm as well as the variability between species and groups in the PSII emission at 685 nm and PSI emission at 730 nm. Combined, these findings support potential methods to discriminate the cyanobacteria fluorescence in mixed communities, and they can be used to determine which excitation-emission pairs provide optimal targets for group-level discrimination. Kinetic or non-kinetic fluorescence

measurements should be conducted using different combinations of excitation wavebands 615 nm (and 445 nm) and emission wavebands among 660 nm, 730 nm and 685 nm targeting respectively PBS, PSI and PSII fluorescence emission. These measurements should be conducted on cultures submitted to different light and nutrients conditions or/and natural samples collected at different time of years, and in areas submitted to different nutrients concentrations. First, the PSI:PSII fluorescence emission ratios $F^r(445, 730)/F^r(445, 684)$ and $F^r(445, 660)/F^r(445\ 684)$ were consistently higher in cyanobacteria than algae, from low-light acclimated conditions and throughout actinic light exposure. This group-level difference may be expected to remain consistent between other cyanobacterial and algal strains and under widely ranging environmental conditions (such as light intensity and nutrient availability).

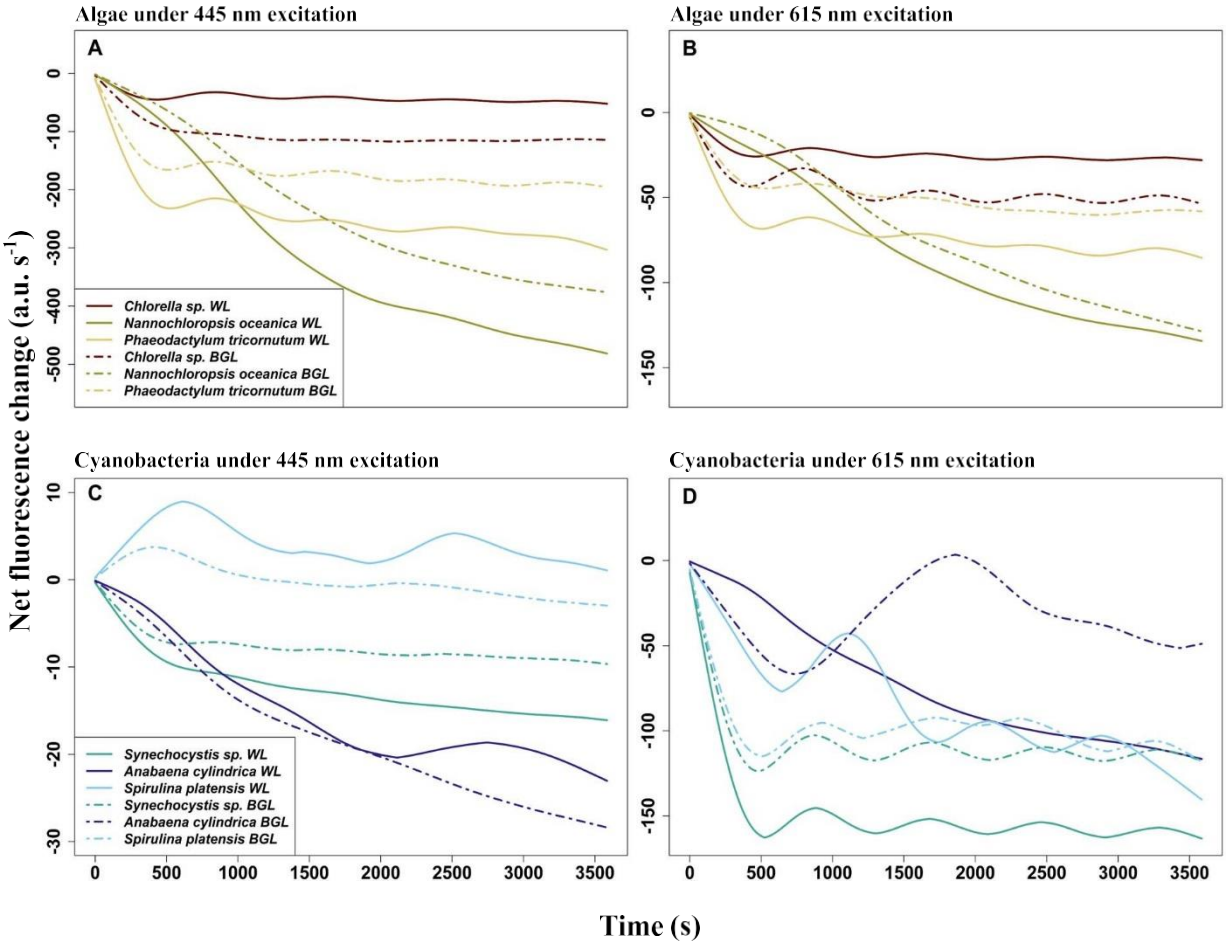

Figure 12. Cumulative temporal change under white actinic and BG actinic (BGL) light. The data are derived from Figs 9 and 10. (A) Algae under blue excitation (445 nm), (B) algae under orange excitation (615 nm), (C) cyanobacteria under blue excitation (445 nm) and (D) cyanobacteria under orange excitation (615 nm). Note different vertical axis scalings.

This is because the assignment of pigments to PBS, PSI and PSII remains diagnostic of cyanobacteria even if the expression of individual pigments is regulated. Cyanobacteria are known to have a lower proportion of Chla linked to PSII than PSI (Mimuro and Fujita, 1977), and the majority of photosynthetic phycobilipigments in natural samples (particularly freshwater) is expected to be associated with cyanobacteria. Thus, observing relatively high PSI:PSII and PBS:PSII fluorescence emission ratios in mixed communities should be indicative of cyanobacteria presence. There is, nevertheless, reason for caution because the PSI:PSII fluorescence emission ratio in *Synechocystis* sp. was only marginally higher (0.29) than the ratio found in algae (around 0.2) in some cases. Various explanations may be found for the wide range of the PSI:PSII fluorescence emission ratio between cyanobacterial cultures. First, natural variability of the proportion of Chla attached to PSI rather than PSII could easily explain the variability between the three cultures. Differences in the efficiency of charge separations in PSII between the strains exposed to the same culturing conditions should also not be ruled out, and this could vary significantly in natural samples. Moreover, stronger quenching of fluorescence emitted by PBS under exposure to BG actinic light, as seen in Figures 6 and 10 and Table II, in *S. platensis and A. cylindrica*, highlights the importance of PBS in discriminating cyanobacteria in mixed communities and support the choice of the emission band 660 nm.

5.4. PSI: PSII fluorescence emission ratio under actinic light exposure

The PSI:PSII fluorescence emission ratio generally increased over time under light exposure as the result of quenching at PSII, with small variations observed in all cultures most likely attributed either to data fitting procedures or slow temperature adjustment in the sample. Larger PSI:PSII fluorescence emission ratio variations could be linked to state transitions as photosynthetic pigment was increasingly decoupled from PSII (Calzadilla and Kirilovsky, 2020). The choice of actinic light source did not differentiate cyanobacteria PSI:PSII fluorescence emission ratio responses. Further measurements of the PSI:PSII fluorescence emission ratio under different light conditions, *in situ* and in laboratory, should be carried out to further model this response. If lower PSI:PSII fluorescence emission ratios in cyanobacteria compared to algae can indeed be generalized, an emission filter centered on emission at 730 nm would be a highly useful addition to future fluorescence sensors in addition to emission bands at 660 nm to target PBS and 684 nm to target PSII.

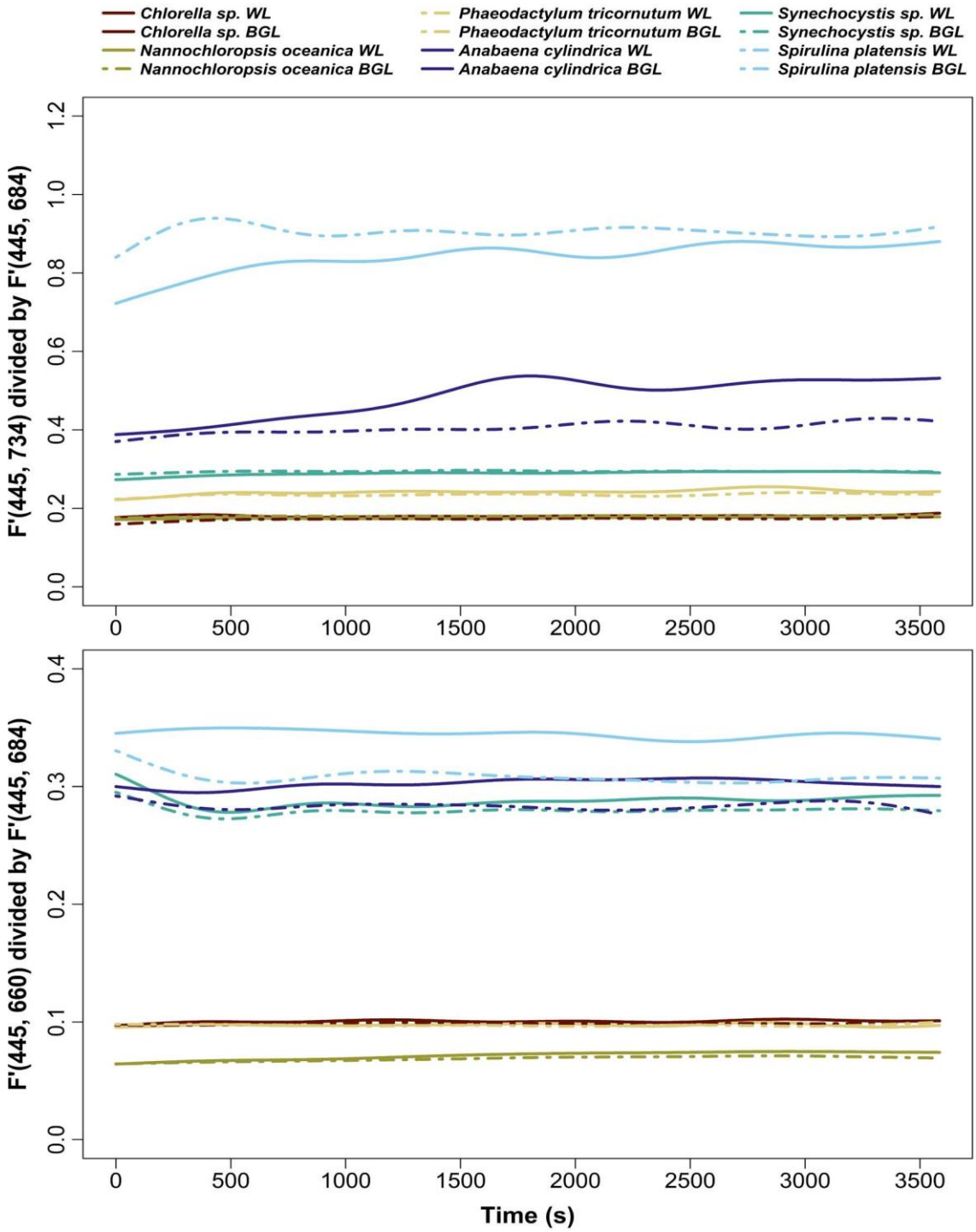

Figure 13. *F* ʳ(445, 734) divided by *F* ʳ(445, 684) (top panel) and *F* ʳ(445, 660) divided by *F* ʳ(445, 684) (bottom panel) over time and submitted to white actinic (WL) and BG actinic (BGL) light treatments.

6. Conclusion

A range of optical configurations were tested to determine suitable optical markers to target cyanobacteria using high spectral resolution fluorescence responses. Fluorescence kinetics measured in the 650–750 nm emission range differentiated responses between cyanobacteria and algae. In particular, three emission wavelengths can be recommended to be implemented in active fluorometry of natural phytoplankton communities, centered around 660, 684 and 730 nm which, respectively, target PBS fluorescence, Chla PSII fluorescence and PSI fluorescence. The choice of blue (445 nm) and orange (615 nm) excitation channels was justified because distinct fluorescence excitation spectra are consistently observed between algae and cyanobacteria, and these wavebands provide maximum separation of absorption by the main photosynthetic pigment groups.

BG actinic treatment did not lead to common responses in the three studied cyanobacterial cultures. A broadband actinic light should be preferred, although BG light does trigger a likely OCP response which could be observable even in natural samples so that it is worth considering a modulated use of BG and white actinic light at the start of the measurement protocol. The protocol duration of 1 hour permitted, in our experiments, the observation of photoacclimation mechanisms in both algal and cyanobacterial cultures. Nevertheless, environmental conditions (photoperiod, light intensity and nutrients' availability) influencing phytoplanktonic species growth and light acclimation consequently induce diverse kinetics responses under a range of actinic light intensities. Those conditions have to be carefully considered before determining the duration and intensity of the actinic light to apply. The ability to change the intensity of the actinic light should, therefore, be included in fluorometer designs. Further work needs to be carried out on 734/684 and 660/684 nm fluorescence emission ratios on a wider range of freshwater species grown under different environmental conditions and excitation wavelengths, while initial results suggest taxonomically distinct responses. Extending the selection of species to additional "spectral groups," according to the pigment composition of the peripheral antenna, is recommended. Ultimately, it may be challenging to combine multiple illumination and emission detection features in (low-cost or other) *in situ* fluorometers, but this is a promising way forward to determine cyanobacterial physiology in mixed natural communities.

CHAPTER 3: OPTIMISING MULTISPECTRAL ACTIVE FLUORESCENCE TO DISTINGUISH THE PHOTOSYNTHETIC VARIABILITY OF CYANOBACTERIA AND ALGAE

This chapter is based on : Courtecuisse, E., Marchetti, E., Oxborough, K., Hunter, P. D., Spyrakos, E., Tilstone, G. H., & Simis, S. G. (2023). Optimising Multispectral Active Fluorescence to Distinguish the Photosynthetic Variability of Cyanobacteria and Algae. Sensors, 23(1), 461.

Author Contributions to the paper: Conceptualisation, E.C., S.G.H.S., G.H.T., E.S., P.D.H. and K.O.; methodology, E.C. and S.G.H.S.; formal analysis, E.C.; investigation, E.C. and E.M.; resources, K.O.; data curation, E.C.; writing—original draft preparation, E.C.; writing—review and editing, S.G.H.S., G.H.T., E.S., P.D.H., E.M. and K.O.; visualisation, E.C.; supervision, S.G.H.S., G.H.T., E.S., P.D.H. and K.O.; project administration, S.G.H.S.; funding acquisition, S.G.H.S. and K.O.

1. Abstract

This study assesses the ability of a new active fluorometer, the LabSTAF, to diagnostically assess the physiology of freshwater cyanobacteria in a reservoir exhibiting annual blooms. Specifically, we analyse the correlation of relative cyanobacteria abundance with photosynthetic parameters derived from fluorescence light curves (FLCs) obtained using several combinations of excitation wavebands, photosystem II (PSII) excitation spectra and the emission ratio of 730 over 685 nm (F_o(730/685)) using excitation protocols with varying degrees of sensitivity to cyanobacteria and algae. FLCs using blue excitation (B) and green–orange–red (GOR) excitation wavebands capture physiology parameters of algae and cyanobacteria, respectively. The green–orange (GO) protocol, expected to have the best diagnostic properties for cyanobacteria, did not guarantee PSII saturation. PSII excitation spectra showed distinct response from cyanobacteria and algae, depending on spectral optimisation of the light dose. F_o(730/685), obtained using a combination of GOR excitation wavebands, F_o(GOR, 730/685), showed a significant correlation with the relative abundance of cyanobacteria (linear regression, *p*-value < 0.01, adjusted R^2 = 0.42). We recommend using, in parallel, F_o(GOR, 730/685), PSII excitation spectra (appropriately optimised for cyanobacteria versus algae), and physiological parameters derived from the FLCs obtained with GOR and B protocols to assess the physiology of cyanobacteria and to ultimately predict their growth. Higher intensity LEDs (G and O) should be considered to reach PSII saturation to further increase diagnostic sensitivity to the cyanobacteria component of the community.

Keywords: active fluorescence; multispectral; phytoplankton; cyanobacteria; algae; population dynamics; limnology

2. Introduction

Anthropogenic activities and climate change are primarily responsible for the increased biomass and occurrence of harmful algal blooms (HABs) (O'Neil et al. 2012, Paerl and Huisman 2008, Paerl and Huisman 2009). In freshwater systems, eutrophic conditions promote cyanobacteria dominance (Paerl, Hall, and Calandrino 2011, Paerl and Paul 2012, Wurtsbaugh, Paerl, and Dodds 2019), with the added risk of proliferation of toxin-producing species (Codd et al. 2005, Codd, Morrison, and Metcalf 2005). Although not every species of cyanobacteria that forms blooms is toxic, and not every strain of toxin-producing species will always produce toxins (Whitton and Potts 2000), regular monitoring for cyanobacteria blooms is critical to manage risk of toxin exposure to wildlife, recreational use or through water consumption, and

to limit the economic cost of mitigation measures. Risk management may include regulation of nutrient loads into water bodies or access to them. Monitoring is required at the global scale and therefore requires cost-efficient methods. Regular monitoring should be able to assess the growth and physiology of cyanobacteria and to determine the status of the bloom or the potential for a bloom to form.

Current monitoring techniques include microscopy identification and quantification, toxin analysis (Carmichael and An 1999, Baker et al. 2002, Oehrle, Southwell, and Westrick 2010), genetics and genomic detection (Pearson and Neilan 2008, Srivastava et al. 2013), and methods based on optical characteristics such as in vivo fluorometry (Beutler et al. 2002), flow cytometry (Becker, Meister, and Wilhelm 2002) and imaging flow cytometry (Campbell et al. 2013). Microscopic identification and quantification, toxicity analysis and genetic methods are highly diagnostic but can be time-consuming and costly. Optical methods, other than microscopy, include diagnostics based on size spectrum analysis, morphology, and absorption and fluorescence characteristics. With the possible exception of image-based classification, which requires training and supervision, these methods are not able to discriminate taxonomic detail beyond functional groups. Fluorometry-based techniques are also limited to distinguishing variations in photosynthetic pigment composition at group-level, but fluorescence can be used to determine photophysiological traits that can be related to population growth.

Several types of fluorometers exist to discriminate between phytoplankton groups, including cyanobacteria. The most affordable fluorometer designs (mostly handheld and sometimes submersible) measure fluorescence from single or multiple excitation wavebands and generally one emission waveband (Huot and Babin 2010, Suggett et al. 2006). These instruments assist in obtaining phytoplankton biomass estimates but are not able to assess phytoplankton physiology (Babin 2008). In contrast, saturating flash fluorometers measure variable fluorescence from which photochemical efficiency can be determined (Huot and Babin 2010). The most elaborate fluorometers in this category saturate photosystem II (PSII) within a single turnover of all reaction centres, while fluorometers operating with a longer 'multiple-turnover' flash can be more affordable (Babin 2008). From the fluorescence emission during the saturating flash, the minimum quantum yield of fluorescence F_o (in dark-adapted state, all reaction centres opened) and the maximum quantum yield of fluorescence F_m (all reaction centres closed) are obtained. From the determination of F_o and F_m, the variable fluorescence F_v (from $F_m - F_o$) and the maximum charge separation at PSII (F_v/F_m) are calculated. By further modulating ambient light availability, daily photosynthetic rates can be

modelled from the fluorescence response (Suggett et al. 2003), which in turn can be combined with nutrient and light availability in the natural environment to model and predict the growth of phytoplankton in a specific sample. Few studies to date have attempted to separate the fluorescence response from phytoplankton associated with specific pigment groups from natural samples (Houliez et al. 2017, Kazama et al. 2021).

Due to overlapping photosynthetic absorption spectra, a combination of fluorescence markers is required to estimate the primary production and photochemistry efficiency of cyanobacteria. Several existing variable fluorescence instruments have multiple excitation wavebands to target different spectral groups (Gorbunov et al. 2020, Schreiber, Klughammer, and Kolbowski 2012, Schuback et al. 2021). To distinguish the fluorescence response of cyanobacteria in the community, the fluorometer requires at least an excitation waveband which excites the main light-harvesting pigments, the phycobilipigments allophycocyanin, phycoerythrin and phycocyanin (Beutler et al. 2002, Gregor and Maršálek 2005, Gregor, Maršálek, and Šípková 2007, Seppälä et al. 2007). The light harvesting system, phycobilisome, constituted of phycobilipigments and the energy transfer in cyanobacteria are shown in Figure 1. Although rhodophytes and glaucophytes are also known to possess these pigments, their abundance is unlikely to be high in environments susceptible to cyanobacteria blooms (Dodds 2002, Dittami et al. 2017, Price et al. 2017). To accurately interpret the fluorescence signal and assess the physiology of cyanobacteria, excitation protocols targeting cyanobacteria should be able to fully saturate PSII through these diagnostic pigments. Moreover, the choice of emission wavebands for fluorometers is important to consider. Fluorescence emission is recorded at PSII chlorophyll *a* (Chla) emission around 685 nm in most fluorometers. In cyanobacteria, most of the Chla is associated with photosystem I (PSI) rather than PSII (Mimuro and Fujita 1977) and therefore has non-variable fluorescence (Johnsen and Sakshaug 2007). The interpretation of the fluorescence signal for the emission of PSII Chla can be complex if the sample contains cyanobacteria. Consistently higher emission ratios of 730 over 685 nm and 660 over 685 nm in cyanobacteria cultures compared to algal cultures was shown by Courtecuisse et al. (2022). Consequently, they suggested implementation of an emission waveband centred on phycobilisomal emission around 660 nm and an emission waveband centred around PSI Chla at 730 nm. Single-turnover fluorometers with emission at 650 nm have not been produced, possibly due to the challenge of cross-talk between excitation sources and emission filters centred on 650 nm.

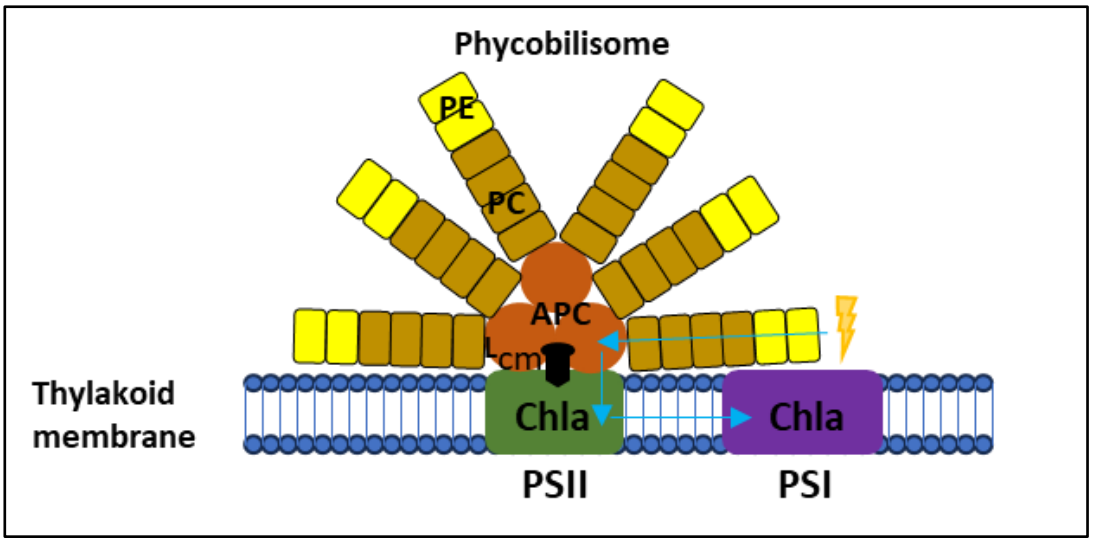

Figure 1. Schematic drawing of photosynthetic apparatus, phycobilisome and energy transfer in cyanobacteria. Chla: Chlorophyll *a*, PE: Phycoerythrin, PC: Phycocyanin, APC: Allophycocyanin, PSII: Photosystem II, PSI: Photosystem I, Lcm: Core-membrane linker. The energy transfer is represented by blue arrows. This figure has been adapted from Mimuro (2004) and Grigoryeva (2020). Rods of PE are not present in all cyanobacteria species.

A new fluorometer, the LabSTAF (Chelsea Technologies Group, UK), shows increased potential to target cyanobacteria in the natural environment. The LabSTAF is a portable robust and compact instrument suited for regular on-site monitoring. The instrument is well suited for long-term continuous and autonomous measurements due to a number of software and hardware features. These include a mixing feature with a flow-through stirrer, temperature control, a sample exchange feature using a separate peristaltic pump controlled by the instrument, as well as an optional cleaning cycle using the pump and additional solenoid valve controller. The instrument has high signal sensitivity (suitable for oligotrophic conditions), which means that the full seasonal phytoplankton variability may be observed. Moreover, the instrument introduces several optical features which increase its potential to target distinct pigment groups, including those diagnostic of cyanobacteria. These include multiple excitation wavebands (see below), emission detection using 685 nm and 730 nm bandpass filters and the automated function to measure photosynthetic excitation spectra. The suitability of these specific features to target cyanobacterial photophysiology is discussed below.

The instrument is based on the concept of a Single Turnover Active Fluorometer (STAF) and uses seven excitation wavebands centered at 416, 452, 473, 495, 534, 594 and 622 nm, which can be combined to target a range of photosynthetic pigments based on their spectral characteristics. Wavebands at 534 (green) and 594 nm (orange) are particularly useful, as these target different forms of phycoerythrin that are common in both oceanic and freshwater cyanobacteria, as well as the short-wavelength tail of phycocyanin absorption (Falkowski and

Raven 2013). The LabSTAF is equipped with a broad-spectrum actinic light source to create Fluorescence Light Curves (FLCs) that are synonymous with photosynthesis–irradiance curves used to estimate and model primary production. The single turnover variable fluorescence is recorded at the waveband 685 nm to target PSII Chla. In addition it obtains F_o, F_m and F_v at 730 nm at the start of a measurement sequence, using a linear actuator to switch between 685 nm and 730 nm bandpass filters (± 10 nm FWHM). This Dual Waveband Measurement (DWM) configuration was initially designed to correct for the pigment packaging effect(Oxborough 2021, Boatman, Geider, and Oxborough 2019). We propose that this configuration may also be sensitive to the presence of cyanobacteria due to allocation of Chla to PSI rather than PSII, resulting in a higher 730 over 685 nm emission ratio when Chla light absorption is targeted. The LabSTAF is further preconfigured to measure the photosynthetic excitation spectrum across the seven excitation wavebands. This is done using one of two distinct protocols, differing in the light dose used at the spectral excitation maximum of algal and cyanobacterial pigment groups, respectively.

In this study, we assess the ability of the LabSTAF fluorometer to target physiological properties of cyanobacteria in a freshwater reservoir where cyanobacteria form annual blooms. Various combinations of fluorescence markers are tested and compared against relative phytoplankton abundance and nutrient availability. Specifically, we analyse the correlation of relative cyanobacteria abundance with photosynthetic parameters derived from FLCs obtained using combinations of excitation wavebands, the interpretation of PSII excitation spectra (both prokaryotic cyanobacteria and eukaryotic algae-optimised protocols), and the emission ratio of 730 over 685 nm obtained with excitation protocols targeting cyanobacteria versus algae. Appropriate predictors of cyanobacterial photophysiology within the phytoplankton community are expected to reflect a positive response of cyanobacteria to conditions favouring their growth, such as reduced N:P ratios and following depletion of silicate in the natural succession from spring (diatoms abundant) to summer (cyanobacteria dominant) community composition. Moreover, we expect fluorescence dynamics to reflect the phytoplankton group abundance estimates from microscopy counts. Comparing the various options for light-excitation protocols, we hypothesise that the photophysiological characterisation of algae and cyanobacteria is best achieved by interpreting single-turnover fluorescence from blue and green–orange light to target diagnostic pigment groups. Saturation and specificity of cyanobacteria fluorescence from green–orange excitation is the most critical test of the system, due to lower excitation energy achieved with light emitting

diodes and the overlap with absorption by phycobilipigments and short-wavelength tails of both chlorophyll *c* and Chla in this range of the spectrum.

3. Materials and Methods

3.1. Study Site

Roadford Lake is the largest drinking water reservoir in Devon County in the United Kingdom (Figure 2), part of the catchment of the river Tamar. It has a net storage of 34,500 million litres and a surface area of 295 hectares. Water is pumped from a draw-off tower situated in the south part of the reservoir, near the dam where there is also an overflow tower (Lawson et al. 1991). The lake is fed by the river Wolf in the northeast and from Westweek inlet, a stream to the northwest.

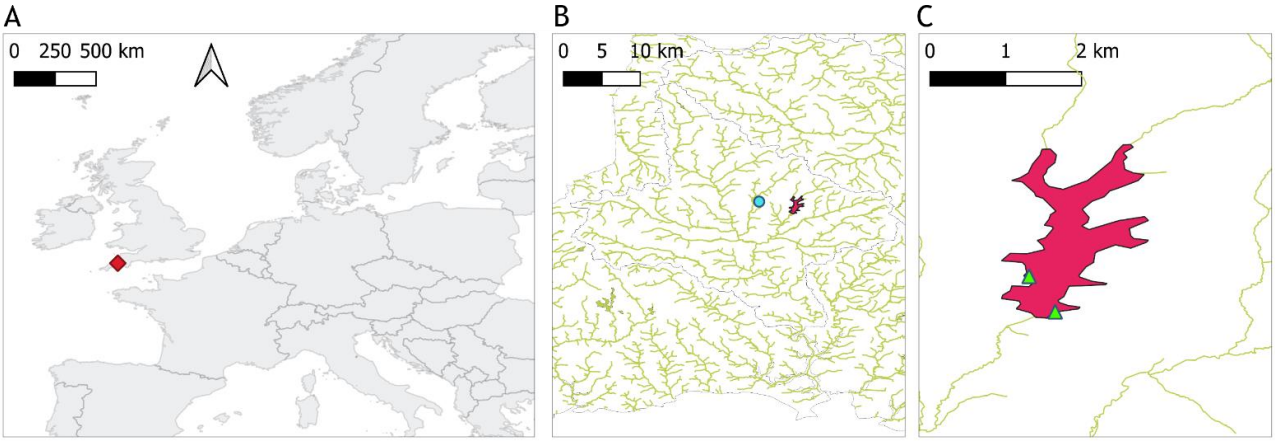

Figure 2. Location of Roadford Lake. A: The location of the reservoir indicated with a red diamond marker. B: The meteorological station "Virginstow, Beaworthy" represented by a turquoise circle to the west of the reservoir in magenta color. C: Green triangles represent the sampling points on the reservoir.

High abundances of cyanobacteria have been recorded in samples analysed by the water utility company using light microscopy, since at least spring 2002, and often year-round (Figure 3, see Section 2.3 for methods). Water samples for this study, 23 in total, were collected between the 12th of April and the 16th of October 2020. Samples were taken every two weeks during the spring period, and weekly during the summer, when high cyanobacteria biomass was expected. Surface water was sampled from a jetty near the western shore with a bucket in the first 0.5 m from the surface in approximately 3 m-deep water (depending on reservoir volume), except for the first seven samples which were taken directly from the east shore whilst access to the jetty was restricted (Figure 2C). During calm weather, any accumulation of cyanobacteria visible at the surface was mixed with the surface water to ensure that the

sample was homogenously representative of conditions in the top layer. Water temperature was recorded at the time of sampling, and approximately 2 litres of water were brought to the laboratory in an insulated container, for further analysis on the same day. Total daily rainfall was retrieved from the National Meteorological Library and Archive of the UK Met Office for station "Virginstow, Beaworthy" (50°42'36.0" N 4°17'45.6" W) which is located around 4 km west of Roadford Lake (Figure 2).

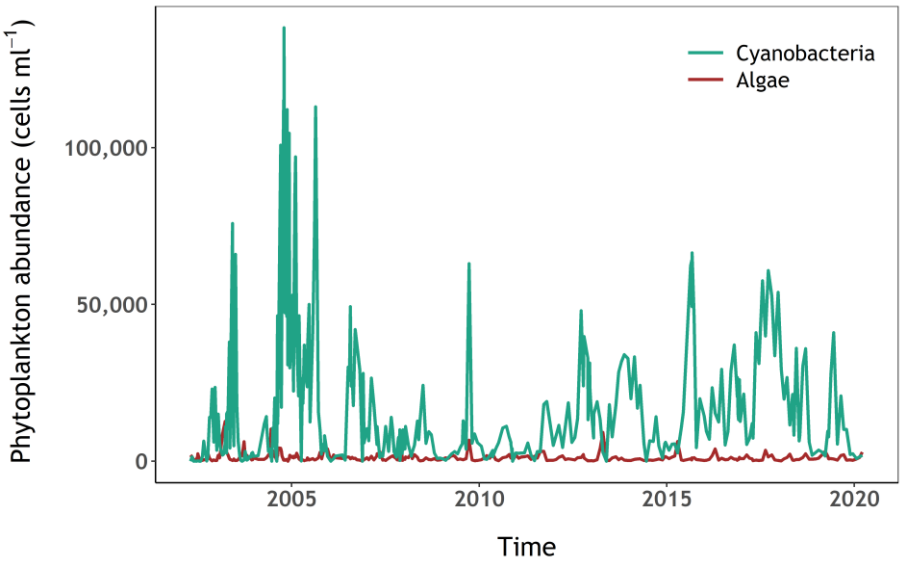

Figure 3. Algae and cyanobacteria abundance (cells mL^{-1}) at Roadford Lake.

3.2. Single-Turnover Fluorescence

A dedicated LabSTAF instrument (serial number 19-0105-006) was used to characterise the photophysiology of phytoplankton at Roadford Lake. FLCs were measured on samples taken from 29th May to 16th October 2020, using the range of fluorescence excitation protocols described in Table 1. These protocols were selected to target semi-isolated pigment groups and the associated phytoplankton taxa through combinations of excitation wavebands expected to lead to full saturation of PSII, based on the work of Bryant et al. (1979) and Johnsen and Sakshaug (1996). Protocols differed in saturation pulse length (100 or 200 µs) to accommodate saturation, and the combination of excitation wavebands denoted B(lue) = 452 nm, G(reen) = 534 nm, O(range) = 594 nm, and R(ed) = 622 nm (Table 1). The Light-Emitting Diodes (LEDs) used to provide the excitation energy were always set to their maximum intensities (G = 10,500, O = 2896 and R = 7594 µmol photons m^{-2} s^{-1}) except for the B LED

which adapted automatically to adjust to the phytoplankton composition and abundance for the B protocol (2 are implemented in the instrument, B1and B2). Moreover, optimal B intensity values within the GORB and GOB protocols were determined prior to any measurements, from exposure using only the B LEDs with a pulse length of 200 µs. These values for the B LED were then adopted in the GORB and GOB protocols with the aim to see if results from separate protocols were additive. Intensity ranges of B LEDs are respectively between 14,108 and 16,819 µmol photons m^{-2} s^{-1} for B1 LED and between 14,068 and 16,719 µmol photons m^{-2} s^{-1}. The intensity range of each protocol through the all sampling period is described in Table 1. Each FLC included 12 actinic light steps from 0 to 1200 µmol photons m^{-2} s^{-1}. The actinic light spectra had a peak at 455 nm and shoulder from 480 nm to 655 nm. Samples were dark adapted for at least 20 min before each analysis to allow all reaction centres to open to correctly measure F_o.

Table 1. Excitation protocols tested to target pigments associated with specific phytoplankton groups, as described by Bryant et al. (1979) and Johnsen and Sakshaug (1996). Phycobilipigments include phycoerythrin, allophycocyanin and phycocyanin.

Protocol	Excitation wavebands (nm at centre)	Intensity range (µmol photons m^{-2} s^{-1})	Pulse length (µs)	Photosynthetic pigment groups targeted	Phytoplankton group targeted
B	452, 452	28,175 — 33,538	100	Chlorophylls *a*/*b*/*c*, carotenoids	Algae, weak signal from cyanobacteria possible
GOR	534, 594, 622	20,990	200	Phycobilipigments Chlorophylls *a*/*b*/*c* and carotenoids	Cyanobacteria with weaker signal from algae likely
GORB	452, 452, 534, 594, 622	49,513 — 54,528	200	Chlorophylls *a*/*b*/*c*, carotenoids and phycobilipigments	Whole community
GOB	452, 452, 534, 594	41,919 — 46,933	200	Chlorophylls *a*/*b*/*c*, carotenoids and phycobilipigments	Whole community with a slower saturation response compared to GORB
GO	534, 594	13,395	200	Phycobilipigments, Chlorophyll *c*, carotenoids	Cyanobacteria, cryptophytes and rhodophytes

Photosynthetic parameters are expressed here as a function of excitation and emission waveband (λ_{ex}, λ_{em}). FLCs parameters and excitation spectrum were reported only for the emission band (λ_{em}) 685 nm, but single turnover curves were also recorded at λ_{em} = 730 nm. Where multiple excitation wavebands are considered, the excitation waveband is referred to by the abbreviations given in Table 1 (e.g., B, GOR). Several photosynthetic parameters were determined from each FLC: $alpha_{PII}$, J_{PII}, P_{max}, σ_{PII}, F_v/F_m and F_o. An example of FLC and ST induction curve obtained with the LabSTAF are shown in the introduction of the thesis (Figure 5 and 6). σ_{PII}, F_o, F_v, F_m (and consequently F_v/F_m) and $alpha_{PII}$ are derived from induction curves at each step of the FLC (Figure 5, Thesis introduction). JPII is a secondary photosynthetic parameter derived from the primary photosynthetic parameter σ_{PII} defined from ST induction

curve and the photon irradiance E. However, P_{max} is defined from the complete FLC (Figure 6, Thesis introduction). The following definitions are repeated from the instrument manual (Oxborough 2021) and the terminology of these photosynthetic parameters is derived from Oxborough (2021) and Schuback et al. (2021).$alpha_{PII}$ defines the initial rate at which photons are used to drive PSII photochemistry during a single turnover (ST) pulse. This parameter is a proxy of saturation of PSII photochemistry. A value of $alpha_{PII}$ between 0.042 and 0.064 is considered optimal and reflects a good ST curve fit. J_{PII} measures the photon flux through the absorption cross section for PSII photochemistry provided by a single PSII complex. J_{PII} is interpreted as electron transport rate (ETR) on the assumption that each photon used to drive PSII photochemistry results in the transfer of an electron out of PSII. ETR, in turn, determines the rate of electron transport which controls phytoplankton carbon fixation and growth (Silsbe et al. 2015). ETR can express the ability of the phytoplankton to achieve metabolic processes. J_{PII} is calculated as:

$$J_{PII} = \sigma_{PII}' \times F_q'/F_v' \times E \qquad (1)$$

Where σ_{PII}' is the absorption cross section of PSII photochemistry of each open PSII complex in nm^2 $PSII^{-1}$, F_v' is the variable fluorescence in light-adapted conditions and F_q' is the difference between F_m' and F_o', which are respectively the maximum and minimum fluorescence in light-adapted conditions and E is photon irradiance in photons m^{-2} s^{-1}. JPII units are electrons $PSII^{-1}$ s^{-1}.

P_{max} is the maximum specific photosynthetic rate which expresses the phytoplankton photosynthetic capacity in optimal ambient light conditions. σ_{PII} is the absorption cross section of PSII, which is the product of the absorption cross section for PSII light-harvesting and the probability that an absorbed photon will be used to drive PSII photochemistry. σ_{PII} is calculated as :

$$\sigma_{PII} = alpha_{PII} \times 100\, EST \qquad (2)$$

Where EST is the irradiance provided to the sample by the LEDs during a ST pulse in photons m^{-2} s^{-1} and $alpha_{PII}$ units are photon $PSII^{-1}$ μs^{-1}.

F_v/F_m measures the photochemistry efficiency, with F_v the variable part of fluorescence obtained from the difference between F_o and F_m, the minimum and maximum fluorescence, respectively. Values of F_o, F_v/F_m, $alpha_{PII}$ and σ_{PII} tend to decrease along the light steps of each FLC. The largest value of these parameters may be observed at or shortly after the first light

step. Consequently, reported values of F_o, F_v/F_m, $alpha_{PII}$ and σ_{PII} were averaged over the first five light steps to characterise each FLC. The maximum value in each FLC was selected to describe the ETR parameter. P_{max} is provided once per FLC.

ST curves were recorded at both emission wavebands (685 and 730 nm) and with the B and GOR protocols, prior to running each FLC. Excitation spectra of $F_v(\lambda_{ex}, 685)$ and $\sigma_{PII}(\lambda_{ex}, 685)$ were also collected before running FLCs. Depending on the $F_o(452, 685)$ response as a proxy for the presence of chlorophylls *b* and *c*, the LabSTAF optimises and scales the excitation spectrum to the response from either blue or orange excitation (Oxborough 2021), here referred to as algae and cyanobacteria-optimised protocols, respectively. The function generating excitation spectra is based on three reps of a combination of seven wavebands (Oxborough 2021). The protocol designed for targeting algae have the common LED waveband 452 nm for all wavebands combination while the other protocol designed for targeting cyanobacteria have the common LED waveband 622 nm for all wavebands combination (Oxborough 2021). The protocol targeting cyanobacteria have all LEDS set to theirs maximum to achieve better saturation while the other protocol has the 1st 452 nm channel set by the auto LED function, the 2nd 452 nm channel fixed at 72 % of the maximum value determined by the auto LED function, the 416 nm and 473 nm channel values set up to be close to the 1st 452 nm channel, and the other channels set up to their maximum values (Oxborough 2021). The choice of the excitation protocol is based on the 452 nm channels values. If these channels are the only one without non-zero value the protocol targeting algae will be automatically chosen. However, if non-zero values are found at other channels, the second protocol will be chosen (Oxborough 2021). F_v and $\sigma_{PII,,}$ are calculated as a difference of values between each LED combinations, considering that saturation has been obtained (Oxborough 2021). For the protocol saturating cyanobacteria, it might be difficult to obtain saturation, so the function have the possibility to increase the pulse length of the LEDs. An example of excitation spectra obtained with the algae-optimised protocol, measured on a natural community is presented in Figure 4.

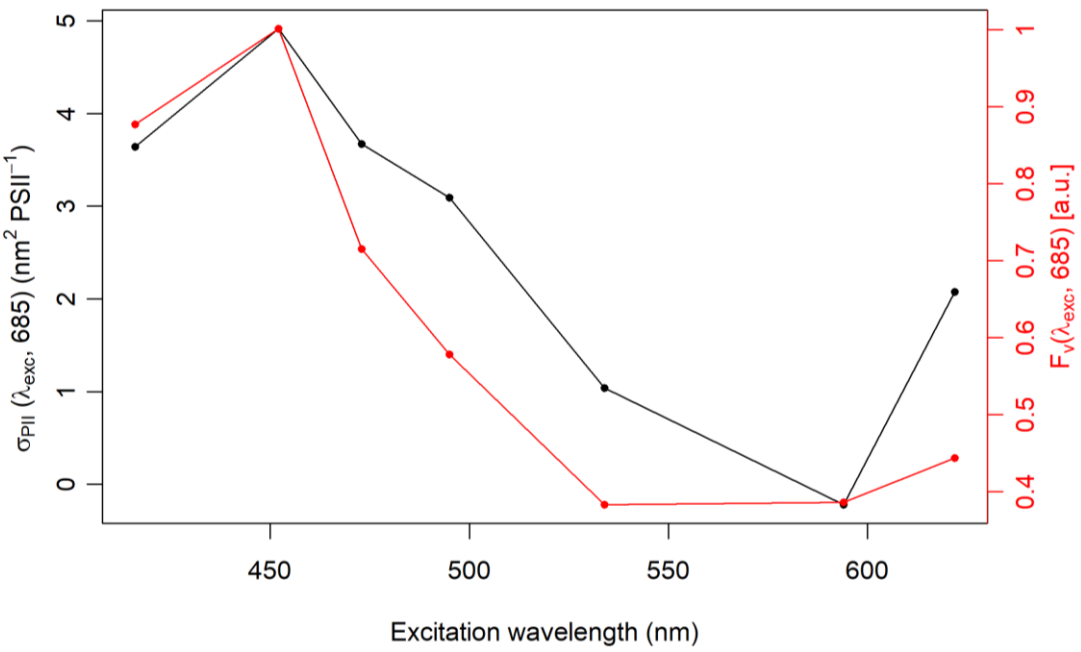

Figure 4. Excitation spectra of $F_v(\lambda_{ex}, 685)$ and $\sigma_{PII}(\lambda_{ex}, 685)$ obtained with the algae-optimised protocol on a natural community.

3.3. Microscopy

Microscopy counts were collected from samples fixed in Lugol's medium. These samples were placed in a 1 mL Sedgewick Rafter Counting Chamber etched with a 20 row x 50 column grid. Samples were examined with a LEICA DM IRB inverted microscope. 100 units of 1µL each were randomly selected and counted to phytoplankton group level to quantify the abundance of diatoms, cyanophytes, chrysophytes, chlorophytes, euglenoids, dinoflagellates and unspecified single-celled eukaryotes. Counts were then multiplied by 10 to yield the abundance per mL.

Microscopy counts and identification to species level were also available from the water utility company (South West Water), from April 2002 to present, generally at monthly intervals. These long-term monitoring data were only used in Figure 3 to inform planning of the sampling campaign. Identification was made to species level, whereas the results reported here are aggregated to either "eukaryotic algae" or "prokaryotic cyanobacteria". The samples were collected from water pumped at the draw-off tower from approximately 5 or 10 m depth, depending on surface water level.

3.4. Nutrients

Dissolved nutrient concentrations including nitrate + nitrite, nitrite, phosphate, ammonium and silicate were determined from 0.2-µm filtrate (Nalgene™ Sterile Syringe Filters 0.2 µm surfactant-free cellulose acetate membrane) using a 5-channel segmented flow

colorimetric SEAL Analytical AAIII autoanalyser. The analytical methods were as described in Woodward and Rees (2001).

4.Results

4.1. Phytoplankton and Nutrient Dynamics

Algae were dominant on the first sampling day followed by cyanobacterial dominance during the rest of the campaign (Figure 5A). Diatoms and chlorophytes dominated the algal community, with diatoms varying over a wide range between samples (Figure 5B,C). A succession of phytoplankton groups was observed through the sampling period and followed variability in nutrient concentrations (Figures 5 and 6). The beginning of the sampling period was marked by an initial increase in diatoms, cyanobacteria and chlorophytes until late April, during which silicate and phosphate concentrations decreased whilst a slight increase of available ammonium was observed. Cyanobacteria and diatoms abundance then decreased sharply until late May, while chlorophytes continued to increase, nitrate decreased, and nitrite availability slowly increased. From mid-May to mid-August, cyanobacteria increased while algae abundance remained relatively low. During this period, a decrease in nitrate and increase in nitrite was observed, while silicate and ammonium availability peaked. From mid-August until the end of the sampling period, algae abundance (notably diatoms and chlorophytes) increased while cyanobacteria showed an overall increasing trend with high variability between samples. Meanwhile, a slow increase of silicate and a decrease of nitrate and nitrite was observed.

There was evidence of phosphate limitation during the whole sampling period (Figure 6B). Phosphate concentration was slightly above the detection limit on the first sampling date and below the limit of detection (0.02 µM) during the remaining period (Figure 6B). Ammonium concentration (Figure 6B) peaked in mid-July, following a period of high precipitation during that period (Figure 7) which likely replenished both nitrite and ammonium from surrounding agricultural sources (Figure 6A,B). Silicate availability is a common driver of early-season phytoplankton succession. Silicate concentration decreased at the beginning of the sampling period when diatoms were relatively abundant, then increased up to the end of the sampling period while cyanobacteria were dominant and available ammonium appeared to be rapidly taken up (Figures 5 and 6A).

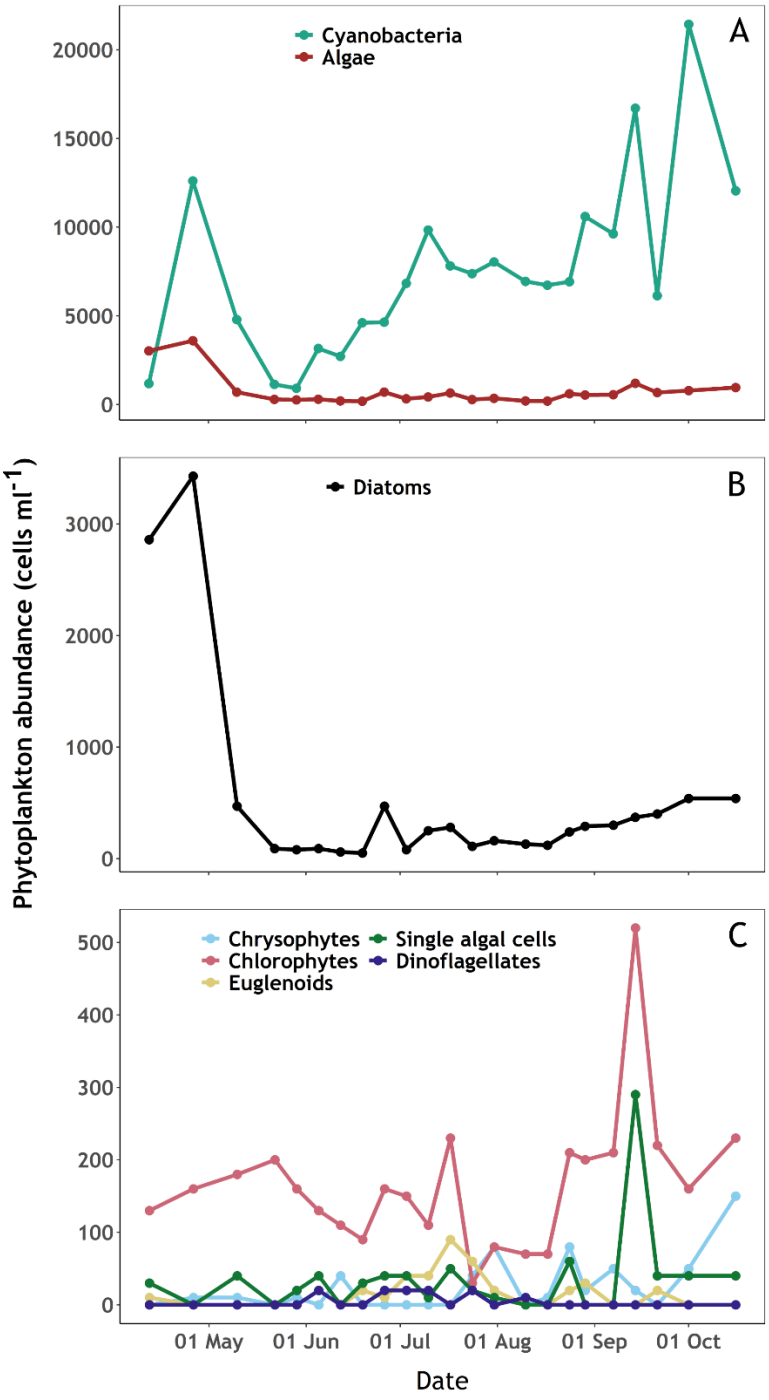

Figure 5. Phytoplankton abundance (cells mL^{-1}) during the sampling period at Roadford Lake. A: Cyanobacteria and algae. B: Diatoms. C: Chrysophytes, Chlorophytes, Euglenoids, Dinoflagellates and single algal cells.

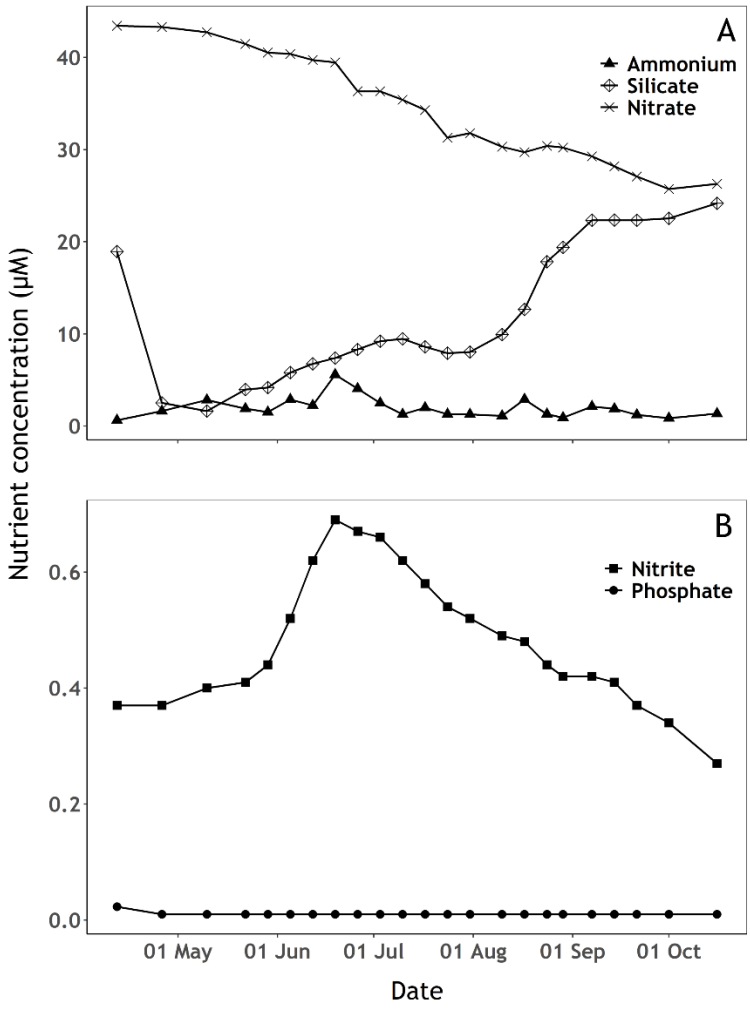

Figure 6. Nutrient concentrations (µM) over the sampling period. A: Ammonium, silicate and nitrate concentration, B: Nitrite and phosphate concentration. When the detection limit was not passed, phosphate concentrations below the limit of detection (0.02 µM) are displayed as 0.01 µM.

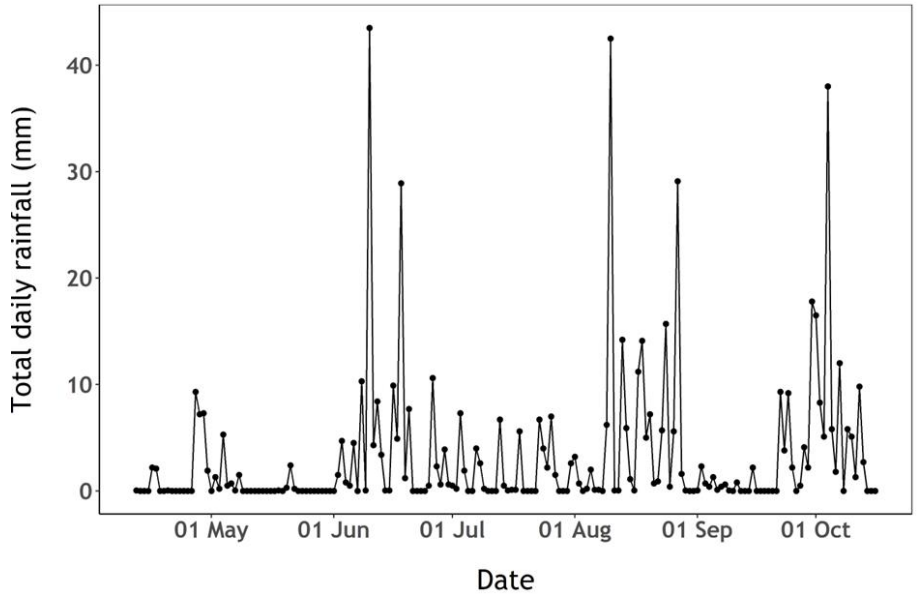

Figure 7. Total daily rainfall (mm) observed at the Virginstow, Beaworthy weather station.

4.2. Fluorescence Dynamics

Negative values observed in Figure 8 are linked to the determination of excitation spectra. Differences of signal between combinations of excitation wavebands might induce negative values for green-orange LEDs, which will show a small fluorescence signal from a community dominated by algae and measured with the protocol optimized for algae. The succession towards increasing cyanobacteria abundance and dominance was clearly reflected in $F_v(\lambda_{ex}, 685)$ and $\sigma_{PII}(\lambda_{ex}, 685)$ (Figure 8). $F_v(\lambda_{ex}, 685)$ showed similar dynamics between the algae and cyanobacteria-optimised protocols (Figure 8A and 8B, respectively). $F_v(594, 685)$ and $F_v(622, 685)$ increased throughout the sampling period, matching changes in cyanobacteria abundance (see Figure 5A) while higher values of $F_v(416, 685)$ and $F_v(452, 685)$ corresponded to higher abundance of algae at the beginning of the sampling period (Figure 8A,B). It should be noted that the algae-optimised protocol showed higher values of F_v than the cyanobacteria-optimised protocol (Figure 8A,B). $\sigma_{PII}(\lambda_{ex}, 685)$ showed distinct responses from different parts of the community between the two protocols (Figure 8C,D). The blue part of the spectrum showed a gentle decrease in σ_{PII} under the algae-optimised protocol while under the cyanobacteria-optimised protocol, σ_{PII} was higher in early April with strong short-term variations until Mid-July. These variations showed contrasting behaviour between blue to orange–red excitation wavebands for σ_{PII} in the cyanobacteria-optimised protocol (Figure 8D), largely absent in the algae-optimised result (Figure 8C). Differences in σ_{PII} between the algae and cyanobacteria-optimised protocols were most significant in the red–orange excitation

wavebands. σ_{PII}(622, 685) increased markedly in the middle of the sampling period using the cyanobacteria-optimised protocol (Figure 8D) while σ_{PII}(534, 685), σ_{PII}(594, 685) and σ_{PII}(622, 685) showed lower values under the algae-optimised protocol.

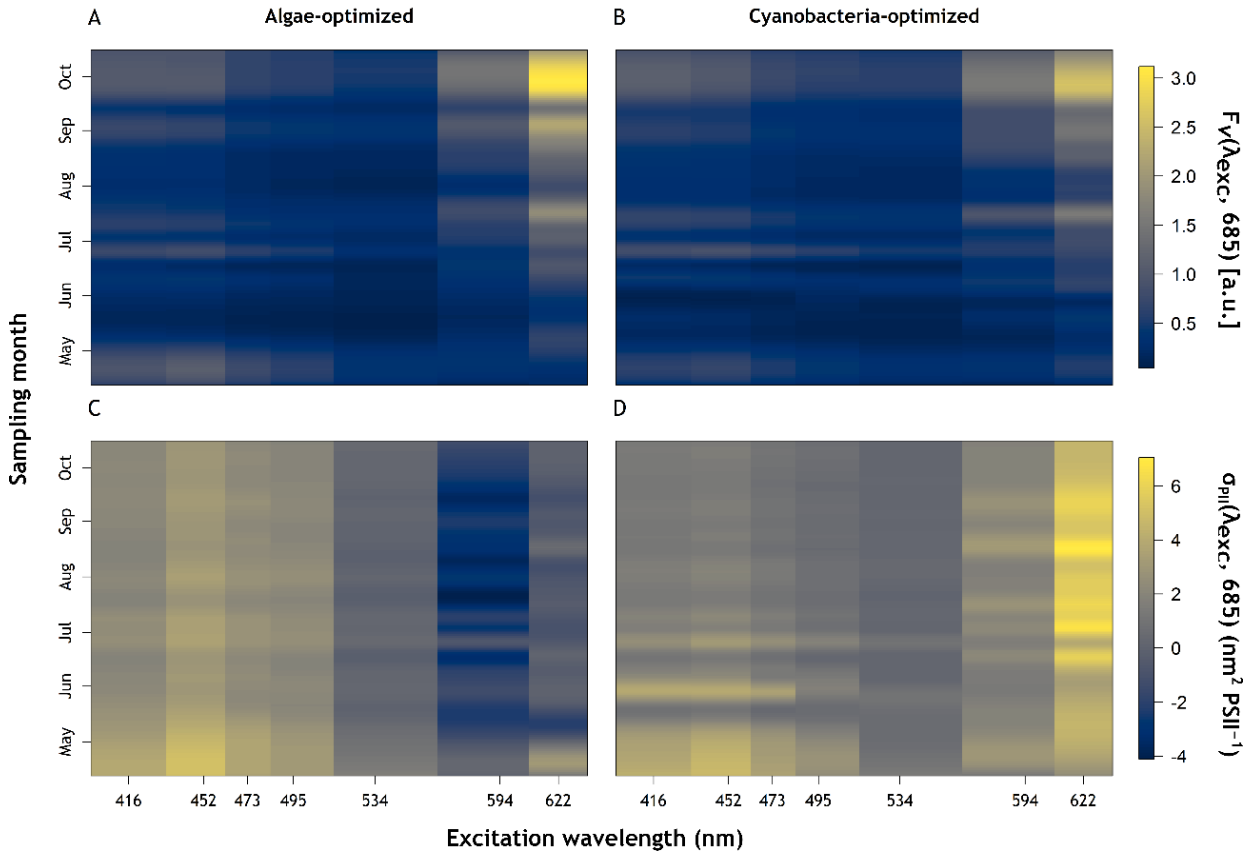

Figure 8. Photosynthetic Excitation spectrum results. (A): $F_v(\lambda_{exc}, 685)$ [a.u.], algae-optimised. (B): $F_v(\lambda_{exc}, 685)$ [a.u.], cyanobacteria-optimised. (C): $\sigma_{PII}(\lambda_{exc}, 685)$ (nm^2 $PSII^{-1}$), algae-optimised. (D): $\sigma_{PII}(\lambda_{exc}, 685)$ (nm^2 $PSII^{-1}$), cyanobacteria-optimised.

4.3. Relative Cyanobacteria Abundance and F_o Dynamics

F_o(GOR) trends followed variations in cyanobacteria abundance over time (Figure 9B, and see Figure 5A). F_o(GO) showed the same trend but with much lower values compared to F_o(GOR), indicating that F_o(GO) was sensitive to cyanobacteria abundance despite lower excitation energy. Abundances of algae and cyanobacteria were significantly correlated with F_o obtained from the five excitation protocols. The abundance of cyanobacteria was more significantly correlated with F_o(GOR) (linear regression, *p*-value < 0.0001, adjusted R^2 = 0.66) than with other protocols (linear regression, *p*-values between *p*-value < 0.01 (GOB) and *p*-value < 0.0001 (GORB), adjusted R^2 ranged between 0.30 (GOB) and 0.58 (GORB)). Reciprocally, the abundance of algae was most strongly correlated with F_o(GORB) (linear

regression, *p*-value < 0.0001, adjusted R^2 = 0.57) than other protocols (linear regression, *p*-value < 0.001 (GOR and B), adjusted R^2 ranged between 0.46 (GOR) and 0.57 (B)).

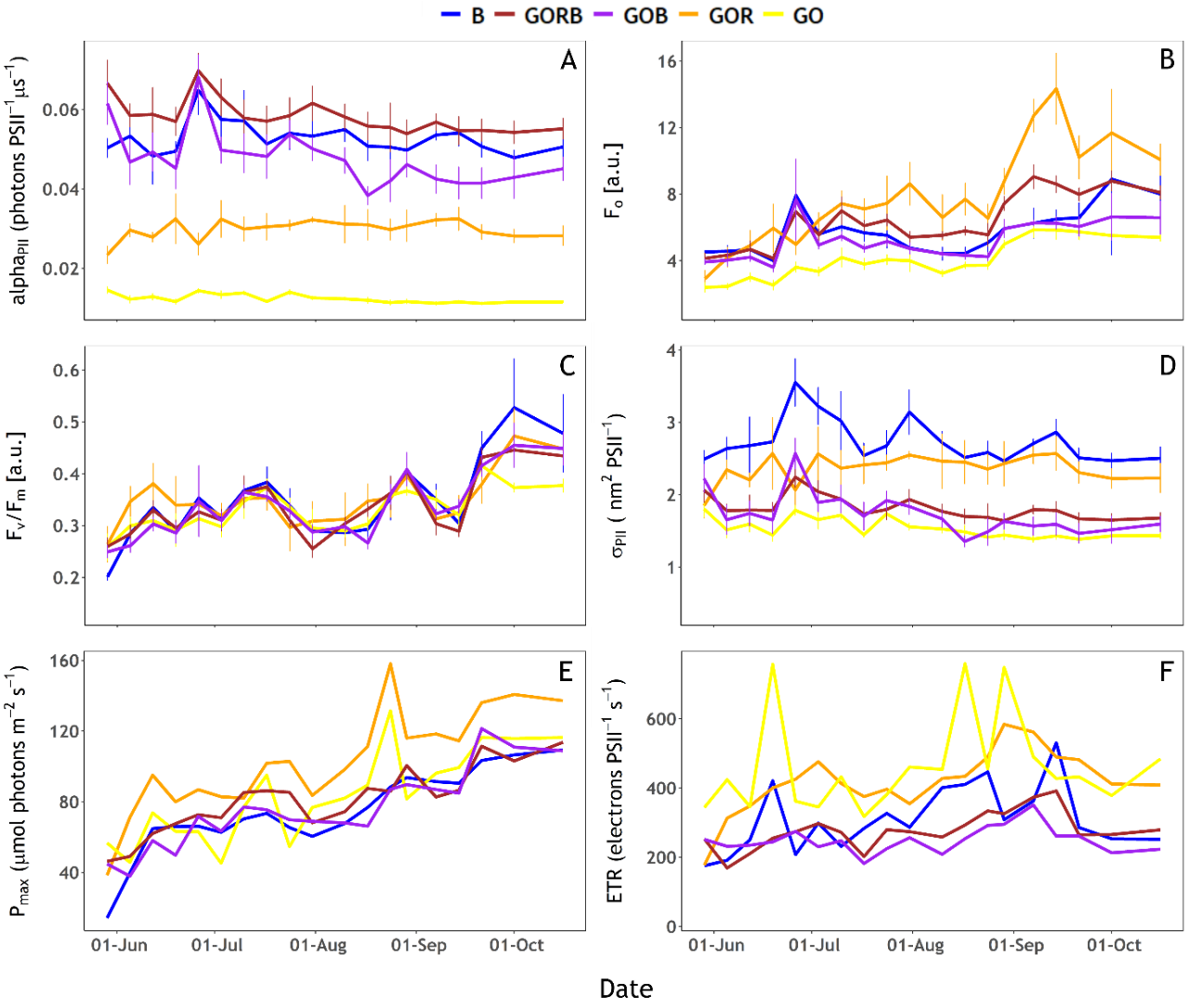

Figure 9. Fluorescence Light Curves (FLCs) photosynthetic parameters obtained with the five excitation protocols (B, GORB, GOB, GOR and GO, see Table 1). A: $alpha_{PII}$ (photons $PSII^{-1}$ μs^{-1}), B: F_o [a.u.] , C: F_v/F_m [a.u.], D: σ_{PII} (nm^2 $PSII^{-1}$), E: P_{max} (µmol photons m^{-2} s^{-1}) and F: ETR (electrons $PSII^{-1}$ s^{-1}). Error bars in panels A, B, C and D represent the standard deviation calculated for F_o, F_v/F_m, $alpha_{PII}$ and σ_{PII} parameters because reported values were averaged over the first five light steps of each FLC.

4.4. Photophysiological Characterisation

When targeting cyanobacteria, full saturation of PSII was not reached with the GOR and GO protocols. $alpha_{PII}$(GO) was < 0.02 and $alpha_{PII}$(GOR) around 0.03 (Figure 9A). The other protocols (B, GORB and GOB) did achieve saturation of the community with $alpha_{PII}$ near or above 0.04. The fitting of ST curves to obtain photophysiological parameters does not necessarily require full saturation as long as the initial fluorescence rise and asymptote (F_m) can be extrapolated from the curve. Nevertheless, GO protocol results should be interpreted with caution.

Photophysiological parameters derived from the FLCs showed multiple trends. P_{max}, F_v/F_m and F_o all increased over time (Figure 9B,C,E). F_v/F_m increased from 0.2—0.3 at the end of May to approximately 0.4—0.5 at the end of the sampling period with minor variations between excitation protocols, detailed below (Figure 9C). By contrast, σ_{PII} showed more short-term variations and a generally decreasing trend (Figure 9D). ETR generally increased up to mid-September before it decreased again, while ETR(GO) results were highly variable (Figure 9F). Assessing specific differences between excitation protocols, P_{max}(GOR) and ETR(GO) showed higher values than other protocols (Figure 9 E-F). P_{max}(GOR) and P_{max}(GO), as well as ETR(GOR) and ETR(GO), followed similar rising trends. When combined with B excitation (GOB and GORB protocols), these trends remained similar, whilst P_{max}(B) lacked some of the short-term variability over the duration of the rising trend. ETR(B) showed a contrasting trend from ETR(GORB) and ETR(GOB). While ETR(GO) and ETR(GOR) trends seem mostly driven by cyanobacteria abundance, ETR(B) trends seem to follow algae abundance (Figure 9F). Moreover, changes in diatoms, chlorophytes and other single-celled algae abundance followed short-term variations of ETR(B) even when algal abundance was low (Figure 9F). σ_{PII}(B) and σ_{PII}(GOR) were both higher than the other excitation light compositions (Figure 9D). σ_{PII}(B) showed three peaks in the time series during late June, late July and mid-September. Only the steady decrease following the September peak was also visible in σ_{PII}(GOR). Short-term variations of σ_{PII}(B) and σ_{PII}(GOR) seemed to follow short-term variations of, respectively algae and cyanobacteria abundance (Figure 9D). The other protocols showed similar trends between them with values decreasing slowly from the end of May up to the end of the sampling period, and a σ_{PII} peak observed at the end of June with GORB, GOB, and GO protocols.

Photochemistry efficiency (F_v/F_m) was similar between excitation light protocols except marked differences at the start of June (higher F_v/F_m(GOR)) and at the end of September (higher F_v/F_m(B) and lower F_v/F_m(GO), Figure 9C). F_o(GOR) was higher than F_o obtained with the other protocols (Figure 9B). F_o(GO) was consistently lower compared to other combinations of

excitation wavebands. F_o(GORB) showed higher values than F_o(B), F_o(GOB) and F_o(GO) protocols from July until the end of the sampling period. F_o(GORB) was lower than F_o(GOR), contrary to expectations considering the GORB protocol operated the GOR LEDs at the same intensities between protocols and received additional energy from the B LEDs.

4.5. Emission Ratio of 730 nm over 685 nm

The emission ratio of 730 over 685 nm, or F_o(GOR, 730/685), corresponded to cyanobacteria biomass as seen in Figure 10. F_o(GOR, 730/685) was positively and significantly correlated with the relative abundance of cyanobacteria of the phytoplankton community (linear regression, *p*-value < 0.01, adjusted R^2 = 0.42). F_o(B, 730/685), in contrast, was not significantly correlated with the relative abundance of either group (linear regression, *p*-value: 0.076, adjusted R^2 = 0.12), although some correspondence of F_o(B, 730/685) with cyanobacteria biomass could be observed.

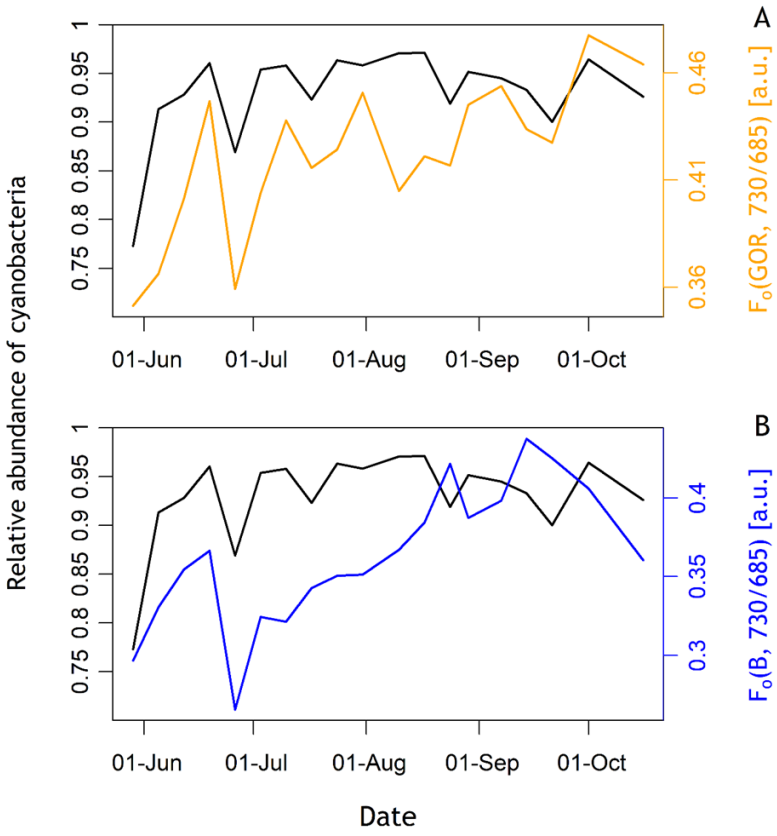

Figure 10. F_o emission ratio using B and GOR excitation protocols compared to the relative abundance of cyanobacteria (black drawn line). A: F_o(GOR, 730/685) [a.u.], B: F_o(B, 730/685) [a.u.].

5. Discussion

5.1. Phytoplankton, Nutrient and Fluorescence Dynamics

The succession of phytoplankton observed from early spring to late summer is typical of the seasonal succession of phytoplankton in temperate lakes (Wetzel 2001, de Figueiredo et al. 2006). The increase of cyanobacteria may be explained by a combination of several factors: temperature increase, replenishment of ammonium, and the ability of cyanobacteria to store phosphorus (Carey et al. 2012).

The use of fluorescence excitation spectra to distinguish pigments groups in phytoplankton forms the basis of all available multispectral phytoplankton fluorescence excitation instruments, and has been described in great detail e.g., (e.g. Beutler et al. 2002, Yoshida, Horiuchi, and Nagasawa 2011). In this study, the shift observed from algae to cyanobacteria dominance was clearly visible in F_o(GOR), and F_o(GO) which tracked variations of cyanobacteria abundance over time. In addition, spectra of $F_v(\lambda_{ex}, 685)$ and $\sigma_{PII}(\lambda_{ex}, 685)$ provide insight into the photosynthetic light uptake potential of the two major phytoplankton groups. In spectra of $F_v(\lambda_{ex}, 685)$, a shift occurred from shorter to longer excitation wavebands as the relative abundance of cyanobacteria increased. Similarly, spectra of $\sigma_{PII}(\lambda_{ex}, 685)$ showed distinct responses from algae and cyanobacteria. This was observed with $\sigma_{PII}(\lambda_{ex}, 685)$ obtained with the algae-optimised protocol at the blue part of the spectrum, following algae abundance. On the other hand, at red–orange wavebands, higher $\sigma_{PII}(\lambda_{ex}, 685)$ values obtained with the cyanobacteria-optimised protocol tracked the abundance of cyanobacteria. These results illustrate the use of PSII excitation spectra to determine the photosynthetic response by either phytoplankton group during natural succession. The fact that the algae-optimised protocol showed low $\sigma_{PII}(\lambda_{ex}, 685)$ in the red–orange part of the spectrum when algae were most abundant, while the cyanobacteria-optimised protocol induced higher $\sigma_{PII}(\lambda_{ex}, 685)$ at blue wavebands illustrates that both protocols induced signal in the other phytoplankton group. The former is explained by the presence of red light at 622 nm in the cyanobacteria-optimised protocol which will induce some Chla absorption in both groups, while the latter points to blue light absorption by Chla in algae and cyanobacterial PSII Chla. The parallel use of the two protocols ensures that there is sufficient signal to extrapolate the photosynthetic parameters, and that differences are associated with the phytoplankton group for which each protocol is optimised. During periods where neither group dominates, no major differences should be expected between the protocols.

5.2. Emission Ratio of 730 nm over 685 nm

The F_o emission ratio F_o(GOR, 730/685) was positively and significantly correlated with the relative abundance of cyanobacteria in the community. F_o(B, 730/685) was not significantly correlated but followed the overall trend and short-term variations of the relative abundance of cyanobacteria. As discussed above, the B and GOR excitation signals are not exclusively diagnostic to either group. It is, therefore, interesting to observe that the emission ratio is sensitive to cyanobacteria in either excitation protocol. These results confirm the potential of interpretating the ratio of 730 nm over 685 nm emission to identify cyanobacteria in the community suggested by Courtecuisse et al. (2022), as well as the importance of the choice of the excitation wavebands. LEDs targeting the orange-to-red spectrum will favour PSII emission from cyanobacteria compared to algae, whilst avoiding the excitation of Chla associated with PSI further enhances the fluorescence emission ratio, as indeed observed here. Nevertheless, we did not observe major variability in time in the relative abundance of cyanobacteria in the community, so these results should be interpreted with some caution. To further confirm the utility of F_o(GOR, 730/685) to identify cyanobacteria, measurements should be repeated alongside group-specific biomass determinations at higher frequency. In this context, the light-acclimation and nutrient history of the samples would have to be considered as these can be expected to influence the ratio of PSI over PSII emission through the expression of accessory pigment as well as photophysiological efficiency. It is known that state transitions induce further variations of the PSII to PSI ratio (Calzadilla and Kirilovsky 2020). In this study, samples were dark-adapted before measuring F_o at both emission wavebands so that state transitions should not influence the observed variability in F_o(GOR, 730/685). Moreover, as described by Luimstra et al. (2018), light conditions in which the cyanobacterium *Synechocystis sp*. PCC 6803 were grown as well as the excitation wavebands have an influence on the PSII:PSI ratio. (Luimstra et al. 2018) showed that the cyanobacterium grown under blue light had a lower PSI:PSII ratio than under orange or red light. Under blue excitation (440 nm), PSI:PSII ratios were higher than under orange excitation (590 nm) (Luimstra et al. 2018). This phenomenon is explained by the fact that the phycobilisomes in cyanobacteria do not efficiently transfer energy from blue light absorption to PSII.

5.3. Photophysiological Characterisation

Differentiated trends between the photosynthetic parameters highlight changes in the physiology of phytoplankton in the lake. The photochemistry efficiency expressed by F_v/F_m more than doubled over the observed period, likely corresponding with improved nutrient availability to the dominant group. F_v/F_m did not vary between the protocols, suggesting that

algae and cyanobacteria populations adjusted similarly to environmental conditions (as also observed by Houliez et al. (2017). In the case of the algal population, this included replacement of diatoms by chlorophytes during a period of silicate depletion.

P_{max} and F_o expectedly increased with overall biomass. σ_{PII} showed a decreasing trend over the sampling period which could be associated with seasonally increasing light availability. Suggett et al. (2009) also showed an inverse correlation between $F_v/F_m(478, \lambda_{em})$ and $\sigma_{PII}(478, \lambda_{em})$, which can be explained by energy requirements: the increasing numbers of pigment molecules in the light-harvesting antenna induce a higher probability of thermal dissipation and a decrease of photochemistry efficiency (Suggett et al. 2009, Lavergne and Joliot 2000). Moreover, the excitation spectra of σ_{PII} showed higher values of $\sigma_{PII}(560, \lambda_{em})$ than $\sigma_{PII}(478, \lambda_{em})$ in cyanobacteria while the opposite was observed in algae (Suggett et al. 2009). In our study, algae abundances were lower than cyanobacteria except at the beginning of the sampling period. We would, thus, expect to see higher σ_{PII}(GOR) than σ_{PII}(B) during periods of cyanobacteria dominance. Nevertheless, σ_{PII}(B) and σ_{PII}(GOR) followed the short-term variations in algae and cyanobacteria abundance, respectively. The fact that σ_{PII}(B) was higher than σ_{PII}(GOR) can be explained, either by the fact that σ_{PII}(B) also targets cyanobacteria or that the ratio of Chla pigments over phycobilipigments was low. This corroborates with the fact that phytoplankton growth was not light-limited and that cyanobacteria regulate their pigment expression (Whitton and Potts 2000). Moreover, σ_{PII} is calculated as the product of $alpha_{PII}$ and EST (Eq. 2., see Oxborough (2021)). Our results suggest lower $alpha_{PII}$ and EST values induced by the GOR protocol compared to the B protocol, which can explain the lower values of σ_{PII}(GOR) compared to σ_{PII}(B). The interpretation of σ_{PII} obtained with the GOR protocol and the B protocol is, therefore, not straightforward here.

PAM (Pulse Amplitude Modulation) and FFR (Fast Repetition Rate) Fluorometers using several induction protocols have been used to estimate the physiology and the biomass of distinct phytoplanktonic groups, including cyanobacteria. Kazama et al. (2021) used the FastOcean (FRRf) and a combination of LEDs to accurately estimate ETR_{PSII} of freshwater cyanobacteria. Parésys et al. (2005) could discriminate cyanobacteria from other phytoplanktonic groups using a PAM fluorometer and blue, green and red LEDs. Raateoja, Seppälä, and Ylöstalo (2004) warned that ST fluorometers equipped solely with blue LEDs lack sensitivity to cyanobacteria without phycoerythrin. Some improvements to group-specific and bulk phytoplankton sensitivity are therefore expected from modern instruments such as used here, equipped with multiple excitation channels and broad-spectrum actinic light. In this work, P_{max} increased over the sampling period and was higher when obtained with GOR and

GO protocols, explained by the increased abundance of cyanobacteria over time. This confirms the importance of using protocols targeting cyanobacteria and especially the GOR protocol (or the GO protocol if saturation can be improved) when trying to predict group-specific population growth. Short-term variations of P_{max} obtained with GOR and GO protocols followed cyanobacteria abundance over time while short-term variations in P_{max} obtained using the other excitation protocols followed algae abundance. The general increasing trend of P_{max} between the excitation protocols suggest that protocols other than GOR and GO also induced a signal in cyanobacteria. ETR generally increased up to mid-September and subsequently decreased with ETR(GOR) and ETR(GO) showing higher values than other protocols. ETR(GOR) followed trends driven by cyanobacteria abundance while ETR(B) trends followed abundance of algae. Moreover, ETR(B) showed a different trend from P_{max}, especially at the end of the sampling period. Wide variability in the 'electron-to-carbon exchange rate' was described by Suggett, MacIntyre, et al. (2009), which highlights the difficulty in linking ETR to C fixation. This is confirmed by the fact that this study focuses on a single lake over a relatively short period of time while nutrient concentrations and light availability remained relatively stable. It was explained by Napoléon and Claquin (2012) that alternative electron sinks can occur for other metabolic processes and physiological mechanisms. Moreover, light and nutrient history effects on ETR values cannot be determined well from this data set due to the relatively long sampling intervals.

5.4. Suitability of LabSTAF for In Situ Assessment of Cyanobacteria

The configuration of the LabSTAF used in this study could not guarantee PSII saturation in the protocols we expected to be most diagnostically sensitive to cyanobacteria, which should be improved using higher intensity LEDs. Ideally, the R LED would only be used comparatively (i.e., combined with B or GO), to determine how well the GO protocol describes the cyanobacteria component of the community. A complete assessment would consist of the spectral excitation measurements providing insights into the efficiency of light uptake through key pigments in the community (providing the first insight into cyanobacteria presence) followed by GO and B fluorescence light curves to determine photophysiological growth parameters which would indicate whether any differences in photosynthetic efficiency are likely between the two major phytoplankton groups.

Due to the nature of overlapping photosynthetic pigment absorption profiles between the major phytoplankton groups, it is essential to consider several optical markers, as confirmed by results presented here. Notably, we recommend using in parallel the ratio of F_o(GOR, 730/685) and the PSII excitation protocols obtained with cyanobacteria and algae-

optimised protocol. Ultimately, parameters derived from the FLCs obtained with GOR and B protocols can then be used to gain insight into likely growth and succession in the phytoplankton community. The DWM emission feature is promising because replacement filters could, in theory, be considered to look at other diagnostic wavebands for targeting cyanobacteria using this approach. The 650 nm emission waveband has been recommended by Courtecuisse et al. (2022) to be implemented in a fluorometer targeting cyanobacteria. Although emission recorded at 650 nm could yield weak fluorescence compared to emission recorded at 685 nm, F_o(GOR, 650/685) would likely give additional valuable diagnostic information on the presence of phycobilisome pigments.

6. Conclusions

This study assessed the ability of a new active fluorometer, the LabSTAF, to diagnostically assess the physiology of freshwater cyanobacteria in a reservoir exhibiting annual blooms.

The reservoir had a typical seasonal succession of phytoplankton of a temperate lake with diatoms being more abundant in spring and cyanobacteria more abundant in summer. PSII excitation spectra optimised for algae or for cyanobacteria showed distinct responses, illustrating the suitability of the instrument to determine the photosynthetic response by either group during their natural succession. FLCs parameters obtained with GOR and B protocols captured physiology parameters of, respectively, cyanobacteria and algae. However, the GO protocol, expected to be most diagnostically sensitive of cyanobacteria, did not reach saturation. Moreover, F_o(GOR, 730/685) was significantly correlated with the relative abundance of cyanobacteria, which shows the potential of the ratio of 730 nm over 685 nm emission to identify cyanobacteria in a mixed phytoplankton community.

Due to the nature of overlapping photosynthetic pigment absorption profiles between the major phytoplankton groups, it is essential to consider several optical markers. We recommend using in parallel excitation spectra obtained with both protocols and F_o(GOR, 730/685) to detect different pigment groups and assess cyanobacteria presence, followed by FLCs obtained with GOR and B protocols to assess the physiology and potential to grow of cyanobacteria and algae. Increased intensity of GO LEDs should be achieved to correctly assess the physiology of cyanobacteria and the R LED should only be used comparatively. Moreover, a 650 nm bandpass filter could be implemented in the DWM feature of the LabSTAF to measure the ratio of 650 nm over 685 nm emission, F_o(GOR, 650/685). The potential of F_o(GOR, 650/685) to be diagnostic of cyanobacteria should also be verified. According to this

study, the LabSTAF is a good candidate to assess the presence and physiology of cyanobacteria in the natural environment.

This instrument is well suited for long-term continuous measurements and its optical features provided suitable optical markers to target cyanobacteria. Improvement or addition of some features are nevertheless recommended to increase the potential of the LabSTAF to be diagnostic of cyanobacteria.

CHAPTER 4: TOWARDS PREDICTING THE ONSET OF CYANOBACTERIA BLOOM FROM MULTISPECTRAL ACTIVE FLUORESCENCE

1. Introduction

Eutrophication and climate change are responsible for the increased frequency of harmful algae blooms (HABs) (O'Neil et al*,* 2012; Paerl and Huisman, 2009, Paerl and Huisman, 2008). In freshwater areas, cyanobacteria can become dominant due to elevated nutrient concentrations (Paerl et al. 2011; Wurtsbaugh et al. 2019). A substantial number of bloom-forming cyanobacteria species produce a diverse range of toxins (Whitton and Potts, 2000) and present a non-negligeable risk to ecosystems and potential users of freshwater areas. Monitoring of the development of cyanobacteria HABs is consequently essential to reduce risks to users. Ultimately, management of these waterbodies includes the reduction of the potential of cyanobacteria HABs to form, by controlling nutrient inputs (Paerl and Barnard 2020), or by active suppression of cyanobacteria HABs with chemical or physical methods (Chen et al. 2022, El Bouaidi et al. 2022, Pan et al. 2006, Wang et al. 2012). Ideally, monitoring methods are able to assess the physiological condition of the cyanobacteria population and, thereby, their potential to grow and form blooms, or for blooms to persist.

A range of techniques are currently used or being developed to monitor the presence of cyanobacteria and development of blooms. Among those methods are identification and quantification of cells by microscopy, toxin analysis (Baker et al. 2002; Carmichael et al. 1999; Oehrle et al. 2010), detection of genetic markers (Pearson and Neilan, 2008; Srivastava et al. 2013), and optical methods such as *in vivo* fluorometry (Beutler et al. 2002), spectrophotometry, flow cytometry (Becker et al. 2002) and imaging flow cytometry (Campbell et al. 2013). Microscopic identification, toxicity analysis and genetic methods are able to give a very accurate assessment of CyanoHABs, but these methods are generally time-consuming and costly. Optical methods, however, are only able to discriminate between taxonomic groups. Fluorescence methods, in particular, are able to discriminate between phytoplankton groups, defined by their photosynthetic pigment composition. Advanced fluorometry techniques also bring the ability to determine phytoplankton physiology, which can be related to population growth, while remaining relatively less costly and fast compared to traditional methods to assess growth, such as oxygen production or carbon fixations methods. Based purely in optics, fluorescence techniques can sample at high frequency with the possibility of *in situ* and real-time measurements, whilst being highly reproducible and non-destructive (Zamyadi et al. 2016).

Current active fluorometers used to observe phytoplankton properties are grouped in two categories. The first category includes instruments which are based on the assumption that

the fluorescence signal is proportional to the concentration of chlorophyll *a* (Chla) and consequently the phytoplankton biomass (Babin, 2008). Those instruments are relatively affordable, portable instruments which sample the fluorescence response from one or more excitation wavebands in one emission waveband. The observed signal is typically used as a proxy of biomass. The second category includes instruments which measure the photochemistry efficiency (F_v/F_m). F_v, the variable fluorescence, is determined by calculating the difference between the maximum of fluorescence (F_m), when all reaction centres (RC) are in their closed state and the minimum of fluorescence (F_o) when RC are in their opened state. Closing RC is achieved using saturating flashes at a high frequency. PAM (Pulse Amplitude Modulation) fluorometers saturate PSII over multiple turnovers (reaction centres open and close repeatedly) while FRR (Fast Repetition Rate) fluorometers (FRRf) saturate PSII over a single turnover, at the microsecond scale. To achieve this, FRRf instruments use higher excitation energy over a shorter saturation period than PAM instruments, which allows repeat sampling over very short time scales and to assess fluorescence relaxation. Instruments in this second category are relatively more costly but with recent technological advances, these differences are diminishing and no longer order-of-magnitude. Both PAM and FRRf fluorometers now generally use multiple excitation wavelengths to target different pigments, and ultimately different groups of phytoplankton. Some instruments may offer several emission wavebands and one or multiple actinic light sources (generally white and blue) to measure photosynthesis–irradiance curves used to estimate and model primary productivity.

To estimate both biomass and physiology of cyanobacteria to assess population growth, PAM and FRRf fluorometers include excitation wavebands targeting phycobilipigments, the main light-harvesting pigments in cyanobacteria (Falkowski and Raven, 2013). However, overlap in the light absorption spectra by these and other photosynthetic pigments leads to challenges to isolate the cyanobacteria response. Moreover, saturating photosystem II (PSII) with only orange-green LEDs is a challenge due to the relatively lower intensity light produced by LEDs in this wavelength range. Therefore, the diagnostic excitation LEDs are typically combined with blue or red LEDs which targets PSII Chla. As a result, photosynthetic parameters derived from the fluorescence response may represent a wider part of the phytoplankton community, presenting a challenge for group-diagnostic interpretation. Nevertheless, it has been shown that blue versus orange based excitation protocols provide some differentiation that can be attributed to a fluorescence response from algae and cyanobacteria groups, respectively (Houliez et al. 2017, Kazama et al. 2021, Courtecuisse et al. 2022). Then, combining the

photosynthetic rates derived from the fluorescence assessment with ambient nutrient and light availability, will help to model and predict phytoplankton growth (Suggett et al. 2003).

The LabSTAF (Chelsea Technologies Group, UK) is a single turnover active fluorometer which already showed potential to diagnostically target cyanobacteria (Courtecuisse et al. 2023). Specific features to support this include two emission filters, at 685 and 730 nm, as well as PSII excitation spectra obtained with distinct protocols to optimise the fluorescence response in algae versus cyanobacteria dominated samples. Finally, Fluorescence Light Curve (FLC) parameters obtained with a strictly blue (B) excitation protocol were shown to principally target algae whereas a combination of Green-Orange-Red (GOR) excitation light is more sensitive to cyanobacteria. The B protocol uses two 452 nm LEDS whereas the GOR bands include wavebands at 534 nm (G), 594 nm (O) and 622 nm (R). The LabSTAF may be considered suitable for monitoring the natural environment because it is portable and weather-sealed and because it can measure continuously and autonomously with built-in flow and temperature control (Oxborough, 2021). However, the use of this instrument is not yet widely documented and more work is needed to verify its sensitivity to the early growth of phytoplankton blooms and cyanobacteria in particular.

In this study we test the ability of the LabSTAF to predict the growth of cyanobacteria versus algae from natural samples brought into nutrient replete laboratory conditions to induce a phytoplankton bloom. Photosynthetic parameters derived from FLCs were recorded over several days to compare the sensitivity of GOR and B excitation protocols to the growing phytoplankton population, aiming to identify photosynthetic parameters that may predict the growth of bulk phytoplankton and discriminate the potential for growth of cyanobacteria, all other conditions such as nutrient supply remaining constant.

2. Materials and Methods

2.1. Study Sites

Roadford Lake (50.694°N, -4.232°E) is the largest drinking water reservoir in county Devon (United Kingdom), part of the catchment of the river Tamar. It has a net storage of 34,500 million litres, a surface area of 295 hectares and a mean depth of 12.4 m. Water is pumped from a draw-off tower situated in the south part of the reservoir, near the dam where there is also an overflow tower (Lawson et al. 1991). The lake is fed by the river Wolf in the northeast and from Westweek inlet, a stream to the northwest.

Blagdon Lake (51.337°N, -2.708°E), previously known as Yeo Reservoir, is a drinking water reservoir in Somerset, United Kingdom. The reservoir is shallow (mean depth 4.75m), and has a surface area of 165 hectares containing 8,456 million litres at maximum capacity. Water is pumped from a pipe through the dam. The lake is fed principally by the Yeo river, by a piped supply from Rickford Spring and by a large stream entering at Butcombe Bay (Wilson et al. 1975).

High abundances of cyanobacteria have previously been recorded in samples from Roadford Lake and analysed by the water utility company using light microscopy, since at least spring 2002, and often year-round. High abundances of cyanobacteria were recorded in Blagdon lake in 2017 and 2019 by the water utility company using light microscopy.

Two experiments used water sampled from Roadford Lake, on 13th May 2022 and 7th July 2022 respectively, from a jetty near the western shore with a bucket in the first 0.5 m from the surface in approximately 3 m-deep water. For the third experiment, surface water was sampled at Blagdon lake on 22nd June 2022, from the south shore of the lake near the dam, with a bucket in the first 0.5 m from the surface. Water temperature was recorded at the time of sampling, and approximately 20 litres of water were brought to the laboratory in an insulated container, for further analysis and the start of the experiments on the same day. The water was filtered with a 250 µm mesh filter on site to remove large grazers and thereby support rapid bloom formation.

2.2. Experimental setup

Sampled water was placed in a transparent glass vessel to a final volume of 13 L for experiment I and 15 L for experiments II and III. The vessel was placed in a temperature controlled room at 19°C, placed on a magnetic stirrer to prevent sedimentation of particles, and aerated with filtered ambient air (Figure 1). Six white LED strips were attached vertically around the vessel and provided continuous light at 200 µmol m^{-2} s^{-1}. Generally, two LabSTAFs measured in parallel to compare excitation light protocols, fed by peristaltic pumps controlled by the instruments, purging the sample between every run of the measurement protocol. The top of the vessel was closed with sterile cotton wool. To avoid heating the sample inside the instruments, water was circulated between the designated water jacket and a large (>10L) container at room temperature. FLC measurements took 1518 to 2096 seconds (GOR) and 1523 - 3855 s (B), depending on the time taken to obtain fluorescence excitation spectra, automatic gain setting and the number of light steps in the FLC. Fluorescence measurements

were interrupted periodically (nominally 3-5 days) to clean the LabSTAF sampling chamber, and several times to investigate technical issues with instruments or pumps.

Samples for laboratory analysis were taken daily using a syringe fed from a tube kept inserted in the vessel, removing any liquid left in the tube first. Laboratory analysis included inorganic nutrient concentrations and microscopy cell counts.

To induce growth of the phytoplankton, nutrients were added to the vessel at 0 - 3 days after incubation. The nutrient additions were based on the BG11 medium and are specified in Table 1. In experiment II the final concentration of $NaNO_3$ (sodium nitrate) in the vessel was divided by 20 compared to experiment I and the final concentration of ammonium ferric citrate green was multiplied by 40 compared to experiment I and III (Table 1). In experiment III, the final concentration of $NaNO_3$ in the vessel was divided by two compared to experiment I (Table 1). The volume in the vessel was topped up with medium of the same nutrient concentrations in experiment I when sample volume was removed for analysis. In experiment III, the volume in the vessel was topped up with medium with nutrient concentrations modified (Ammonium ferric citrate concentrations multiplied by three for the three first top ups, and multiplied by five for the next three top ups, $NaNO_3$ was not added for the last three top ups) when sample volume was removed for analysis. Top ups of nutrient are indicated in Figure 2 by red-arrows. Concentrations of nutrients topped up are comparatively small with concentration of nutrients added in the initial addition. The experiments ended once it was evident that the peak of the bloom had passed or when wall growth was deemed to interfere with the interpretation of results, respectively after 17, 13 and 11 days after nutrient addition in experiments I, II and III.

Figure 1. Experiment setup.

Table 1. Final concentrations (mg L^{-1}) of nutrients added in each vessel following initial nutrient additions.

Nutrients	I	II	III
$NaNO_3$	1500	75	750
K_2HPO_4	40	40	40
$MgSO4.7H_2O$	75	75	75
$CaCl_2.2H2O$	36	36	36
Citric acid	6	6	6
Ammonium ferric citrate	6	240	6
$EDTANa_2$	1	1	1
Na_2CO_3	20	20	20
H_3BO_3	2.86	2.86	2.86
$MnCl_2.4H_2O$	1.81	1.81	1.81
$ZnSO_4.7H_2O$	0.22	0.22	0.22
$Na_2MoO_4.2H_2O$	0.39	0.39	0.39
$CuSO_4.5H_2O$	0.08	0.08	0.08
$Co(NO_3)2.6H_2O$	0.05	0.05	0.05

2.3. Single-turnover fluorescence

FLCs were obtained using the fluorescence excitation protocols detailed in Table 2. These protocols were selected to target semi-isolated pigment groups and the associated phytoplankton taxa through combinations of excitation wavebands expected to lead to full saturation of PSII, based on the work of Bryant et al. (1979) and Johnsen and Sakshaug (1996). The protocols differed in saturation pulse length (100 or 300 µs) to further accommodate light saturation, and the combination of excitation wavebands. In turn, the LEDs used differed in the excitation energy delivered to the sample and was automatically adjusted before each FLC. The Light-Emitting Diodes (LEDs) used to provide the excitation energy had an intensity ranging from 9,123 to 10,842 µmol photons m^{-2} s^{-1} (G), from 2,266 to 2,691 µmol photons m^{-2} s^{-1} (O), and from 5,967 to 7,838 µmol photons m^{-2} s^{-1} (R) for the GOR protocol and from 11,976 to 18,363 µmol photons m^{-2} s^{-1} (B1) and from 12,640 to 19,509 µmol photons m^{-2} s^{-1} (B2) for the B protocol.

Table 2. Excitation protocols tested to target pigments associated with specific phytoplankton groups, as described by Bryant et al. (1979) and Johnsen and Sakshaug (1996). Phycobilipigments include phycoerythrin, allophycocyanin and phycocyanin.

Protocol	Excitation wavebands (nm at centre)	Full intensity range (µmol photons m^{-2} s^{-1})	Pulse length (µs)	Photosynthetic pigment groups targeted	Phytoplankton group targeted
B	452, 452	24,616 — 37,871	100	Chlorophylls *a*/*b*/*c*, carotenoids	Algae, weak signal from cyanobacteria possible
GOR	534, 594, 622	17,357 — 21,371	300	Phycobilipigments Chlorophylls *a*/*b*/*c* and carotenoids	Cyanobacteria with weaker signal from algae likely

Each FLC included 12 actinic light steps from 0 to an intensity varying from 676 to 2000 µmol photons m^{-2} s^{-1} (GOR) and from 439 to 1984 µmol photons m^{-2} s^{-1} (B). The actinic light spectra had a peak at 455 nm and shoulder from 480 nm to 655 nm. The dark adaptation of the sample lasted 60s which corresponded to the first step of the FLC.

The LabSTAF, despite having two emission wavebands, only switches to the 730 nm band for brief periods, and FLC parameters are therefore only available for the emission waveband at 685 nm. Where multiple (combinations of) excitation wavebands are considered, the excitation waveband is referred to by the same abbreviations given in Table 2 (i.e. B, GOR). Several photosynthetic and fluorescence parameters were determined from each FLC: $alpha_{PII}$, J_{PII}, P_{max}, F_v/F_m and F_o. An example of FLC and ST induction curve obtained with the LabSTAF are shown in the introduction of the thesis (Figure 5 and 6). σ_{PII}, F_o, F_v, F_m (and consequently F_v/F_m) and $alpha_{PII}$ are derived from induction curves at each step of the FLC (Figure 5, Thesis introduction). JPII is a secondary photosynthetic parameter derived from the primary photosynthetic parameter σ_{PII} defined from ST induction curve and the photon irradiance E. However, P_{max} is defined from the complete FLC (Figure 6, Thesis introduction).The following definitions are repeated from the instrument manual (Oxborough 2021) and the terminology of these photosynthetic parameters is derived from Oxborough (2021) and Schuback et al. (2021). J_{PII} measures the photon flux through the absorption cross section for PSII photochemistry provided by a single PSII complex. J_{PII} is interpreted as and reported henceforth as the electron transport rate (ETR) on the assumption that each photon used to drive PSII photochemistry results in the transfer of an electron out of PSII. ETR, in turn,

determines the rate of electron transport which controls phytoplankton carbon fixation and growth (Silsbe et al. 2015). ETR can express the ability of the phytoplankton to achieve metabolic processes. J_{PII} is calculated as:

$$J_{PII} = \sigma_{PII}' \times F_q'/F_v' \times E$$

Where σ_{PII}' is the absorption cross section of PSII photochemistry of each open PSII complex in nm^2 $PSII^{-1}$, F_v' is the variable fluorescence in light-adapted conditions and F_q' is the difference between F_m' and F_o', which are respectively the maximum and minimum fluorescence in light-adapted conditions and E is photon irradiance in photon m^{-2} s^{-1}. J_{PII} units are electrons $PSII^{-1}$ s^{-1}.

P_{max} is the maximum specific photosynthetic rate which expresses the phytoplankton photosynthetic capacity in optimal ambient light conditions. σ_{PII} is the absorption cross section of PSII, which is the product of the absorption cross section for PSII light-harvesting and the probability that an absorbed photon will be used to drive PSII photochemistry. σ_{PII} is calculated as :

$$\sigma_{PII} = alpha_{PII} \times 100\ EST$$

Where EST is the irradiance provided to the sample by the LEDs during a ST pulse in photon m^{-2} s^{-1} and $alpha_{PII}$ units are photon $PSII^{-1}$ μs^{-1}.

F_v/F_m measures the photochemistry efficiency, with F_v the variable part of fluorescence obtained from the difference between F_o and F_m, the minimum and maximum fluorescence, respectively. Values of F_o, F_v/F_m, $alpha_{PII}$ and σ_{PII} tend to decrease along the light steps of each FLC. The largest value of these parameters may be observed at or shortly after the first light step. Consequently, reported values of F_o and F_v/F_m were averaged over the first five light steps to characterise each FLC. Due to the high frequency of measurements, standard errors were not plotted but their values were small compared to the averaged values. The maximum value in each FLC was selected to describe the ETR parameter. P_{max} is provided once per FLC.

2.4. Microscopy

Cell counts were obtained from samples fixed in Lugol's medium. These samples were placed in a 1 mL Sedgewick Rafter Counting Chamber etched with a 20 row x 50 column grid. Samples were examined with a LEICA DM IRB inverted microscope. 100 units of 1µL each were randomly selected and counted to phytoplankton group level to quantify the abundance of diatoms, cyanophytes, chrysophytes, chlorophytes, euglenoids, dinoflagellates and unspecified single-celled eukaryotes. Identification was made to species level to the extent possible,

although the results reported here are aggregated to either eukaryotic algae or prokaryotic cyanobacteria. Growth rate (*m*) of algae and cyanobacteria were calculated as:

$$m = \ln(C_f/C_i)/(t_f - t_i)$$

Where C_f is the final cell abundance, C_i the initial cell abundance and t_f and t_i are respectively the time when were recorded the final cell abundance, and the time were recorded the initial cell abundance.

2.5 Nutrients

Concentrations of dissolved nitrate, nitrite, phosphate, ammonium, and silicate were determined from 0.2-µm filtrate (Nalgene™ Sterile Syringe Filters 0.2 µm surfactant-free cellulose acetate membrane) using a 5-channel segmented flow colorimetric SEAL Analytical AAIII autoanalyser. The analytical methods were as described in Woodward and Rees (2001).

3. Results

3.1. Ecophysiological conditions and growth dynamics

Experiments I and II were characterized, prior to nutrient addition, by phosphate limitation and a high N:P ratio (983 and 233, respectively) as shown in Figure 2. Experiment III started from a likely nitrogen limitation, with low N:P ratio (≈5) and lower phytoplankton abundance compared to the other experiments (Figure 3). The physiological state of the phytoplankton community, prior to nutrient addition, was typical of nutrient limitation with F_v/F_m values in the 0.26 to 0.38 range (Figure 3 P-R).

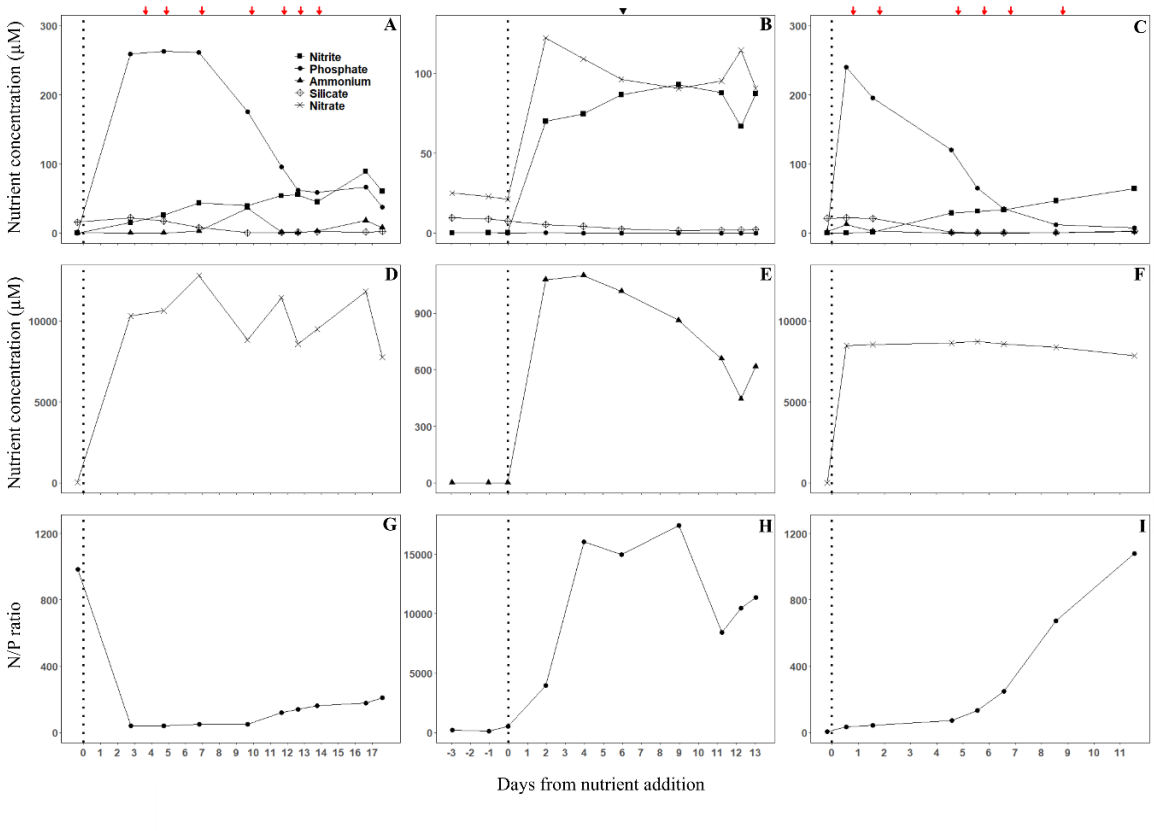

Figure 2. Concentrations of (A-C) nitrite, phosphate, ammonium, and silicate and (D-F) nitrate, and (G-I) N/P ratios during the three experiments (from left to right). Vertical dashed lines mark the initial nutrient enhancement. Red arrows in Expriments I and III indicate the top ups of nutrients. The black triangle in experiment II indicates when the precipitation of ferric phosphate was removed from the vessel.

The addition of nutrients induced exponential growth in all experiments. In experiments I and III, the addition resulted in rapid uptake of phosphate leaving excess nitrate. In experiment II, ammonium availability was increased relative to nitrate to encourage cyanobacterial over algal growth (Figure 2E). Phosphate availability remained low due to rapid uptake by phytoplankton, reflected by exponential growth, and in part by precipitation of ferric phosphate (from ammonium ferric citrate and potassium phosphate). Different growth dynamics of algae and cyanobacteria were observed between experiments I and II despite the same lake origin. Experiment I saw an increase in algae and cyanobacteria growth rates which reached a maximum at days 4-5 from nutrient addition, an exponential increase of cyanobacteria abundance from day 4-5, and an exponential increase of algae from day 6-7 (Figure 3D,G). In experiment III, the algal growth rate peaked around day 1, then steadily declined, while the cyanobacterial growth rate peaked around day 5-6 (Figure 3I), likely the result of the different nutrient treatment. As a result, algae abundance increased exponentially from day 1-2 while cyanobacteria abundance only showed a slight increase between days 5 and 6 (Figure 3A,C).

In experiment II, nutrient additions induced an exponential increase of algae and cyanobacteria abundance. Maximum growth rates in cyanobacteria and algae were observed around 9 days from the nutrient additions, which was later than observed in the other experiments and is likely due to depletion and slow recycling of phosphate or release from precipitate, although these nutrient dynamics cannot be reconstructed with certainty (Figure 3B,E,H). Moreover, phytoplankton growth rates in experiment II initially decreased before increasing from day 4 in algae and from around day 6 in cyanobacteria (Figure 3H).

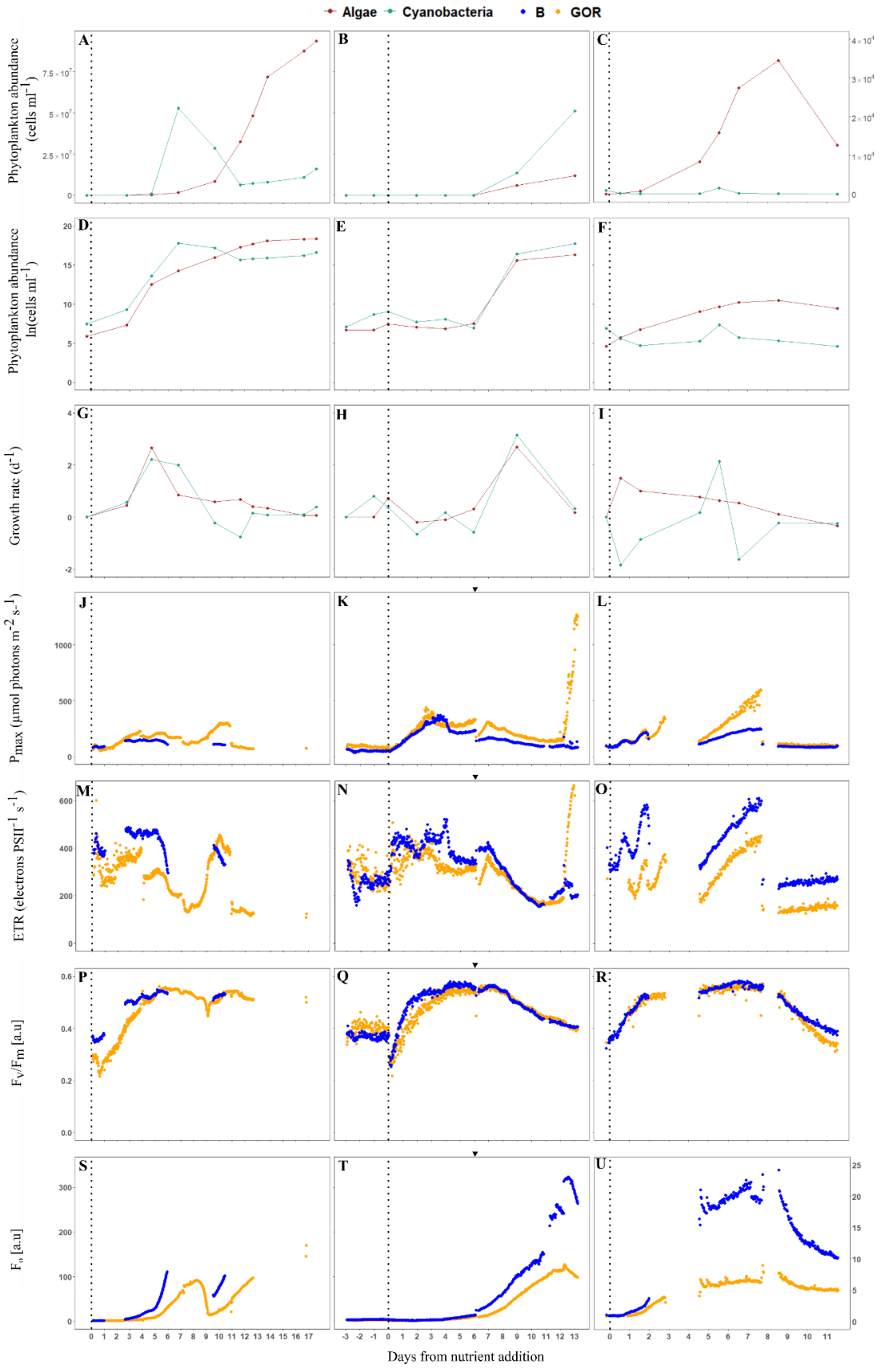
Algae
Cyanobacteria
B
GOR
Phytoplankton abundance (cells ml-1)
Phytoplankton abundance ln(cells ml-1)
Growth rate (d-1)
Pmax (µmol photons m-2 s-1)
ETR (electrons PSII-1 s-1)
Fv/Fm [a.u]
Fo [a.u]
Days from nutrient addition

Figure 3. A-C) Phytoplankton abundance (cells ml^{-1}), (D-F) Phytoplankton abundance (ln transformed), (G-I) phytoplankton growth rate (d^{-1}), (J-L) P_{max} (µmol photons m^{-2} s^{-1}), (M-O) ETR (electrons $PSII^{-1}$ s^{-1}), (P-R) F_v/F_m, and (S-U) F_o with panels horizontally corresponding to experiments I, II and III (from left to right). Dashed lines mark the initial nutrient enhancement. The black triangle in experiment II indicates when the precipitation of ferric phosphate was removed from the vessel. Panel C scale is different from the scale of panels A and B and is plotted on the ride side of the panel. Panel U scale is different from the scale of panels S and T and is plotted on the ride side of the panel.

F_v/F_m increased from approximately 0.3 to 0.5-0.6 in all experiments at 5-7 days from lifting nutrient limitations on growth (Figure 3P,Q,R). In experiment II, the initial, sharp decrease of F_v/F_m upon nutrient addition (Figure 3Q) was likely caused by a change in light availability due to formation of ferric phosphate kept in suspension and absorbing light at longer wavelengths. The sharp decrease of F_v/F_m coincided with a decrease in the growth rate determined from cell counts, corroborating the impact of the light climate on physiology regardless of improved nutrient availability (Figure 3H,Q). F_v/F_m reached a plateau lasting between several days up to a week in all experiments before decreasing again. In experiments II and III F_v/F_m decreased from around 8 - 9 days from nutrient additions. F_v/F_m reached 0.4 on day 13 of experiment II, and 0.3 (GOR) and 0.38 (B) on day 12 in experiment III, when these experiments were stopped (Figure 3Q,R). Experiment I was still at a plateau of approximately 0.5 (GOR) when the experiment was terminated due to instrumentation issues. Short-lived depressions and recovery in F_v/F_m(GOR) between 0.5 and 0.6 were observed around day 9 of experiment I (Figure 3P) which could be linked to a change in growth rates of parts of the phytoplankton community (Figure 3G).

The decrease of F_v/F_m towards the end of experiment II and III was most likely related to the combination of two factors: the decrease of light availability due to wall growth and phosphate limitation.

3.2. F_o and population dynamics

F_o matched the abundance of phytoplankton in all experiments (Figure 3A-C,S-U). The relative magnitude of F_o(B) and F_o(GOR) did vary considerably between experiments. In experiment III, where algae were predominant, F_o obtained with either excitation protocol tracked the algal abundance (Figure 3C,F,U) due to the low abundance of cyanobacteria. In experiment I, F_o(GOR) corresponded to the local peak of cyanobacteria abundance on the day 7 but following a faster rise in F_o(B). Both then further tracked an increase in algal abundance from towards the end of the experiment, around days 10-11 (Figure 3A,D,S).

Peak growth rates, determined from cell counts, were observed 3 - 4 days prior to peak F_o(GOR) in experiment I and to the peak in both F_o excitation protocols in experiment II. In

experiment III, although fluorescence measurements were interrupted several days, the difference was likely in the order of 1-3 days (Figure 3).

3.3. Phytoplankton dynamics predicted by photosynthetic parameters derived from FLCs

With few exceptions, ETR(GOR) was lower than ETR(B) and P_{max}(GOR) higher than P_{max}(B) (Figure 3J-O). Compared to growth rates, it can be observed that increased divergence between P_{max}(GOR) and P_{max}(B) generally corresponded to elevated cyanobacterial growth rates within several days, although the interval between cell counts introduces some uncertainty. Similar observations can be made on the divergence between ETR(B) and ETR(GOR). Specifically, in experiment I ETR(B) exceeded ETR(GOR) by approximately 250 electron $PSII^{-1}$ s^{-1} over days 4-5, followed by a change from cyanobacteria to algae as the fastest growing group between days 7 and 10 (Figure 3A,M). During experiment II, P_{max}(GOR) was marginally higher than P_{max}(B) prior to nutrient addition, while cyanobacteria growth rates outpaced algae (Figure 3B,H,K). However, following nutrient addition and up to day 3, P_{max} was briefly equal between protocols and the difference in growth rates also narrowed, lasting at least up until day 6. Then, following a gap in laboratory observations, cyanobacteria growth exceeded algae around day 9 and cyanobacteria abundance continued to increase faster than algae until the experiment ended. This corresponded to a steady increase in P_{max}(GOR) relative to P_{max}(B) signal increasing from day 4, both before and after some of the precipitate of ferric phosphate was manually removed (indicated in Figures 2-3 by a black symbol on day 6). In experiment III, algae were far more abundant than cyanobacteria, which translated in clear differences between ETR(GOR) and ETR(B) (Figure 3O). The dynamics of P_{max} are particularly interesting, showing a first period without significant differences between excitation protocols (likely caused by only one phytoplankton group dominating the fluorescence response regardless of excitation protocol), followed by a steady divergence while cyanobacteria growth rates sharply peaked (subject to some uncertainty in magnitude, due to low cell numbers), and finally returning to very similar values as the cyanobacteria growth waned (Figure 3L). These fluorometric observations were interrupted due to a pump failure on day 2 which was resolved on day 5, and further maintenance on day 8.

Changes in ETR and P_{max}, irrespective of excitation waveband set, generally preceded observed changes in growth rate and cell numbers. This is most clearly observable in experiment II because fluorescence was already recorded from several days before nutrient addition. Nutrient additions led to an immediate change in ETR, a gradual increase in P_{max} over four days, while the lag phase of observed cell counts lasted at least six days. In experiment I, the

maximum growth rate of cyanobacteria and algae on days 4 - 5 was preceded by one to two days in a rise in P_{max}(B) and P_{max}(GOR) (Figure 3G, J). P_{max} peaked 3-5 days prior to the highest count of cyanobacteria cells on day 7. The highest values of ETR(B) and ETR(GOR) were observed on day 3 which preceded the maximum growth rate of cyanobacteria by 1-2 days and the highest cell number found in cyanobacteria in this experiment by 4 days. Moreover, P_{max} and ETR increased again from day 7-8 which may be attributed to the next exponential increase of algae cells around day 10, although data at this point are likely less reliable due to wall growth in the vessel and connecting tubing.

In experiment II, P_{max}(GOR) and P_{max}(B) peaks observed, respectively, on days 2-3 and 4, preceded the peak growth rate seen around day 9, marking a difference of 5 - 6 days (Figure 3H,K). Moreover, the exponential increase of cell numbers on day 6 was preceded by increased P_{max} 6 days earlier, on the day of nutrient addition. Equivalent results were observed in the dynamics of ETR which increased from nutrient addition six days before algae and cyanobacteria cell numbers increased. ETR(GOR) and ETR(B) peaks observed on days 2-3 preceded the maximum growth rates observed on day 9.

4. Discussion

4.1. Conditions controlling growth

Increased growth rates leading to high cell abundance were the result of removing the nutrient limitations encountered in the samples taken from the two reservoirs. In experiment II, removing the phosphate limitation in addition to providing elevated ammonium contributed to higher abundance of cyanobacteria because ammonium is a preferred source of nitrogen for cyanobacteria (Tandeau de Marsac and Houmard 1993). The ability to store phosphorus (Carey et al. 2012) may also have been a factor promoting cyanobacteria growth because the precipitation of iron phosphate limited the access of phosphate to phytoplankton after the initial rapid uptake. In the other experiments the phytoplankton community encountered in the field sample did not significantly alter following nutrient treatment. In the first experiment the removal of phosphate limitation promoted the growth of both algae and cyanobacteria, while in experiment III it may be concluded that the only bloom-forming species were eukaryotic algae, despite a slightly higher cyanobacteria cell number in the starting sample. Phytoplankton physiology observed from fluorescence was closely coupled to the dynamics observed from cell counts, witnessed by the increase of F_v/F_m from approximately 0.3 to 0.5-0.6 in all experiments within 5-7 days from lifting nutrient limitations on growth.

In experiment II and III, phytoplankton physiology was negatively affected from around 8-9 days after nutrient addition, likely due to factors such as wall growth contributing to lower nutrient availability and incident light. In experiment I, phytoplankton physiological parameters remained in favour of growth but no firm conclusions can be drawn towards the end of the experiment, due to large data gaps caused by instrument malfunction.

4.2. Observed fluorescence properties in relation to phytoplankton community composition

F_o values matched abundances of phytoplankton in the three experiments, which was expected and supports the use of fluorescence tools for biomass assessment. However, sensitivity of the protocols targeting blue versus green-red absorption to algae and cyanobacteria varied considerably between experiments, leading to inconsistent results. This is explained by the fact that the B protocol also targets PSII Chla in cyanobacteria, even though the fluorescence response may be considered low in comparison (Courtecuisse et al. 2022, Simis et al. 2012). More importantly, the red LED used in the GOR protocol targets both algae and cyanobacteria. Here, the response from algae and cyanobacteria may be expected of similar magnitude but when cyanobacteria are present an additional response is to be expected from the green-orange LEDs. This combination was still required because these LEDs are not sufficiently bright to produce a saturating pulse in cyanobacteria, even with the extended duration of the saturating flash used. The total photon flux produced with the GOR protocol was, in fact, still weaker than the B protocol (Table 2). Discussion of these differences has been previously detailed by Courtecuisse et al. (2022). Both excitation protocols can still be used in parallel to provide a comparative picture of phytoplankton abundance, whilst a saturating light dose from green and particularly orange LEDs remains highly desirable to further the diagnostic relevance of the instrument to freshwater cyanobacteria.

4.3. Predicting phytoplankton dynamics from photosynthetic parameters derived from FLCs

F_v/F_m did not vary between protocols B and GOR in the three experiments, suggesting that the algal and cyanobacteria subpopulations adjusted similarly to environmental conditions, as also observed by Houliez et al. (2017) in a seasonal study of the Baltic Sea with a dual-excitation FRRf. When P_{max} and ETR results were of similar value between excitation protocols, we may similarly assume that the two phytoplankton groups responded similarly. However, because

the two protocols are not fully selective, the signal from either protocol may also be largely driven by one group dominating biomass, which is observed in several instances in the experiments presented here. This is confirmed by the fact that when P_{max} and ETR values diverged, differences in growth rates and ultimately abundance between cyanobacteria and algae increased as well. These results confirm the benefit of applying multiple excitation protocols in parallel or in sequence, to predict the growth of algae versus cyanobacteria in the community.

ETR is the product of photon irradiance and σ_{PII} which is the absorption cross section of PSII. σ_{PII}(GOR) produced lower values than σ_{PII}(B) in the three experiments (data not shown) which explains the lower values of ETR(GOR) compared to ETR(B). The fact that σPII(B) was higher than σ_{PII}(GOR) can be explained, either by the fact that σPII(B) also targets cyanobacteria or that the ratio of Chla pigments over phycobilipigments was high. Analysis of the particulate absorption coefficient partitioned into pigment ($a_\phi(\lambda)$, with λ denoting wavelength) and other fractions, using the filter pad method inside an integrating sphere following Simis and Kauko (2012), confirmed that the ratio $a_\phi(675)$ over $a_\phi(615)$ varied between 1.93 and 4.23 (results not shown). This supports the understanding that cyanobacterial accessory pigment was present in relatively low concentrations. P_{max}(GOR) was higher than P_{max}(B) for the majority of each experiment, which can also be explained by the low affinity of cyanobacteria to green-orange excitation light, as well as the fact that the red LED also targets PSII Chla in algae. This may readily explain possible false positives such as the peak of P_{max}(GOR) in experiment III around day 4-5 preceding high abundances of algae while cyanobacteria were all but absent.

P_{max} and ETR peaks are of particular interest as likely precursors of efficient growth when environmental conditions allow. The lag observed between elevated P_{max} and ETR on the one hand, and peak growth rates on the other, was longer in experiment II than in the other experiments, which may be due to a lower light dose due to precipitated iron phosphate. Nevertheless, these results confirm that measuring ETR and P_{max} obtained with both excitation protocols can predict phytoplankton growth periods. Combined with F_o obtained with diagnostic excitation bands and any corresponding elevation of F_v/F_m should provide clear cues to enhanced phytoplankton growth from exclusively fluorescence-based parameters. This should be of significant practical use in freshwater monitoring where the pulsed introduction of nutrients from catchments should lead to very similar responses.

The sensitivity of the protocols targeting blue versus green-red absorption to algae and cyanobacteria varied considerably between experiments. Predicting the growth of

cyanobacteria versus algae with ETR and P_{max} fluorescence using GOR and B protocols only is then challenging. Nevertheless, the labSTAF is also able to measure excitation spectra, obtained with a protocol targeting algae and a protocol targeting cyanobacteria, which illustrates the photosynthetic action spectrum (pigment groups) as described by Courtecuisse et al. (2022). Both excitation spectra and ETR and P_{max} fluorescence under GOR and B protocols can be measured in parallel to predict the growth of cyanobacteria versus algae. However, low concentrations of PC were found in this study, which indicates that the prediction of cyanobacteria versus algae using excitation spectra as well, will be not certain.

The proportion of nitrogen inputs, *i.e.* ammonium versus nitrate, is considered key in determining the dominance of phytoplankton functional groups in the environment (Glibert et al. 2016). A higher proportion of ammonium generally favours flagellates, cyanobacteria and chlorophytes while overall production will be characterized by smaller cells, whilst a higher proportion of nitrate favours diatoms and production dominated by larger cells. If the N:P ratio is already monitored, this information combined with fluorescence measurements on an instrument such as the LabSTAF will likely aid in the accurate prediction of cyanobacteria growth, with N:P decreasing, from the addition of phosphorus source, more likely to favour bloom-forming cyanobacteria (Levich 1996).

Overall, the observed phytoplankton dynamics and lead times between fluorescence-based cues and observed growth reported here should be considered short estimates, compared to the situation that would be encountered in the field. This is by design, as the sample was transferred from natural light into a continuous light period and any large grazers were removed from the sample, to induce rapid growth. Thus, fluorescence-based precursors of 2-3 days may well correspond to a week or longer in natural conditions, which would be highly appropriate for regular observation practises as an early warning for the bloom of potentially harmful cyanobacteria.

CHAPTER 5: DISCUSSION

1. Identifying optical markers specific to cyanobacteria photo-physiology responses

One of the first aspects of this research was to define fluorescence excitation and emission wavebands diagnostic of the presence and photophysiology of cyanobacteria. Chapter 2 confirmed the benefit of combining excitation wavebands centered at 445 nm and 615 nm, respectively targeting chlorophyll *a* (Chla) and phycocyanin pigment absorption, to separate the fluorescence response by cyanobacteria from algae. In the same chapter, emission wavebands centred at 660 nm, 685 nm and 730 nm differentiate the fluorescence response between cyanobacteria and algae. The waveband at 660 nm is useful to record the fluorescence from PC and APC, alongside fluorescence at 685 nm to target PSII Chla while the waveband at 730 nm targets fluorescence from PSI. Furthermore, fluorescence from kinetics measurements showed a high fluorescence signal and high values of slope of fluorescence changes at emission 730 nm, observed only in cyanobacteria, which highlights the importance of considering this emission waveband.

In Chapter 3, excitation protocols B (Blue LED, 452 nm) and GOR (Green-Orange-Red LEDs, 534, 594 and 622 nm), generated by the LabSTAF instrument, captured the physiology of algae and cyanobacteria, respectively. The GO excitation protocol (Green-Orange LEDs, 534, 594), was considered particularly promising for diagnostically targeting cyanobacteria because it included LEDs targeting PC (594 nm) and PE (534 nm) without using a red LED that would further include PSII Chla, present in all photosynthetic organisms. However, this protocol did not achieve saturation, so that photosynthetic parameters could not be accurately derived. This is not ideal, and it is recommended that future instruments use excitation protocols which principally target phycobilipigments with sufficiently high intensity to saturate RC in PSII. In addition, to improve saturation, the length of pulses can be extended, which has been described in Chapter 3 and 4 with pulse lengths of 100 µs for the B protocol compared to 200 µs (Chapter 3) and 300 µs (Chapter 4) for the GOR protocol.

Chapter 2 and 3 further explored the role of fluorescence emission ratios as optical markers to target cyanobacteria. Fluorescence emission (F') ratios of 734: 684 and 660: 684, under 445 nm excitation, were consistently higher in cyanobacteria cultures than algae cultures (Chapter 2). Moreover, the fluorescence emission ratio (F_o) 730: 685 measured prior to FLC curves with the LabSTAF obtained with the GOR excitation protocol was positively and significantly correlated to the relative abundance of cyanobacteria (Chapter 3). This confirmed the potential of the emission ratio 730: 685 as an indicator of PSI: PSII fluorescence, as an optical marker targeting cyanobacteria. The LabSTAF is not the only fluorometer which has the

potential to measure fluorescence around 730 nm; the LIFT-FRR fluorometer (Soliense, US) has the possibility to measure fluorescence at six emission wavebands using a filter wheel. The Dual PAM-100 (WALZ, Germany) contains filters to separate fluorescence shorter and longer than 700 nm (Pfündel, Stichs, and Tanis 2021), which could be useful to target PSI fluorescence in cyanobacteria. Emission filters targeting the 660 nm waveband would ideally be included to measure the PBS: Chla fluorescence ratio as an optical marker of accessory pigments most commonly found in cyanobacteria. The emission ratio PBS: Chla will be responsive to environmental conditions which means that this ratio should be tested on cultures grown under different light and nutrient conditions.

Chapter 3 then explored the potential of the LabSTAF fluorometer to target cyanobacteria by combining several optical features. Those features included the excitation protocols GOR and B and emission ratio (F_o) 730: 685, described above, and excitation spectra obtained with protocols optimized to algae and cyanobacteria, respectively. Excitation spectra of σ_{PII}, measured at 685 nm emission showed distinct responses between algae and cyanobacteria. Excitation spectra of F_v, measured at emission 685 nm, further captured shifts in abundance between algae and cyanobacteria. Excitation spectra of σ_{PII} and F_v were determining to characterize the phytoplankton community. Although excitation spectra have been previously used in multispectral fluorometer to discriminate pigment groups (Beutler et al. 2002, Yoshida et al. 2011), we recommend using excitation spectra to determine the dominant pigment group.

The research in Chapter 2 also explored the NPQ mechanism induced by the OCP protein in cyanobacteria cultures under blue-green actinic light, as a potential optical marker. Blue-green actinic light showed distinct fluorescence kinetic responses from white actinic light in two out of three studied cyanobacteria strains. Considering the small number of cultures tested and the fact that NPQ induced by OCP protein was not observed in all cultures, it is not considered a suitable optical marker to target cyanobacteria.

2. Predicting growth

Chapter 4 tested the potential of the LabSTAF to predict the growth of cyanobacteria versus algae from fluorometry. Photosynthetic parameters derived from FLC curves were obtained with two excitation protocols targeting cyanobacteria or algae, as determined relatively suitable in Chapter 3. We found that ETR and P_{max} obtained with both excitation protocols could predict phytoplankton growth periods with a lead period of several days. These results

mean that enhanced phytoplankton growth could be predicted in advance, to the benefit of water quality managers in affected areas, such as recreational or drinking water bodies. ETR and P_{max} measured with both excitation protocols, combined with F_v/F_m to estimate differences in physiology between phytoplankton groups, and F_o measured with the most diagnostic excitation wavebands for biomass assessment, constitute the key fluorescence parameters to monitor. For enhanced assessment of phytoplankton group dynamics, excitation spectra, as explored in Chapter 3, and the 730: 685 emission ratio, explored in Chapter 2 and 3, should then be added. These combined optical markers as well as fluorescence and photosynthetic parameters would allow reasonable prediction of cyanobacteria versus algae growth potential using exclusively fluorescence-based parameters.

In the last experiments, phytoplankton was grown under artificial continuous light and large grazers had been removed (Chapter 4). Whilst this helped promote phytoplankton growth, it may also underestimate the lead time of predicting phytoplankton bloom. The prediction will need to be adjusted to natural environment for a more accurate diagnostic of cyanobacteria growth.

3. Towards lower-cost fluorometry

With an increasing number of optical markers, the price of the ideal fluorometer is likely to increase as well. Thus, optical features should be carefully selected and ranked. First, excitation and emission wavebands should be chosen to limit the number of filters and LEDs to implement in the instrument. Ideally, excitation wavebands 445 nm and 615 nm and narrow (10 nm) emission wavebands at 685 nm and either 730 or 660 nm should be considered. Only one type of actinic light colour should be chosen, and as suggested in Chapter 2, a broadband actinic light should be preferred. The sensitivity requirement for single turnover fluorometers generally extends from low phytoplanktonic concentrations (oligotrophic conditions) to hyper-eutrophic conditions. However, a trade-off between cost and sensitivity suggests that reduced sensitivity of the instrument may be considered for applications targeting eutrophic water bodies, where the risk of toxic concentrations of cyanobacteria is high. Photodiode detectors can be 200 - 10,000 times cheaper (Geng et al. 2017) than the photomultiplier tubes commonly used now in ST fluorometers.

An instrument measuring the physiology and estimating the biomass of phytoplankton, i.e., fluorometers using flash-stimulated techniques, should be preferred to provide the rich information exploited in Chapter 3 and 4 of this thesis, to identify potential HABs. However,

this preference will increase the cost of the instrument and PAM fluorometers may be preferred for their lower cost compared to faster fluorometers capable of achieving single turnover saturation.

4. Towards routine applications: practical considerations for developers

Schuback et al. (2021) provides a recent overview of ST-fluorometer protocols, applications and recommendations to potential users. Protocols for fluorometers using flash-stimulated techniques are relatively complex. A large number of parameters can be optimized, including the length of pulses for RC saturation, the maximum irradiance and number of steps for FLC curves, the duration of dark adaptation and the choice and combination of LEDs. In order to popularize the use of ST and MT fluorometers or to produce an easy-to-use fluorometer, step-by-step protocols, should be designed alongside tutorials to make a measurement and extract useful data.

As there are still many options available, accessible protocols should guide the users in the choice of parameters to use according to the type of measurements they want to operate. Primary considerations for the investigation of phytoplankton productivity in natural samples should include:

- Required sensitivity (low to high biomass)
- Influence of light history and temperature
- Phytoplankton group discrimination versus bulk phytoplankton assessment
- Discrete versus continuous measurements
- Selection of photo-physiological parameters to report

Whether samples are taken from oligo-, meso- or eutrophic conditions will influence the sensitivity required from the instrument. The light history will further determine the pre-illumination irradiance and duration prior to FLC curve measurements and the maximum photon irradiance to apply in the FLC curve. The latter in turn determines the number of increasing light steps needed to fit the FLC curve. For non-expert users these settings should be automated.

For phytoplankton group discrimination, multiple excitation LED groups will be needed in sequency and their intensity optimised. Pre-set excitation protocols for different

phytoplankton groups would ideally be provided, with the option to automatically adjust excitation LEDs combination and intensity for an optimal fluorescence response. The pulse length of LEDs should also be adjusted as needed to reach saturation. Features such as the PSII:PSI ratio and excitation spectra should be assessed to provide proxies for the cyanobacteria component of the community. Guidelines should nevertheless be included to the user for helping discriminate cyanobacteria physiology based on notably the work done is this thesis. This include chosen excitation and emission spectra, the LED pulse length, as well as the use of extra features (excitation spectra obtained with two distinct protocols and PSI:PSII ratio measurement).

Depending on the application, continuous or discrete measurements may be preferred. A single instrument may be taken to numerous field sites or have samples (e.g. weekly) transported to it. In those cases where samples are discrete, light history effects will likely need to be removed by low-light acclimation, whilst temperature should be kept consistent with the natural environment. NPQ mechanisms will be less likely to provide valuable insight as they are likely to vary in the course of the day, and can be removed from the assessment. In continuous (on site) measurements, the repeat frequency should capture light history and vertical mixing effects, whilst stirring, temperature control and regular cleaning of instrument optics will be required.

If possible, simpler diagnostic tools should be provided, linking the results from fitted photosynthetic parameters to the presence, biomass estimate and physiological state of cyanobacteria in the sample. Such diagnostics should provide clear predictions of the potential for cyanobacteria to grow if environmental conditions remain as they are. These diagnostic tools should include an analysis tool kit to retrieve the data from the measurements and based on F_v/F_m, F_o, ETR, P_{max} and E_k measured under different excitation protocol, the current biomass estimate and physiology and the potential to grow of cyanobacteria versus algae could be assessed. F_o and F_v/F_m will give an assessment of the current biomass of both types of phytoplankton while P_{max}, ETR, the elevation of F_v/F_m and E_k will give the potential to grow of cyanobacteria versus algae. Excitation protocols targeting cyanobacteria and algae should be able to saturate PSII and a Green-Orange protocol should be preferred to target cyanobacteria. The instrument should have a simple interface identifying the estimate biomass and proportion of cyanobacteria with a level of uncertainty and a health indication (Good, moderate, bad). A prediction of growth, constancy or decline will be presented on a set time scale with a level of uncertainty, according to nutrients and light conditions. Potential growth

peaks could also be indicated. An example of the interface shown by the diagnostic tool is shown in Figure 1.

For long-term deployments there are additional practical considerations:

- Preventing bio-fouling
- Protection from the elements
- Data transmission

In continuous deployments, purging and changing of samples, as well as washing cycles with clean water or detergents, requires pumps and valves to be included in the sampling setup. The cleaning system avoids growth in tubing and on optical surfaces. A protective environment will be needed to avoid excessive temperature fluctuations, power backup solutions, and the system will need to include remote monitoring provisions.

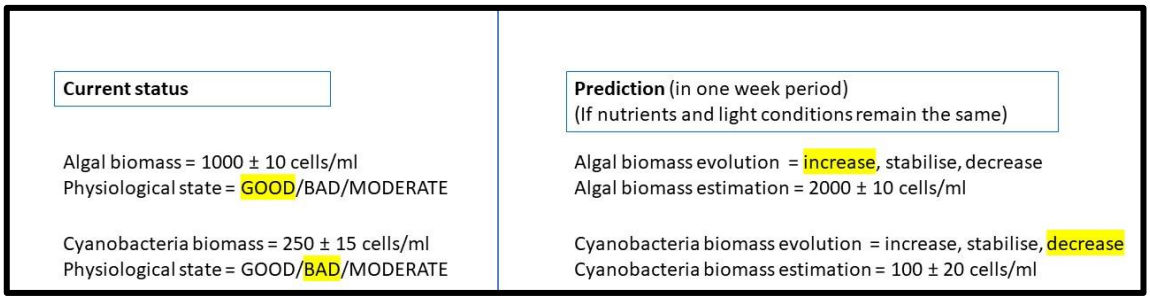

Figure 1. Example of a simple fluorometer diagnostic tool interface which indicates the current algal and cyanobacteria biomass and their respective physiological state of the sample and the evolution and estimation of their biomass if nutrients and light level stay unchanged.

5. Limitations and future research for cyanobacteria monitoring with the LabSTAF

As mentioned above, to accurately predict the potential for cyanobacteria growth, the excitation protocol must be specific to cyanobacteria, to maximise group separation and to obtain PSII saturation for the assessment of primary and secondary photosynthetic parameters. We recommend an excitation protocol using green-orange LEDs which are brighter than those used in Chapter 3 and 4. Moreover, we suggest testing the potential of the fluorescence emission ratio 650:685 nm as a primary optical marker of cyanobacteria presence, noting that this does not strictly require single-turnover fluorescence methodology.

We recommend not using the dual waveband measurement (DWM) for correcting the package effect. Indeed, our results in Chapter 3 indicate that the DWM value is biased by the nature of

the phytoplankton (cyanobacteria versus algae). However, this feature can be used for discriminating cyanobacteria, as suggested in Chapter 3, and other filter could be used to target other emission waveband, including 650 nm which is has the potential of being diagnostic of cyanobacteria.

Results from Chapter 4 give a first insight into predicting cyanobacteria versus algae growth using F_v/F_m, σ_{PII} and ETR obtained with two distinct excitation protocols. However, these experiments were operated under constant illumination and nutrient replete conditions induced in natural samples. Further studies are recommended to optimise the approach. First, we recommend generating artificial communities, increasing in complexity. Going from single cultures of algae and cyanobacteria, artificial communities composed of one or more cyanobacteria and algae species would be observed. Fluorescence would be measured from cultures grown under different light and nutrient conditions to optimize the prediction of growth from algae and cyanobacteria. Fluorescence measurements would ideally be carried out on two LabSTAF instruments in parallel using the two distinct excitation protocols, but following optimisation of the GO excitation set. This will allow further separation of the fluorescence response from algae versus cyanobacteria than what was the case in Chapter 4.

The LabSTAF is presently developed for expert users. A simpler version of the instrument interface and handbook could be provided for non-expert users, including step-by-step protocols to facilitate considerations described in the previous section. Automated signal optimisation will be preferred by non-expert users. These include options already present in the LabSTAF, notably “Auto LED” which optimises excitation LED group intensities against sample phytoplankton (pigment) composition, "Auto PMT” which adjusts the sensitivity of the instrument to the amplitude of the signal, “Repeat FLC” which automatically repeats new FLC measurement, in combination with “Auto set” which automatically adjust the maximum actinic irradiance based on the E_k derived from the previous FLC. Other parameter settings could still be automated, including the length of pulses for RC saturation, the number and length of steps for FLC curves, the duration of dark adaptation and the details of the induction protocol, including the time gap (and gap characteristics) between the two pulses, the duration of the sequence interval, the number of sequences by acquisition and the number of acquisitions per super acquisition. Moreover, an analysis tool kit should be provided to help retrieve and understand key data from the FLC, induction curves and excitation spectra data.

6. Fluorescence in water quality management

The instrument (LabSTAF) tested in Chapters 3 and 4 showed its flexibility in terms of deployment. The LabSTAF is designed not only for discrete measurements (Chapter 3) but also for continuous measurements (Chapter 4). The instrument is particularly suitable for long-term continuous measurements thanks to a sample exchange feature using a peristaltic pump controlled by the instrument, a flow-through stirrer, a cleaning cycle using a pump and a solenoid valve controller and temperature control (Oxborough, 2021). These features indicate that the instrument can be maintained with relatively low maintenance effort, other than regular cleaning of the sampling chamber, retrieving data from the computer associated with the instrument and periodically checking if the instrument is running correctly.

If fluorescence measurements such as those performed with LabSTAF instruments are operated continuously, high volumes of data will be produced which will need analyzing and archiving. In Chapter 4, FLC curves, lasting between 25 min to 1h05, were measured back to back, following the purging and refill of the sample. This high frequency of measurements is recommended to explore short-term variations of photo-photophysiology and photosynthetic rates. However, a lower frequency might be considered to look at longer-term variations of photosynthetic parameters and ultimately to reduce the analysis effort and even the bandwidth required for data transfer. The LabSTAF has the possibility to adjust the frequency of FLC measurements when continuous measurements are operated, and this feature is important to consider for other ST and MT fluorometers targeting cyanobacteria.

7. Other applications of the LabSTAF instrument

The LabSTAF has a high signal sensitivity and dynamic range which makes this instrument suitable from oligotrophic to eutrophic conditions. Other than the interpretation of the 730:685 nm emission which is heavily influenced by cyanobacteria presence, this implies that the instrument is suitable for determining phytoplankton productivity in the continuum from oceans to freshwater areas. Moreover, the LabSTAF is able to measure continuously and support a cleaning system which permits prolonged deployment. A submersible version of the LabSTAF could also be considered. The LabSTAF is particularly suitable to fulfil a role in the management of water quality. Measuring fluorescence from all phytoplanktonic community or from different types of phytoplankton on a regular basis can indicate the water quality status through the year, particularly related to nutrient availability. This type of instrument can be used at drinking water reservoirs, recreational water bodies and water bodies with known

health risks due to harmful algal blooms. Fluorescence measurements can be used to give a warning status before additional analysis including microscopy or toxins analysis for a precise and advanced diagnostic, at relatively low cost.

The LabSTAF has the potential to collect valuable reference information in satellite-derived ocean colour studies of primary production, by relating the sun-induced Chla fluorescence observed with satellites to (diurnal) variability in phytoplankton productivity. Such studies would benefit from long-term station and transect data collected from moorings, research vessels and even autonomous vehicles.

Other industries than the water utilities may also find benefit from enhanced routine investigation of phytoplankton productivity from fluorescence. Examples include the assessment of ballast water to ensure its safe release into port environments, phytoplankton productivity in and around aquaculture sites (those requiring phytoplankton to feed on, or those adding nutrients into the system). The high sensitivity of modern active fluorescence instruments provide rapid assessment capabilities and the potential for a rapid response to subtle changes in phytoplankton productivity.

8. Conclusion

The research carried out in this thesis has helped to further our understanding on how to capture the photo-physiology of cyanobacteria, confirming the accuracy of existing and new optical markers. The potential for specific optical markers to discriminate cyanobacteria in mixed communities was tested with active fluorescence methods *in vitro*, including on manipulated natural samples. A new ST instrument combining several of the recommended optical features, developed in parallel to this research, was tested for its potential to follow cyanobacteria growth, providing promising results whilst marking further possible improvements. This research helped to determine a combination of optical markers suitable to implement in a fluorescence protocol suited for either ST or MT fluorometers. In Chapter 4, findings on the prediction of phytoplankton growth from photosynthetic parameters could be extended to the development of protocols targeting cyanobacteria. The combination of these findings will help to build a better understanding of the photo-physiology of cyanobacteria in freshwater bodies, which remains crucial for the development of an ideal fluorescence protocol that is diagnostic of cyanobacteria.

References

Abbasi, Tasneem, and Shahid A Abbasi. 2012. *Water quality indices*: Elsevier.

Allen, Mary Mennes. 1984. "Cyanobacterial cell inclusions." *Annual reviews of microbiology* 38 (1):1-25.

Arnold, William, and Henry I Kohn. 1934. "The chlorophyll unit in photosynthesis." *The Journal of General Physiology* 18 (1):109.

Babin, M. 2008. "Phytoplankton fluorescence: theory, current literature and in situ measurement." *Real-Time Coastal Observing System for Marine Ecosystem Dynamics and Harmful Algal Blooms*:237-280.

Baker, Judith A., Barrie Entsch, Brett A. Neilan, and David B. McKay. 2002. "Monitoring changing toxigenicity of a cyanobacterial bloom by molecular methods." *Applied and Environmental Microbiology* 68 (12):6070-6076.

Barbour, Michael T. 1999. *Rapid bioassessment protocols for use in wadeable streams and rivers: periphyton, benthic macroinvertebrates and fish*: US Environmental Protection Agency, Office of Water.

Becker, Annette, Armin Meister, and Christian Wilhelm. 2002. "Flow cytometric discrimination of various phycobilin-containing phytoplankton groups in a hypertrophic reservoir." *Cytometry: The Journal of the International Society for Analytical Cytology* 48 (1):45-57.

Bender, Douglas J, and Alan J Laub. 1987. "The linear-quadratic optimal regulator for descriptor systems: discrete-time case." *Automatica* 23 (1):71-85.

Beutler, M., Karen Helen Wiltshire, Bettina Meyer, C. Moldaenke, C. Lüring, M. Meyerhöfer, U.-P. Hansen, and H. Dau. 2002. "A fluorometric method for the differentiation of algal populations in vivo and in situ." *Photosynthesis research* 72 (1):39–53.

Bidigare, Robert R, Mikel Latasa, Zachary Johnson, Richard T Barber, Charles C Trees, and William M Balch. 1997. "Observations of a Synechococcus-dominated cyclonic eddy in open-oceanic waters of the Arabian Sea." Ocean Optics XIII.

Bidigare, Robert R, Michael E Ondrusek, John H Morrow, and Dale A Kiefer. 1990. "In-vivo absorption properties of algal pigments." Ocean Optics X.

Birk, Sebastian, Wendy Bonne, Angel Borja, Sandra Brucet, Anne Courrat, Sandra Poikane, Angelo Solimini, Wouter Van De Bund, Nikolaos Zampoukas, and Daniel Hering. 2012. "Three hundred ways to assess Europe's surface waters: an almost complete overview of biological methods to implement the Water Framework Directive." *Ecological indicators* 18:31-41.

Boatman, Tobias G, Richard J Geider, and Kevin Oxborough. 2019. "Improving the accuracy of single turnover active fluorometry (STAF) for the estimation of phytoplankton primary productivity (PhytoPP)." *Frontiers in Marine Science* 6:319.

Borja, Angel, Javier Franco, and V Pérez. 2000. "A marine biotic index to establish the ecological quality of soft-bottom benthos within European estuarine and coastal environments." *Marine pollution bulletin* 40 (12):1100-1114.

Bower, Peter M, Carol A Kelly, Everett J Fee, John A Shearer, Doug R DeClercq, and David W Schindler. 1987. "Simultaneous measurement of primary production by whole-lake and bottle radiocarbon additions." *Limnology and Oceanography* 32 (2):299-312.

Bryant, Donald A. 1995. *The molecular biology of cyanobacteria*. Vol. 1: Springer Science & Business Media.

Bryant, Donald A, Gérard Guglielmi, Nicole Tandeau de Marsac, Anne-Marie Castets, and Germaine Cohen-Bazire. 1979. "The structure of cyanobacterial phycobilisomes: a model." *Archives of Microbiology* 123 (2):113-127.

Caffarri, Stefano, Tania Tibiletti, Robert C Jennings, and Stefano Santabarbara. 2014. "A comparison between plant photosystem I and photosystem II architecture and functioning." *Current Protein and Peptide Science* 15 (4):296–331.

Calzadilla, Pablo I., and Diana Kirilovsky. 2020. "Revisiting cyanobacterial state transitions." *Photochemical & Photobiological Sciences* 19 (5):585-603.

Campbell, Douglas. 1996. "Complementary chromatic adaptation alters photosynthetic strategies in the cyanobacterium Calothrix." *Microbiology* 142 (5):1255-1263.

Campbell, Lisa, Darren W Henrichs, Robert J Olson, and Heidi M Sosik. 2013. "Continuous automated imaging-in-flow cytometry for detection and early warning of Karenia brevis blooms in the Gulf of Mexico." *Environmental Science and Pollution Research* 20 (10):6896-6902.

Carey, Cayelan C, Bas W Ibelings, Emily P Hoffmann, David P Hamilton, and Justin D Brookes. 2012. "Eco-physiological adaptations that favour freshwater cyanobacteria in a changing climate." *Water research* 46 (5):1394-1407.

Carmichael, Wayne W., and Jisi An. 1999. "Using an enzyme linked immunosorbent assay (ELISA) and a protein phosphatase inhibition assay (PPIA) for the detection of microcystins and nodularins." *Natural toxins* 7 (6):377-385.

Chamberlin, WS, CR Booth, DA Kieffer, JH Morrow, and R Co Murphy. 1990. "Evidence for a simple relationship between natural fluorescence, photosynthesis and chlorophyll in the sea." *Deep Sea Research Part A. Oceanographic Research Papers* 37 (6):951-973.

Chen, Min, and Robert E Blankenship. 2011. "Expanding the solar spectrum used by photosynthesis." *Trends in plant science* 16 (8):427-431.

Chen, Min, Martin Schliep, Robert D Willows, Zheng-Li Cai, Brett A Neilan, and Hugo Scheer. 2010. "A red-shifted chlorophyll." *Science* 329 (5997):1318-1319.

Chen, Zhihao, Meiqing Chen, Kok Yuen Koh, Wenyang Neo, Choon Nam Ong, and J Paul Chen. 2022. "An optimized CaO2-functionalized alginate bead for simultaneous and efficient removal of phosphorous and harmful cyanobacteria." *Science of The Total Environment* 806:150382.

Codd, Geoffrey A., Jaime Lindsay, Fiona M. Young, Louise F. Morrison, and James S. Metcalf. 2005. "Harmful cyanobacteria." In *Harmful cyanobacteria*, 1–23. Springer.

Codd, Geoffrey A., Louise F. Morrison, and James S. Metcalf. 2005. "Cyanobacterial toxins: risk management for health protection." *Toxicology and Applied Pharmacology* 203 (3):264-272.

Courtecuisse, Emilie, Elias Marchetti, Kevin Oxborough, Peter D Hunter, Evangelos Spyrakos, Gavin H Tilstone, and Stefan GH Simis. 2023. "Optimising Multispectral Active Fluorescence to Distinguish the Photosynthetic Variability of Cyanobacteria and Algae." *Sensors* 23 (1):461.

Courtecuisse, Emilie, Kevin Oxborough, Gavin H Tilstone, Evangelos Spyrakos, Peter D Hunter, and Stefan G H Simis. 2022. "Determination of optical markers of cyanobacterial physiology from fluorescence kinetics." *Journal of Plankton Research* 44 (3):365-385. doi: 10.1093/plankt/fbac025.

Cronberg, G, EJ Carpenter, and WW Carmichael. 2003. "Taxonomy of harmful cyanobacteria." *Manual on harmful marine microalgae. UNESCO publishing*:523-562.

de Figueiredo, Daniela R, Ana SSP Reboleira, Sara C Antunes, Nelson Abrantes, Ulisses Azeiteiro, Fernando Goncalves, and Mario J Pereira. 2006. "The effect of environmental parameters and cyanobacterial blooms on phytoplankton dynamics of a Portuguese temperate lake." *Hydrobiologia* 568 (1):145-157.

De Marsac, N Tandeau, and J Houmard. 1988. "[34] Complementary chromatic adaptation: physiological conditions and action spectra." In *Methods in enzymology*, 318-328. Elsevier.

Delrue, Florian, Emilie Alaux, Lagia Moudjaoui, Clément Gaignard, Gatien Fleury, Amaury Perilhou, Pierre Richaud, Martin Petitjean, and Jean-François Sassi. 2017. "Optimization of Arthrospira platensis (Spirulina) Growth: From Laboratory Scale to Pilot Scale." *Fermentation* 3 (4):59.

Demmig-Adams, Barbara. 1990. "Carotenoids and photoprotection in plants: a role for the xanthophyll zeaxanthin." *Biochimica et Biophysica Acta (BBA)-Bioenergetics* 1020 (1):1-24.

Diaz, Robert J, Martin Solan, and Raymond M Valente. 2004. "A review of approaches for classifying benthic habitats and evaluating habitat quality." *Journal of environmental management* 73 (3):165-181.

Dittami, Simon M., Svenja Heesch, Jeanine L. Olsen, and Jonas Collén. 2017. "Transitions between marine and freshwater environments provide new clues about the origins of multicellular plants and algae." *Journal of phycology* 53 (4):731-745.

Dodds, Walter. 2002. *Freshwater ecology: concepts and environmental applications*: Elsevier.

El Bouaidi, Widad, Giovanni Libralato, Mountasser Douma, Abdelaziz Ounas, Abdelrani Yaacoubi, Giusy Lofrano, Luisa Albarano, Marco Guida, and Mohammed Loudiki. 2022. "A review of plant-based coagulants for turbidity and cyanobacteria blooms removal." *Environmental Science and Pollution Research* 29 (28):42601-42615.

Elmorjani, K, J -C Thomas, and P Sebban. 1986. "Phycobilisomes of wild type and pigment mutants of the cyanobacterium Synechocystis PCC 6803." *Archives of microbiology* 146:186-191.

Emerson, Robert, and William Arnold. 1932. "The photochemical reaction in photosynthesis." *The Journal of general physiology* 16 (2):191-205.

Falkowski, Paul G., and John A. Raven. 2013. *Aquatic Photosynthesis: (Second Edition)*, *Aquatic Photosynthesis: (Second Edition)*: Princeton University Press.

Ficek, D, R Majchrowski, M Ostrowska, and B Wozniak. 2000. "Influence of non-photosynthetic pigments on the measured quantum yield of photosynthesis." *Oceanologia* 42 (2).

Field, Christopher B, Michael J Behrenfeld, James T Randerson, and Paul Falkowski. 1998. "Primary production of the biosphere: integrating terrestrial and oceanic components." *science* 281 (5374):237-240.

Förster, Th. 1948. "Intermolecular energy transfer and fluorescence." *Ann. Phys. Leipzig.* 2:55-75.

Förster, Th. 1960. "Transfer mechanisms of electronic excitation energy." *Radiation Research Supplement*:326-339.

Franck, Fabrice, Philippe Juneau, and Radovan Popovic. 2002. "Resolution of the photosystem I and photosystem II contributions to chlorophyll fluorescence of intact leaves at room temperature." *Biochimica et Biophysica Acta (BBA)-Bioenergetics* 1556 (2-3):239-246.

Fukuzaki, Koji, Ichiro Imai, Keitaro Fukushima, Ken-Ichiro Ishii, Shigeki Sawayama, and Takahito Yoshioka. 2014. "Fluorescent characteristics of dissolved organic matter produced by bloom-forming coastal phytoplankton." *Journal of plankton research* 36 (3):685-694.

Gaffron, Hans, and Kurt Wohl. 1936. "Zur theorie der assimilation." *Naturwissenschaften* 24 (6):81-90.

Gantt, Elisabeth. 1975. "Phycobilisomes: Light-harvesting pigment complexes." *Bioscience* 25 (12):781-788.

Gault, Percy M, and Harris J Marler. 2009. *Handbook on cyanobacteria*: Nova Science Publishers.

Geider, Richard J, and Julie La Roche. 2002. "Redfield revisited: variability of C [ratio] N [ratio] P in marine microalgae and its biochemical basis." *European Journal of Phycology* 37 (1):1-17.

Geng, Xuhui, Yan Gao, Chunbo Feng, and Yafeng Guan. 2017. "A facile and high sensitive micro fluorimeter based on light emitting diode and photodiode." *Talanta* 175:183-188.

Giacometti, GM, and T Morosinotto. 2013. "Photoinhibition and Photoprotection in Plants, Algae, and Cyanobacteria."

Glibert, Patricia M, Frances P Wilkerson, Richard C Dugdale, John A Raven, Christopher L Dupont, Peter R Leavitt, Alexander E Parker, JoAnn M Burkholder, and Todd M Kana. 2016. "Pluses and minuses of ammonium and nitrate uptake and assimilation by phytoplankton and implications for productivity and community composition, with emphasis on nitrogen-enriched conditions." *Limnology and Oceanography* 61 (1):165-197.

Gorbunov, Maxim Y, Evgeny Shirsin, Elena Nikonova, Victor V Fadeev, and Paul G Falkowski. 2020. "A multi-spectral fluorescence induction and relaxation (FIRe) technique for physiological and taxonomic analysis of phytoplankton communities." *Marine Ecology Progress Series* 644:1-13.

Gregor, Jakub, and Blahoslav Maršálek. 2005. "A simple in vivo fluorescence method for the selective detection and quantification of freshwater cyanobacteria and eukaryotic algae." *Acta hydrochimica et hydrobiologica* 33 (2):142-148.

Gregor, Jakub, Blahoslav Maršálek, and Helena Šípková. 2007. "Detection and estimation of potentially toxic cyanobacteria in raw water at the drinking water treatment plant by in vivo fluorescence method." *Water Research* 41 (1):228-234.

Grigoryeva, Natalia. 2020. "Studying Cyanobacteria by Means of Fluorescence Methods: A Review." In, 3-33.

Grossman, AR. 1990. "Chromatic adaptation and the events involved in phycobilisome biosynthesis." *Plant, Cell & Environment* 13 (7):651-666.

Gwizdala, Michal, Adjele Wilson, and Diana Kirilovsky. 2011. "In vitro reconstitution of the cyanobacterial photoprotective mechanism mediated by the Orange Carotenoid Protein in Synechocystis PCC 6803." *The Plant Cell* 23 (7):2631-2643.

Hallegraeff, Gustaaf M, Donald Mark Anderson, Allan D Cembella, and Henrik O Enevoldsen. 2004. *Manual on harmful marine microalgae*: Unesco.

Harel, Yariv, Itzhak Ohad, and Aaron Kaplan. 2004. "Activation of photosynthesis and resistance to photoinhibition in cyanobacteria within biological desert crust." *Plant Physiology* 136 (2):3070-3079.

Houliez, Emilie, Stefan Simis, Susanna Nenonen, Pasi Ylöstalo, and Jukka Seppälä. 2017. "Basin-scale spatio-temporal variability and control of phytoplankton photosynthesis in the Baltic Sea: The first multiwavelength fast repetition rate fluorescence study operated on a ship-of-opportunity." *Journal of Marine Systems* 169:40-51.

Hu, Qiang, Hideaki Miyashita, Ikuko Iwasaki, Norihide Kurano, Shigetoh Miyachi, Masayo Iwaki, and Shigeru Itoh. 1998. "A photosystem I reaction center driven by chlorophyll d in oxygenic photosynthesis." *Proceedings of the National Academy of Sciences* 95 (22):13319-13323.

Hughes, David J, Douglas A Campbell, Martina A Doblin, Jacco C Kromkamp, Evelyn Lawrenz, C Mark Moore, Kevin Oxborough, Ondřej Prášil, Peter J Ralph, and Marco F Alvarez. 2018. "Roadmaps and detours: active chlorophyll-a assessments of primary productivity across marine and freshwater systems." *Environmental science & technology* 52 (21):12039-12054.

Hunter, Peter D, Andrew N Tyler, Mátyás Présing, Attila W Kovács, and Tom Preston. 2008. "Spectral discrimination of phytoplankton colour groups: The effect of suspended particulate matter and sensor spectral resolution." *Remote Sensing of Environment* 112 (4):1527-1544.

Huot, Yannick, and Marcel Babin. 2010. "Overview of Fluorescence Protocols: Theory, Basic Concepts, and Practice." In *Chlorophyll a Fluorescence in Aquatic Sciences: Methods and Applications*, edited by David J. Suggett, Ondrej Prášil and Michael A. Borowitzka, 31-74. Dordrecht: Springer Netherlands.

Hur, Jin, Soon-Jin Hwang, and Jae-Ki Shin. 2008. "Using synchronous fluorescence technique as a water quality monitoring tool for an urban river." *Water, air, and soil pollution* 191:231-243.

Hurley, Tim, Rehan Sadiq, and Asit Mazumder. 2012. "Adaptation and evaluation of the Canadian Council of Ministers of the Environment Water Quality Index (CCME WQI) for use as an effective tool to characterize drinking source water quality." *Water research* 46 (11):3544-3552.

Inagaki, Noritoshi. 2022. "Processing of D1 Protein: A Mysterious Process Carried Out in Thylakoid Lumen." *International Journal of Molecular Sciences* 23 (5):2520.

Itoh, Shigeru, and Kana Sugiura. 2004. "Fluorescence of Photosystem I." In *Chlorophyll a Fluorescence: A Signature of Photosynthesis*, edited by George Christos Papageorgiou and Govindjee, 231-250. Dordrecht: Springer Netherlands.

Jacoby, Jean M, Diane C Collier, Eugene B Welch, F Joan Hardy, and Michele Crayton. 2000. "Environmental factors associated with a toxic bloom of Microcystis aeruginosa." *Canadian Journal of Fisheries and Aquatic Sciences* 57 (1):231-240.

Jeffrey, SW, M Vesk, and RF Mantoura. 1997. "Phytoplankton pigments: windows into the pastures of the sea."

Johnsen, G., and Egil Sakshaug. 1996. "Light harvesting in bloom-forming marine phytoplankton: speciesspecificity and photoacclimation." *Sci. Mar.* 60:47-56.

Johnsen, Geir, and Egil Sakshaug. 2007. "Biooptical characteristics of PSII and PSI in 33 species (13 pigment groups) of marine phytoplankton, and the relevance for pulse-amplitude-modulated and fast-repetition-rate fluorometry ¹." *Journal of Phycology* 43 (6):1236-1251.

Kana, Todd M, and Patricia M Glibert. 1987. "Effect of irradiances up to 2000 µE m− 2 s− 1 on marine Synechococcus WH7803—I. Growth, pigmentation, and cell composition." *Deep Sea Research Part A. Oceanographic Research Papers* 34 (4):479-495.

Katyal, Deeksha. 2011. "Water quality indices used for surface water vulnerability assessment." *International journal of environmental sciences* 2 (1).

Kawamura, Michio, Mamoru Mimuro, and Yoshihiko Fujita. 1979. "Quantitative relationship between two reaction centersin the photosynthetic system of blue-green algae." *Plant and Cell Physiology* 20 (4):697-705.

Kazama, Takehiro, Kazuhide Hayakawa, Victor S Kuwahara, Koichi Shimotori, Akio Imai, and Kazuhiro Komatsu. 2021. "Development of photosynthetic carbon fixation model using multi-excitation wavelength fast repetition rate fluorometry in Lake Biwa." *PLoS One* 16 (2):e0238013.

Kerfeld, Cheryl A., Matthew R. Melnicki, Markus Sutter, and Maria Agustina Dominguez-Martin. 2017. "Structure, function and evolution of the cyanobacterial orange carotenoid protein and its homologs." *New Phytologist* 215 (3):937-951.

Kirilovsky, Diana, and Cheryl A Kerfeld. 2012. "The orange carotenoid protein in photoprotection of photosystem II in cyanobacteria." *Biochimica et Biophysica Acta (BBA)-Bioenergetics* 1817 (1):158-166.

Kirk, John TO. 1994. *Light and photosynthesis in aquatic ecosystems*: Cambridge university press.

Kolber, Zbigniew S, and Paul G Falkowski. 1992. Fast repetition rate (FRR) fluorometer for making in situ measurements of primary productivity. Brookhaven National Lab., Upton, NY (United States).

Kolber, Zbigniew S, F Gerald, Plumley, Andrew S Lang, J Thomas Beatty, Robert E Blankenship, Cindy L VanDover, Costantino Vetriani, Michal Koblizek, and Christopher Rathgeber. 2001. "Contribution of aerobic photoheterotrophic bacteria to the carbon cycle in the ocean." *Science* 292 (5526):2492-2495.

Kolber, Zbigniew S, Ondřej Prášil, and Paul G Falkowski. 1998. "Measurements of variable chlorophyll fluorescence using fast repetition rate techniques: defining methodology and experimental protocols." *Biochimica et Biophysica Acta (BBA)-Bioenergetics* 1367 (1-3):88-106.

Kopf, Uwe, and Juergen Heinze. 1984. "2, 7-Bis (diethylamino) phenazoxonium chloride as a quantum counter for emission measurements between 240 and 700 nm." *Analytical Chemistry* 56 (11):1931–1935.

Kowalczuk, Piotr, William J Cooper, Robert F Whitehead, Michael J Durako, and Wade Sheldon. 2003. "Characterization of CDOM in an organic-rich river and surrounding coastal ocean in the South Atlantic Bight." *Aquatic Sciences* 65:384-401.

Krall, John P, and Gerald E Edwards. 1992. "Relationship between photosystem II activity and CO2 fixation in leaves." *Physiologia Plantarum* 86 (1):180-187.

Kromkamp, Jacco. 1987. "Formation and functional significance of storage products in cyanobacteria." *New Zealand Journal of Marine and Freshwater Research* 21 (3):457-465.

Larkum, Anthony WD, and Michael Kühl. 2005. "Chlorophyll d: the puzzle resolved." *Trends in plant science* 10 (8):355-357.

Lavergne, Jérôme, and Pierre Joliot. 2000. "Thermodynamics of the excited states of photosynthesis." *Biophysics textbook onLine. Biophysical Society, Bethesda, MD*:1-12.

Lawaetz, Anders Juul, and Colin A Stedmon. 2009. "Fluorescence intensity calibration using the Raman scatter peak of water." *Applied spectroscopy* 63 (8):936-940.

Lawson, JD, HT Sambrook, DJ Solomon, and G Weilding. 1991. "The Roadford scheme: minimizing environmental impact on affected catchments." *Water and Environment Journal* 5 (6):671-681.

Levich, AP. 1996. "The role of nitrogen-phosphorus ratio in selecting for dominance of phytoplankton by cyanobacteria or green algae and its application to reservoir management." *Journal of Aquatic Ecosystem Health* 5:55-61.

Likens, Gene E. 1975. "Primary production of inland aquatic ecosystems." *Primary productivity of the biosphere*:185-202.

Liu, Lu-Ning. 2016. "Distribution and dynamics of electron transport complexes in cyanobacterial thylakoid membranes." *Biochimica et Biophysica Acta (BBA)-Bioenergetics* 1857 (3):256-265.

Long, Stephen P, S Humphries, and Paul G Falkowski. 1994. "Photoinhibition of photosynthesis in nature." *Annual review of plant biology* 45 (1):633-662.

Longhi, Maria L, and Beatrix E Beisner. 2010. "Patterns in taxonomic and functional diversity of lake phytoplankton." *Freshwater Biology* 55 (6):1349-1366.

Luimstra, Veerle M, J Merijn Schuurmans, Antonie M Verschoor, Klaas J Hellingwerf, Jef Huisman, and Hans CP Matthijs. 2018. "Blue light reduces photosynthetic efficiency of cyanobacteria through an imbalance between photosystems I and II." *Photosynthesis research* 138 (2):177-189.

Mackey, Katherine RM, Adina Paytan, Ken Caldeira, Arthur R Grossman, Dawn Moran, Matthew McIlvin, and Mak A Saito. 2013. "Effect of temperature on photosynthesis and growth in marine Synechococcus spp." *Plant physiology* 163 (2):815-829.

Mann, Kenneth Henry. 1982. *Ecology of coastal waters: a systems approach*. Vol. 8: Univ of California Press.

Mann, Kenneth Henry. 2009. *Ecology of coastal waters: with implications for management*: John Wiley & Sons.

Manning, Winston M, and Harold H Strain. 1943. "Chlorophyll d, a green pigment of red algae." *Journal of Biological Chemistry* 151 (1):1-19.

Mauzerall, D. 1976. "Multiple excitations in photosynthetic systems." *Biophysical Journal* 16 (1):87-91.

Metcalfe, Janice L. 1989. "Biological water quality assessment of running waters based on macroinvertebrate communities: history and present status in Europe." *Environmental pollution* 60 (1-2):101-139.

Mimuro, Mamoru. 2004. "Photon capture, exciton migration and trapping and fluorescence emission in cyanobacteria and red algae." In *Chlorophyll a fluorescence: a signature of photosynthesis*, 173-195. Springer.

Mimuro, Mamoru, and Yoshihiko Fujita. 1977. "Estimation of chlorophyll a distribution in the photosynthetic pigment systems I and II of the blue-green alga Anabaena variabilis." *Biochimica et Biophysica Acta (BBA)-Bioenergetics* 459 (3):376–389.

Mitchell, B. Greg, Mati Kahru, John Wieland, Malgorzata Stramska, and J. L. Mueller. 2002. "Determination of spectral absorption coefficients of particles, dissolved material and phytoplankton for discrete water samples." *Ocean optics protocols for satellite ocean color sensor validation, Revision* 3 (2):231.

Mullineaux, Conrad W, Mark J Tobin, and Gareth R Jones. 1997. "Mobility of photosynthetic complexes in thylakoid membranes." *Nature* 390 (6658):421-424.

Murphy, Kathleen R. 2011. "A note on determining the extent of the water Raman peak in fluorescence spectroscopy." *Applied Spectroscopy* 65 (2):233-236.

Nielsen, E Steemann. 1952. "The use of radio-active carbon (C14) for measuring organic production in the sea." *ICES Journal of Marine Science* 18 (2):117-140.

O'Carra, P, RF Murphy, and SD Killilea. 1980. "The native forms of the phycobilin chromophores of algal biliproteins. A clarification." *Biochemical Journal* 187 (2):303-309.

O'Neil, J. M., T. W. Davis, M. A. Burford, and C. J. Gobler. 2012. "The rise of harmful cyanobacteria blooms: the potential roles of eutrophication and climate change." *Harmful algae* 14:313-334.

Oehrle, Stuart A., Ben Southwell, and Judy Westrick. 2010. "Detection of various freshwater cyanobacterial toxins using ultra-performance liquid chromatography tandem mass spectrometry." *Toxicon* 55 (5):965-972.

Organelli, Emanuele, Caterina Nuccio, Luigi Lazzara, Julia Uitz, Annick Bricaud, and Luca Massi. 2017. "On the discrimination of multiple phytoplankton groups from light absorption spectra of assemblages with mixed taxonomic composition and variable light conditions." *Applied Optics* 56 (14):3952-3968.

Oxborough, Kevin. 2021. "LabSTAF and RunSTAF Handbook."

Paerl, and Jef Huisman. 2009. "Climate change: a catalyst for global expansion of harmful cyanobacterial blooms." *Environmental Microbiology Reports* 1 (1):27-37.

Paerl, Hans W, and Malcolm A Barnard. 2020. "Mitigating the global expansion of harmful cyanobacterial blooms: Moving targets in a human-and climatically-altered world." *Harmful Algae* 96:101845.

Paerl, Hans W, and Timothy G Otten. 2013. "Harmful cyanobacterial blooms: causes, consequences, and controls." *Microbial ecology* 65:995-1010.

Paerl, Hans W., Nathan S. Hall, and Elizabeth S. Calandrino. 2011. "Controlling harmful cyanobacterial blooms in a world experiencing anthropogenic and climatic-induced change." *Science of the total environment* 409 (10):1739-1745.

Paerl, Hans W., and Jef Huisman. 2008. "Blooms Like It Hot." *Science* 320 (5872):57-58.

Paerl, Hans W., and Valerie J. Paul. 2012. "Climate change: links to global expansion of harmful cyanobacteria." *Water research* 46 (5):1349-1363.

Pan, Gang, Ming-Ming Zhang, Hao Chen, Hua Zou, and Hai Yan. 2006. "Removal of cyanobacterial blooms in Taihu Lake using local soils. I. Equilibrium and kinetic screening on the flocculation of Microcystis aeruginosa using commercially available clays and minerals." *Environmental Pollution* 141 (2):195-200.

Parésys, Gérard, Claude Rigart, Bernard Rousseau, AWM Wong, F Fan, J-P Barbier, and Johann Lavaud. 2005. "Quantitative and qualitative evaluation of phytoplankton communities by trichromatic chlorophyll fluorescence excitation with special focus on cyanobacteria." *Water Research* 39 (5):911-921.

Patil, PN, DV Sawant, and RN Deshmukh. 2012. "Physico-chemical parameters for testing of water-a review." *International journal of environmental sciences* 3 (3):1194.

Pearson, Leanne A, and Brett A Neilan. 2008. "The molecular genetics of cyanobacterial toxicity as a basis for monitoring water quality and public health risk." *Current Opinion in Biotechnology* 19 (3):281-288.

Pfündel, Katrin, Anja Stichs, and Kerstin Tanis. 2021. *Muslimisches Leben in Deutschland 2020: Studie im Auftrag der Deutschen Islam Konferenz*. Vol. 38: DEU.

Pinto, Rute, Joana Patrício, Alexandra Baeta, Brian D Fath, Joao M Neto, and Joao Carlos Marques. 2009. "Review and evaluation of estuarine biotic indices to assess benthic condition." *Ecological indicators* 9 (1):1-25.

Poikane, Sandra, Martyn G Kelly, Fuensanta Salas Herrero, Jo-Anne Pitt, Helen P Jarvie, Ulrich Claussen, Wera Leujak, Anne Lyche Solheim, Heliana Teixeira, and Geoff Phillips. 2019. "Nutrient criteria for surface waters under the European Water Framework Directive: Current state-of-the-art, challenges and future outlook." *Science of the Total Environment* 695:133888.

Porter, G, CJ Tredwell, GFW Searle, and J Barber. 1978. "Picosecond time-resolved energy transfer in Porphyridium cruentum. Part I. In the intact alga." *Biochimica et Biophysica Acta (BBA)-Bioenergetics* 501 (2):232-245.

Price, Dana C., Jürgen M. Steiner, Hwan Su Yoon, Debashish Bhattacharya, and Wolfgang Löffelhardt. 2017. "Glaucophyta." In *Handbook of the Protists: Second Edition*, 23-87. Springer International Publishing.

Rabinowitch, E, and Govindgee. 1969. " Photosynthesis. John Wileyand Sons." *Inc., New York*.

Rahmanian, Nejat, Siti Hajar Bt Ali, M Homayoonfard, NJ Ali, M Rehan, Y Sadef, and AS Nizami. 2015. "Analysis of physiochemical parameters to evaluate the drinking water quality in the State of Perak, Malaysia." *Journal of Chemistry* 2015:1-10.

Raps, Shirley, Kevin Wyman, Harold W Siegelman, and Paul G Falkowski. 1983. "Adaptation of the cyanobacterium Microcystis aeruginosa to light intensity." *Plant Physiology* 72 (3):829-832.

Rascher, Uwe, Michael Lakatos, Burkhard Büdel, and Ulrich Lüttge. 2003. "Photosynthetic field capacity of cyanobacteria of a tropical inselberg of the Guiana Highlands." *European Journal of Phycology* 38 (3):247-256.

Redfield, Alfred C. 1958. "The biological control of chemical factors in the environment." *American scientist* 46 (3):230A-221.

Renström-Kellner, Eva, and Birgitta Bergman. 1990. "Glycolate metabolism in cyanobacteria. IV. Uptake, growth and metabolic pathways." *Physiologia Plantarum* 78 (2):285–292.

Reynolds, Colin S. 1980. "Phytoplankton assemblages and their periodicity in stratifying lake systems." *Ecography* 3 (3):141-159.

Schreiber, U, U Schliwa, and W1 Bilger. 1986. "Continuous recording of photochemical and non-photochemical chlorophyll fluorescence quenching with a new type of modulation fluorometer." *Photosynthesis research* 10:51-62.

Schreiber, Ulrich, and Christof Klughammer. 2021. "Evidence for variable chlorophyll fluorescence of photosystem I in vivo." *Photosynthesis Research* 149 (1-2):213-231.

Schreiber, Ulrich, Christof Klughammer, and Jörg Kolbowski. 2012. "Assessment of wavelength-dependent parameters of photosynthetic electron transport with a new type of multi-color PAM chlorophyll fluorometer." *Photosynthesis research* 113 (1):127-144.

Schuback, Nina, Philippe D Tortell, Ilana Berman-Frank, Douglas A Campbell, Aurea Ciotti, Emilie Courtecuisse, Zachary K Erickson, Tetsuichi Fujiki, Kimberly Halsey, and Anna E Hickman. 2021. "Single-turnover variable chlorophyll fluorescence as a tool for assessing phytoplankton photosynthesis and primary productivity: Opportunities, caveats and recommendations." *Frontiers in Marine Science*:895.

Schubert, Hendrik, Ulrich Schiewer, and Erhard Tschirner. 1989. "Fluorescence characteristics of cyanobacteria (blue-green algae)." *Journal of plankton research* 11 (2):353-359.

Seppälä, J., P. Ylöstalo, S. Kaitala, S. Hällfors, M. Raateoja, and P. Maunula. 2007. "Ship-of-opportunity based phycocyanin fluorescence monitoring of the filamentous cyanobacteria bloom dynamics in the Baltic Sea." *Estuarine, Coastal and Shelf Science* 73 (3-4):489-500.

Shen, Ding-Wu, Lynn M Pouliot, Matthew D Hall, and Michael M Gottesman. 2012. "Cisplatin resistance: a cellular self-defense mechanism resulting from multiple epigenetic and genetic changes." *Pharmacological reviews* 64 (3):706-721.

Sidler, Walter A. 1994. "Phycobilisome and phycobiliprotein structures." In *The molecular biology of cyanobacteria*, 139-216. Springer.

Silsbe, Greg M, Kevin Oxborough, David J Suggett, Rodney M Forster, Sven Ihnken, Ondřej Komárek, Evelyn Lawrenz, Ondřej Prášil, Rüdiger Röttgers, and Michal Šicner. 2015. "Toward autonomous measurements of photosynthetic electron transport rates: An evaluation of active fluorescence-based measurements of photochemistry." *Limnology and Oceanography: Methods* 13 (3):138-155.

Simeonov, V, JA Stratis, C Samara, G Zachariadis, Dimitra Voutsa, A Anthemidis, Michail Sofoniou, and Th Kouimtzis. 2003. "Assessment of the surface water quality in Northern Greece." *Water research* 37 (17):4119-4124.

Simis, Stefan G. H., Yannick Huot, Marcel Babin, Jukka Seppälä, and Liisa Metsamaa. 2012. "Optimization of variable fluorescence measurements of phytoplankton communities with cyanobacteria." *Photosynthesis Research* 112 (1):13-30.

Simis, Stefan GH, and Hanna M Kauko. 2012. "In vivo mass-specific absorption spectra of phycobilipigments through selective bleaching." *Limnology and Oceanography: Methods* 10 (4):214-226.

Sluchanko, Nikolai N, Konstantin E Klementiev, Evgeny A Shirshin, Georgy V Tsoraev, Thomas Friedrich, and Eugene G Maksimov. 2017. "The purple Trp288Ala mutant of Synechocystis OCP persistently quenches phycobilisome fluorescence and tightly interacts with FRP." *Biochimica et Biophysica Acta (BBA)-Bioenergetics* 1858 (1):1-11.

Srivastava, Ankita, Shweta Singh, Chi-Yong Ahn, Hee-Mock Oh, and Ravi Kumar Asthana. 2013. "Monitoring approaches for a toxic cyanobacterial bloom." *Environmental science & technology* 47 (16):8999-9013.

Stadnichuk, Igor N, Natalya I Romanova, and Irina O Selyakh. 1985. "A phycourobilin-containing phycoerythrin from the cyanobacterium Oscillatoria sp." *Archives of microbiology* 143:20-25.

Staehelin, LA. 1986. "Chloroplast structure and supramolecular organization of photosynthetic membranes." In *Photosynthesis III: photosynthetic membranes and light harvesting systems*, 1-84. Springer.

Suggett, David J, C Mark Moore, Anna E Hickman, and Richard J Geider. 2009. "Interpretation of fast repetition rate (FRR) fluorescence: signatures of phytoplankton community structure versus physiological state." *Marine Ecology Progress Series* 376:1-19.

Suggett, David J, C Mark Moore, Kevin Oxborough, and Richard J Geider. 2006. "Fast repetition rate (FRR) chlorophyll a fluorescence induction measurements." *West Molesey: Chelsea Technologies Group*:1-53.

Suggett, David J, Kevin Oxborough, Neil R Baker, Hugh L MacIntyre, Todd M Kana, and Richard J Geider. 2003. "Fast repetition rate and pulse amplitude modulation chlorophyll a

fluorescence measurements for assessment of photosynthetic electron transport in marine phytoplankton." *European Journal of Phycology* 38 (4):371-384.

Suggett, David, Gijsbert Kraay, Patrick Holligan, Margaret Davey, Jim Aiken, and Richard Geider. 2001. "Assessment of photosynthesis in a spring cyanobacterial bloom by use of a fast repetition rate fluorometer." *Limnology and Oceanography* 46 (4):802-810.

Swanson, Ronald V, LJ Ong, Sigurd M Wilbanks, and AN Glazer. 1991. "Phycoerythrins of marine unicellular cyanobacteria. II. Characterization of phycobiliproteins with unusually high phycourobilin content." *Journal of Biological Chemistry* 266 (15):9528-9534.

Tandeau de Marsac, Nicole, and Jean Houmard. 1993. "Adaptation of cyanobacteria to environmental stimuli: new steps towards molecular mechanisms." *FEMS microbiology reviews* 10 (1-2):119-189.

Tian, Lijin, Ivo H. M. van Stokkum, Rob B. M. Koehorst, Aniek Jongerius, Diana Kirilovsky, and Herbert van Amerongen. 2011. "Site, Rate, and Mechanism of Photoprotective Quenching in Cyanobacteria." *Journal of the American Chemical Society* 133 (45):18304-18311.

Trask, BJ, GJ Van den Engh, and JHBW Elgershuizen. 1982. "Analysis of phytoplankton by flow cytometry." *Cytometry: The Journal of the International Society for Analytical Cytology* 2 (4):258-264.

Trudgill, Stephen, Tim Burt, Penny Johnes, and Louise Heathwaite. 1997. "Improving lake water quality in Slapton Ley National Nature Reserve, south Devon, UK-amelioration by wetlands or drainage basin source management?" *IAHS Publication* 243:299.

Vincent, Warwick F. 1980. "MECHANISMS OF RAPID PHOTOSYNTHETIC ADAPTATION IN NATURAL PHYTOPLANKTON COMMUNITIES. II. CHANGES IN PHOTOCHEMICAL CAPACITY AS MEASURED BY DCMU-INDUCED CHLOROPHYLL FLUORESCENCE 1." *Journal of Phycology* 16 (4):568-577.

Wang, Zhicong, Dunhai Li, Hongjie Qin, and Yinxia Li. 2012. "An integrated method for removal of harmful cyanobacterial blooms in eutrophic lakes." *Environmental Pollution* 160:34-41.

Weithoff, Guntram. 2003. "The concepts of'plant functional types' and'functional diversity'in lake phytoplankton: a new understanding of phytoplankton ecology."

Werdell, P. Jeremy, Lachlan I.W. McKinna, Emmanuel Boss, Steven G. Ackleson, Susanne E. Craig, Watson W. Gregg, Zhongping Lee, Stéphane Maritorena, Collin S. Roesler, Cécile S. Rousseaux, Dariusz Stramski, James M. Sullivan, Michael S. Twardowski, Maria Tzortziou, and Xiaodong Zhang. 2018. "An overview of approaches and challenges for retrieving marine inherent optical properties from ocean color remote sensing." *Progress in Oceanography* 160:186-212.

Wetzel, Robert G. 2001. *Limnology: lake and river ecosystems*: gulf professional publishing.

Whitton, Brian A. 1992. "Diversity, ecology, and taxonomy of the cyanobacteria." In *Photosynthetic prokaryotes*, 1-51. Springer.

Whitton, Brian A., and Malcolm Potts. 2000. *The ecology of cyanobacteria: their diversity in time and space*. Edited by Brian A. Whitton and Malcolm Potts. Dordrecht: Kluwer Acad.

Wilson, Adjélé, Claire Punginelli, Andrew Gall, Cosimo Bonetti, Maxime Alexandre, Jean-Marc Routaboul, Cheryl A. Kerfeld, Rienk van Grondelle, Bruno Robert, and John TM Kennis. 2008. "A photoactive carotenoid protein acting as light intensity sensor." *Proceedings of the National Academy of Sciences* 105 (33):12075–12080.

Wilson, RS, MA Sleigh, TRA Maxwell, G Mance, and RA Milne. 1975. "Physical and chemical aspects of Chew Valley and Blagdon Lakes, two eutrophic reservoirs in North Somerset, England." *Freshwater Biology* 5 (4):357-377.

Woodward, EMS, and AP Rees. 2001. "Nutrient distributions in an anticyclonic eddy in the northeast Atlantic Ocean, with reference to nanomolar ammonium concentrations." *Deep Sea Research Part II: Topical Studies in Oceanography* 48 (4-5):775-793.

Wright, Simon W, and SW Jeffrey. 2006. "Pigment markers for phytoplankton production." *Marine organic matter: biomarkers, isotopes and DNA*:71-104.

Wurtsbaugh, Wayne A., Hans W. Paerl, and Walter K. Dodds. 2019. "Nutrients, eutrophication and harmful algal blooms along the freshwater to marine continuum." *WIREs Water* 6 (5):e1373. doi: https://doi.org/10.1002/wat2.1373.

Xiaoli, Chai, Liu Guixiang, Zhao Xin, Hao Yongxia, and Zhao Youcai. 2012. "Fluorescence excitation–emission matrix combined with regional integration analysis to characterize the composition and transformation of humic and fulvic acids from landfill at different stabilization stages." *Waste management* 32 (3):438-447.

Yentsch, Charles S., and Clarice M. Yentsch. 1979. "Fluorescence spectral signatures: the characterization of phytoplankton populations by the use of excitation and emission spectra." *J. mar. Res* 37 (3):471–483.

Yoshida, Mitsuo, Tomohiro Horiuchi, and Yasuhiro Nagasawa. 2011. "In situ multi-excitation chlorophyll fluorometer for phytoplankton measurements: Technologies and applications beyond conventional fluorometers." OCEANS'11 MTS/IEEE KONA.

Zamyadi, Arash, Florence Choo, Gayle Newcombe, Richard Stuetz, and Rita K. Henderson. 2016. "A review of monitoring technologies for real-time management of cyanobacteria: Recent advances and future direction." *TrAC Trends in Analytical Chemistry* 85:83-96.

Zapata, Manuel, José L Garrido, and Shirley W Jeffrey. 2006. "Chlorophyll c pigments: current status." *Chlorophylls and bacteriochlorophylls: biochemistry, biophysics, functions and applications*:39-53.